RATIONAL PROCEDURE FOR DAMAGE BASED SERVICEABILITY DESIGN OF STEEL BUILDINGS UNDER WIND LOADS
AND
A SIMPLE LINEAR RESPONSE HISTORY PROCEDURE FOR BUILDING CODES

Kevin Paul Aswegan

Thesis submitted to the faculty of the
Virginia Polytechnic Institute and State University
in partial fulfillment of the requirements for the degree of

MASTER OF SCIENCE

in

CIVIL ENGINEERING

Finley A. Charney

Roberto T. Leon

Cristopher D. Moen

August 7, 2013
Blacksburg, Virginia

Keywords: wind drift, serviceability, fragility, steel, linear response history analysis, spectral matching

RATIONAL PROCEDURE FOR DAMAGE BASED SERVICEABILITY DESIGN OF STEEL BUILDINGS UNDER WIND LOADS
AND
A SIMPLE LINEAR RESPONSE HISTORY PROCEDURE FOR BUILDING CODES

Kevin Paul Aswegan

ABSTRACT

This thesis is divided into two topics: the development of a procedure for wind serviceability design of steel buildings and the development of a simple linear response history analysis for building codes.

In the United States the building codes are generally silent on the issue of serviceability. This has led to a wide variation in design practices related to service level wind loads. Chapter 2 of this thesis contains a literature review which discusses pertinent aspects of wind drift serviceability, including selecting the mean recurrence interval (MRI), mathematical modeling of the structure, and establishment of rational deformation limits. Chapter 3 contains a journal article submitted to *Engineering Journal* which describes the recommended procedure for damage based wind serviceability design of steel structures. The procedure uses a broad range of MRIs, bases damage measurement on shear strains, includes all sources of deformation in the model, and bases deformation limits on fragility curves.

Chapter 4 of this thesis contains a literature review which examines issues related to performing linear response history analysis. Chapter 5 contains a conference paper submitted to the *Tenth U.S. National Conference on Earthquake Engineering* which serves as a position paper

promoting the inclusion of a linear response history analysis procedure in future editions of the NEHRP Recommended Seismic Provisions and ASCE 7. The procedure address the following issues: selection and scaling of ground motions, the use of spectral matched ground motions, design for dependent actions, and the scaling of responses with the response modification coefficient (R) and the deflection amplification factor (C_d).

ACKNOWLEDGEMENTS

I would like to express my deepest appreciation and gratitude to my Committee Chair Dr. Finley Charney for providing guidance and insight during my studies. I have learned much from him, both in the classroom and in our research meetings and discussions. I would also like to thank Dr. Cristopher Moen and Dr. Roberto Leon for serving on my committee and providing feedback and suggestions for my research.

I also would like to thank my friends and family for their support through my educational career. Specifically I want to thank my wife, Toni Carroll Aswegan, for her unwavering encouragement and support; my mother, Catherine Aswegan for always being there for me; my father, Douglas Aswegan; my sister, Janet; my best friend, Jacob Ellenwood; and all of my grandparents, aunts, uncles, and cousins who have helped make me who I am today.

A great deal of appreciation is owed to Virginia Tech, where I first came to know structural engineering. I would like to thank the faculty and staff of the university for everything I have learned since I started my studies. I owe a special thanks to the Charles E. Via Department of Civil and Environmental Engineering for providing me with funding to complete my graduate research. And last, but certainly not least, I would like to thank all of the great friends I have made at Virginia Tech. You have made my stay here truly fun.

Attribution

Jordan Jarrett, the third author of the journal paper presented in Chapter 3 of this thesis, is a graduate student pursuing the degree of PhD in the Department of Civil and Environmental Engineering at Virginia Tech. Contributions to the journal paper include overall feedback and corrections as well as primary authorship of the "Application the FEMA P-58 Methodology" section.

Table of Contents

List of Figures

List of Tables

1 Introduction

The two topics of this thesis, although unrelated to one another, each address an identified design or analysis deficiency within the structural engineering field. The first topic considers the serviceability design of steel structures for wind loads and the second topic considers the design and analysis of structures using linear response history analysis.

1.1 Wind Serviceability

1.1.1 Motivation

Serviceability issues have long been considered critical design considerations. Engineers and researchers in the past have assessed the state-of-the-practice and recommended changes and research needs. In 1986 the Ad Hoc Committee on Serviceability Research reviewed the issues related to structural serviceability limit states and determined areas and topics in need of improvement. Recognizing the need for guidance, but attempting to avoid a prescriptive serviceability standard, the committee provided the following thoughts (Ellingwood 1986):

> *"Serviceability guidelines need to be flexible and adaptable to different occupancies, use requirements, and techniques for integrating nonstructural components. The guidelines ought to be negotiable, within limits, between the engineer, architect, and building owner."*

As discussed in Chapter 2, the design community lacks clear guidance relating to the serviceability design of steel structures for service level wind loads. There is a wide variation within the design community in terms of the design mean recurrence interval (MRI), the

complexity and accuracy of the structural model, the damage measure (e.g. interstory drift ratio), and the source of the damage limits. Furthermore, the traditional approach to wind drift design is outdated and does not take full advantage of modern computing power and techniques.

1.1.2 Research Objectives

The objective of the research is to develop a rational damage-based procedure for the design of steels buildings under service level wind loads. The proposed procedure should address the following issues:

- Incorporation of select concepts from the field of Performance Based Earthquake Engineering (PBEE)
- Identification of the appropriate MRI for wind drift design
- Identification and use of a logical damage measure for nonstructural components
- Selection and computation of damage limits based on test results tied to the damageable material in question

Furthermore, a principal theme found throughout the procedure is that the method should be nonprescriptive, leaving the large decisions to be made in consultation between the engineer, architect, owner, and other decision makers.

1.1.3 Organization of the Report

Chapter 2 of this report contains a detailed literature review of the issues related to wind drift and wind serviceability design. Key topics reviewed in this section are the overall state of the practice, a discussion of the traditional damage measure and the proposed revised measure, the use of fragility curves to obtain damage limits, calculation of wind loads and selection of

appropriate mean recurrence intervals, and accurate structural modeling and important sources of stiffness to include in the model.

Chapter 3 contains a journal article detailing the proposed wind serviceability design procedure, supported by the literature review of Chapter 2. The article, titled "Recommended Procedures for Damage Based Serviceability Design of Steel Buildings" has been submitted to the American Institute of Steel Construction's (AISC) *Engineering Journal*.

1.2 Linear Response History Analysis

1.2.1 Motivation

Linear response history analysis (LRHA) is a technique to compute the response of a structural system to a specific excitation (usually a ground motion) using numerical integration. The technique is more accurate than both the Equivalent Lateral Force (ELF) procedure and Response Spectrum Analysis (RSA) procedure of ASCE 7 (2010). Unlike ELF, LRHA is capable of explicitly handling higher mode effects, and unlike RSA, the signs of the responses are not lost due to combination rules. LRHA is an important option available to engineers, whether used as a method to design a structure, validate design results from other methods, or as a step in a chain of increasingly complex analyses culminating in nonlinear response history analysis. A further advantage of linear response history analysis is the information generated related to the history of the forces and displacements. This is significant because pairs of responses can be plotted over time (i.e. the history of axial load and moment in a column can be used to design the column for interaction effects) rather than assuming some relation between the peak values as is done for response spectrum analysis.

1.2.2 Research Objectives

The objective of the research is to identify key issues associated with current linear response history analysis procedures and to provide analysis and discussion of the issues in the context of building code applications. The provisions of ASCE 7 are evaluated along with the European, Canadian, and New Zealand building codes, amongst others. Significant issues addressed by the research are:

- The use of spectral matched ground motions to reduce the required number of analyses
- Ground motion scaling requirements for 3D analysis
- Handling of dependent actions (force and moment interaction)
- Modeling and analysis for accidental torsion
- Scaling of responses using the R and C_d factors

Furthermore, it is intended that any proposed LRHA procedure for building codes should be concise and simple to understand for practicing engineers. In general, it should be of equal or only slightly more complexity than the current response spectrum analysis procedure.

1.2.3 Organization of the Report

Chapter 4 of this report contains a literature review related to the issues identified in the previous section. These issues include ground motion selection and scaling, spectral matching (including the methods used to match ground motions), the response modification coefficient R, modeling concerns (damping, direction of loading, etc.), and an overview of current procedures as specified in various building codes and standards.

Chapter 5 contains a draft conference paper to be submitted to the *Tenth U.S. National Conference on Earthquake Engineering* (held in July 2014 in Anchorage, Alaska). The paper, supported by the literature review of Chapter 4, serves as a position paper promoting the inclusion of LRHA in future editions of ASCE 7. The appendix of the paper contains draft code language proposed for future building codes.

Chapter 6 is used for discussion, conclusions, and recommendations for future research related to the two topics of the thesis.

2 Wind Serviceability – Literature Review

2.1 Introduction

Designing to prevent damage due to lateral wind loads has historically been an area dominated by rules-of-thumb. The benefit is that the design remains relatively simple, while the potential drawbacks are inefficiency or unconservatism. These drawbacks have led some to question the usefulness of traditional wind drift design methods. Smith (2011) points out several problems related to wind serviceability design, such as the fact that interstory drift is a flawed damage measure as well as the fact that designers should be using deflection limits that take into account the damageable materials.

In order to rationally design for wind drift, several important topics must first be addressed. These topics include establishing a correct definition for drift, determining material-specific drift limits, selecting appropriate wind loads (related to selecting a mean recurrence interval), and accurately modeling the structure. The purpose of this literature survey is to review key information relating to these topics.

2.2 State of the Practice

In 1984 ASCE created the Task Committee on Drift Control of Steel Building Structures. The goal of the committee was to assess the state-of-the-art of wind drift design practices. A survey was conducted of structural engineering firms, and in 1988 the results were published (ASCE 1988). The committee sent the survey to 132 firms and received 35 responses. Its goal was to

obtain information relating to wind drift design practices, including modeling techniques, drift limits, and wind loads.

The task committee examined the responses to the survey and made several recommendations and observations. These include:

- Wind drift should be a consideration in design, but generally speaking, it should not be codified.
- It is reasonable to use a different mean recurrence interval (MRI) for wind drift than for the strength design.
- Drift calculations should include column axial deformations, shear deformations, panel-zone deformations, width of beam to column joints, and P-delta effects.
- Responses concerning allowable interstory drift limits varied widely, from 1/600 to 1/200.

The task committee survey illustrated that wind drift design practices varied widely within the design community. The responses indicated that there was no consensus on which wind loads to use, how to model the structure, or which drift limits to employ.

Charney (1990b) proposed research needs related to wind drift design, including the establishment of drift limits based on material tests and the establishment of modeling techniques to calculate drift that accurately represent the behavior of a building. Griffis (1993) also identified several issues related to wind drift. He recommended the use of a 10-year mean recurrence interval, as well as making the point that accurate wind drift calculations must include the effects mentioned by the ASCE task committee as well as beam and column flexural

deformations. Griffis tabulated recommended deflection limits for various materials, such as brick veneer, gypsum drywall, and unreinforced concrete masonry.

A second survey, intended to assess the state of the wind drift serviceability design practice, was developed by the ASCE/SEI Committee on the Design of Steel Building Structures. It was administered in 2006 and the results confirm that within the design community there is still much variation in terms of wind drift design practices (Charney and Berding 2007). Two examples from the survey can be used to represent this variation. The first example is that forty percent of respondents reported using a 10-year MRI to check wind drift, while the rest used a 50- or 100-year MRI. The second example is on the question of including shear deformations in columns. Of the respondents, 27.3% usually include shear deformations, 33.3% sometimes do, and 39.4% rarely do. This wide variation could be due to many reasons, but it demonstrates the lack of consistency in the structural engineering industry with regards to structural modeling.

2.3 Drift Limits

2.3.1 Definition of Drift

There are several traditional measures of the drift of a level of a building. The most common measures are *total drift* (the lateral displacement at a level with respect to a particular datum, usually the ground level) and *interstory drift* (the relative lateral displacement between two adjacent levels in a building). The *total drift index* can be obtained by dividing the total drift by the height of the level above the datum. Similarly, the *interstory drift index* (or interstory drift ratio) can be obtained by dividing the interstory drift by the height of the story (Charney 1990b). The goal of limiting wind drift is usually to prevent damage to building elements, and so

interstory drift is more useful than total drift. For example, a large interstory drift at the ground level of a building will affect the interior partitions at that level, but will not affect the interior partitions at any other levels above it. Using the interstory drift index instead of interstory drift is important because it normalizes the deformation by the height of the story. A drift of 1 in. will be of greater concern for a story height of 10 ft. than for a story height of 13 ft.

The traditional measures of drift are not always entirely accurate measures of the true damage in a building element. Interstory drift includes rigid body rotation (which should not be included) and does not include vertical racking (which should be included). To remedy these problems, Charney (1990b) and Griffis (1993) recommend measuring damage using a *drift damage index* (DDI) which takes into account horizontal racking, vertical racking, and rigid body rotation. Mathematically the DDI is the equivalent of the shear strain in the material. To calculate the DDI, a *drift damageable zone* must first be defined. This zone typically will span from one level to the next, and between adjacent column lines. It is the region where damage is measured, representing, for example, a section of gypsum drywall. Figure 2-1 defines a drift damageable zone and the definitions are used to calculate the DDI, which can be determined using Eq. 2.1.

$$DDI = 0.5\left[\frac{X_A - X_C}{H} + \frac{X_B - X_D}{H} + \frac{Y_D - Y_C}{L} + \frac{Y_B - Y_A}{L}\right] \qquad (2.1)$$

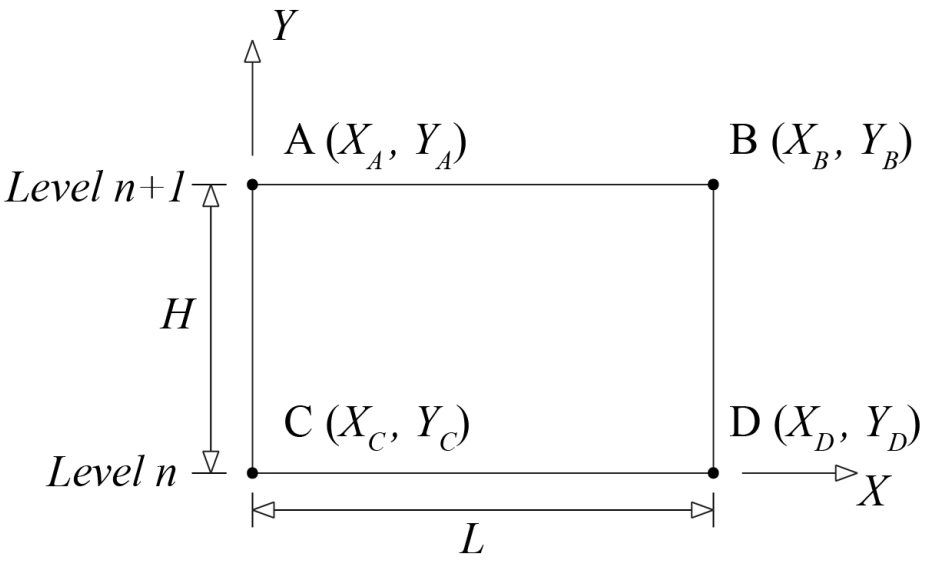

Figure 2-1. Drift Damageable Zone

Charney and Griffis present examples to illustrate the differences between interstory drift and DDI, and the inherent deficiencies of using interstory drift as a damage measure. The example from Charney (1990) is repeated below. In the example, two 10 story frames were subjected to the same lateral loads. Figure 2-2 shows the frames (one moment frame and one braced frame).

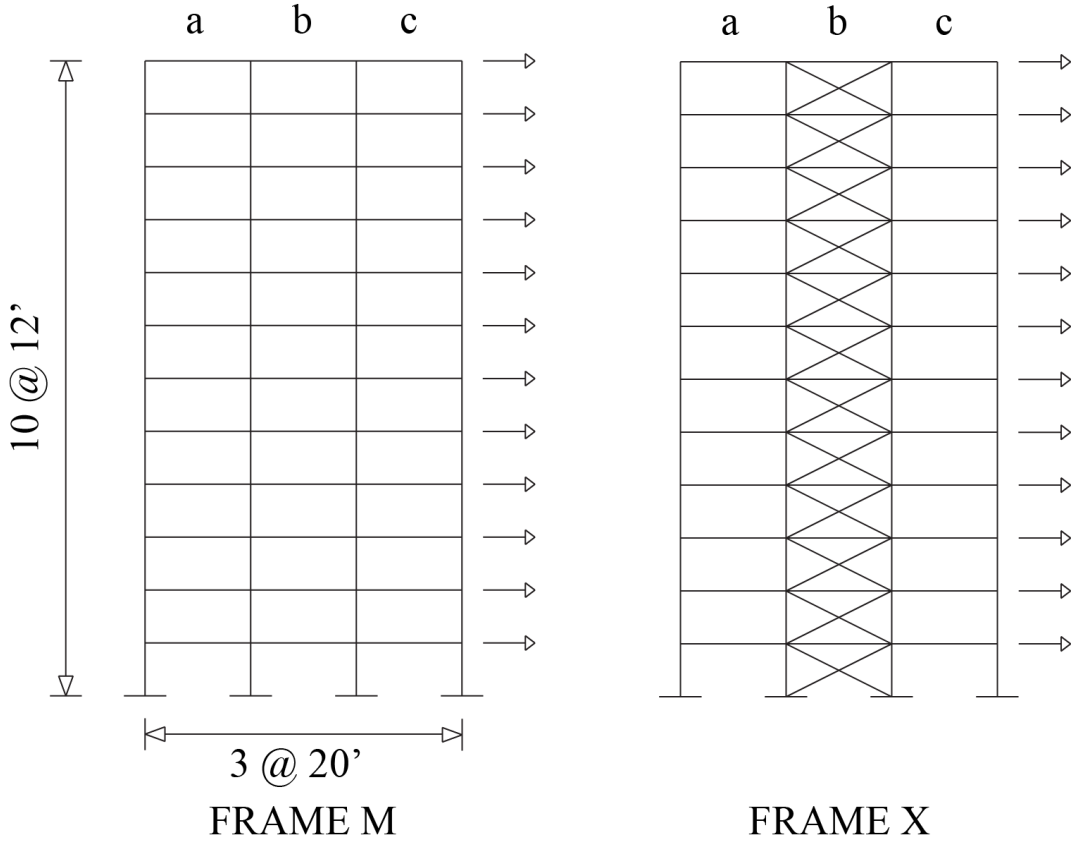

Figure 2-2. Interstory Drift and Drift Damage Index

Table 2-1 contains a comparison of the interstory drift and the drift damage index for each of the two frames. For the applied loads, the interstory drift is equal (0.00267) for both frames for all three bays. The DDI, however, ranges from a low of 0.00083 to a high of 0.00358. This spans a wide range, from 31% of the interstory drift to 134%. This range can be higher for other cases, especially for tall braced frame or frame-wall systems (Charney 1990b).

Table 2-1. Comparison of Interstory Drift with Drift Damage Index

		Interstory Drift	Drift Damage Index	(Drift Damage Index) / (Interstory Drift)
Frame M	Bay *a*	0.00267	0.00219	0.820
	Bay *b*	0.00267	0.00267	1.000
	Bay *c*	0.00267	0.00219	0.820
Frame X	Bay *a*	0.00267	0.00358	1.341
	Bay *b*	0.00267	0.00083	0.311
	Bay *c*	0.00267	0.00358	1.341

Although shear strain (DDI) is the most accurate measure of damage in a building element, interstory drift is still the most commonly used parameter. In the 2006 ASCE-sponsored wind drift survey 97% of respondents reported using interstory drift, total drift, or a combination of the two. None of the respondents reported using shear strain as the wind drift damage measure.

2.3.2 Commonly Used Drift Limits

There are no standard drift limits used within the design community. In 1988, ASCE reported the results of a survey which showed that designers were using interstory drift index limits ranging from 1/600 to 1/200 (ASCE 1988). Galambos and Ellingwood (1986) compiled interstory drift index limits at which various serviceability problems might occur. The limits are repeated in Table 2-2. It should be noted that the commonly use drift limits reported by the ASCE survey fall within the serviceability limits given in the table.

Table 2-2. Interstory Drift Limits at Which Serviceability Problems Develop (Galambos and Ellingwood 1986). Used under fair use, 2013.

Interstory Drift Limit (Fraction of Height)	Deformation Visibility	Typical Behavior
≤ 1/1000	Not Visible	Cracking of brickwork
1/500	Not Visible	Cracking of partition walls
1/300	Visible	General architectural damage Cracking in reinforced walls Cracking in secondary members Damage to ceiling and flooring Façade damage Cladding leakage Visual Annoyance
1/200 - 1/300	Visible	Improper damage
1/100 - 1/200	Visible	Damage to lightweight partitions, windows, finishes Impaired operation of removable components such as doors, windows, sliding partitions

Furthermore, Griffis (1993) compiled recommended interstory drift limits to prevent material damage to building elements due to wind loading. The building elements for which he reported limits include metal roofs, skylights, brick veneer, unreinforced concrete masonry, curtain walls, gypsum drywall, and tile. Selected building elements and their associated drift limits reported by Griffis are repeated in Table 2-3.

Table 2-3. Selected Recommended Interstory Drift Limits (Griffis 1993). Used under fair use, 2013.

Building Element	Supporting Structural Element	Deformation Type	Recommended Limit
Brick Veneer	Wind Frame	Shear Strain	1/400
Concrete Masonry Unreinforced (Exterior)	Wind Frame (1 story)	Shear Strain	1/600
	Wind Frame (2 story)	Shear Strain	1/400
Concrete Masonry Reinforced (Exterior)	Wind Frame (1 story)	Shear Strain	1/200
	Wind Frame (2 story)	Shear Strain	1/400
Gypsum Drywall, Plaster	Wind Frame	Shear Strain	1/400
Brick (Interior Partition)	Wind Frame	Shear Strain	1/1250

Other sources provide drift limits similar to those above. For example, AISC Design Guide 3 (Serviceability Design Considerations) gives a general recommendation of H/500 as the interstory drift limit when the model includes the bare frame only and the wind load is due to a 10-year wind event (West et al. 2003). Another source cites the typical allowable interstory drift range to be H/750 to H/250, with H/400 the most common (Chan and Huang 2010). For seismic loads the serviceability-related interstory drift limits used are typically different than those used for wind. Dymiotis-Wellington and Vlachaki (2004) summarize the employed seismic interstory drift limits, with a median value of approximately H/250.

Building codes are generally vague on drift limits. ASCE 7 (2010) states “lateral deflection or drift of structures and deformation of horizontal diaphragms and bracing systems due to wind effects shall not impair the serviceability of the structure.” It provides no limits on the drift itself.

The Commentary to ASCE 7 cites common drift limits of 1/600 to 1/400, taken from ASCE (1988) and Griffis (1993). Unlike most other national building codes, the National Building Code of Canada (2010a) gives explicit drift limits. Sentence (3) of Section 4.1.3.5 of the NBCC states that "the total drift per storey under service wind and gravity loads shall not exceed 1/500 of the storey height". The Commentaries (2010b) to the NBCC recommend a total drift limit between 1/250 and 1/1000 of the total building height.

In summary, the allowable interstory drift used by the design community varies within a wide range. Generally, the range is between H/700 and H/200, although values outside this range are used on occasion. Using only one particular value of interstory drift for design, however, poses multiple problems. It fails to account for the fact that interstory drift is a flawed damage measure (because it does not include the effects of vertical racking), and it also fails to differentiate between damageable materials. For example, it is possible (likely, in fact) that two different drift limits should be used for drywall and unreinforced concrete masonry.

2.3.3 Fragility Curves

A fragility curve is a relationship between "structural response parameters such as interstory drift ratio or peak floor acceleration and the level of damage in structural and non-structural components" (Miranda 2006). In the context of wind drift, an example would be the probability of a gypsum wall experiencing cracking vs. interstory drift ratio. An example of a fragility curve of this type is shown in Figure 2-3. This fragility curve was generated with Performance Assessment Calculation Tool (PACT), a program released by FEMA (2013b). The green line represents damage state 1 (DS1) which is screws popping out and minor cracking. The yellow

line (DS2) is moderate cracking or crushing of the gypsum. The red line (DS3) is significant cracking or crushing. The horizontal axis is the interstory drift ratio and the vertical axis is the probability of exceeding the damage limit state. For example, for an interstory drift ratio of 0.002 (H/500) there is approximately a 50% chance of minor damage (DS1). Physically this means that if a number of specimens of gypsum walls were racked to an interstory drift of 0.002, half of them would experience minor damage, and half would not. A fragility curve is useful to an engineer because the probability of exceedance for a limit state can be determined given any level of the response parameter (e.g. interstory drift).

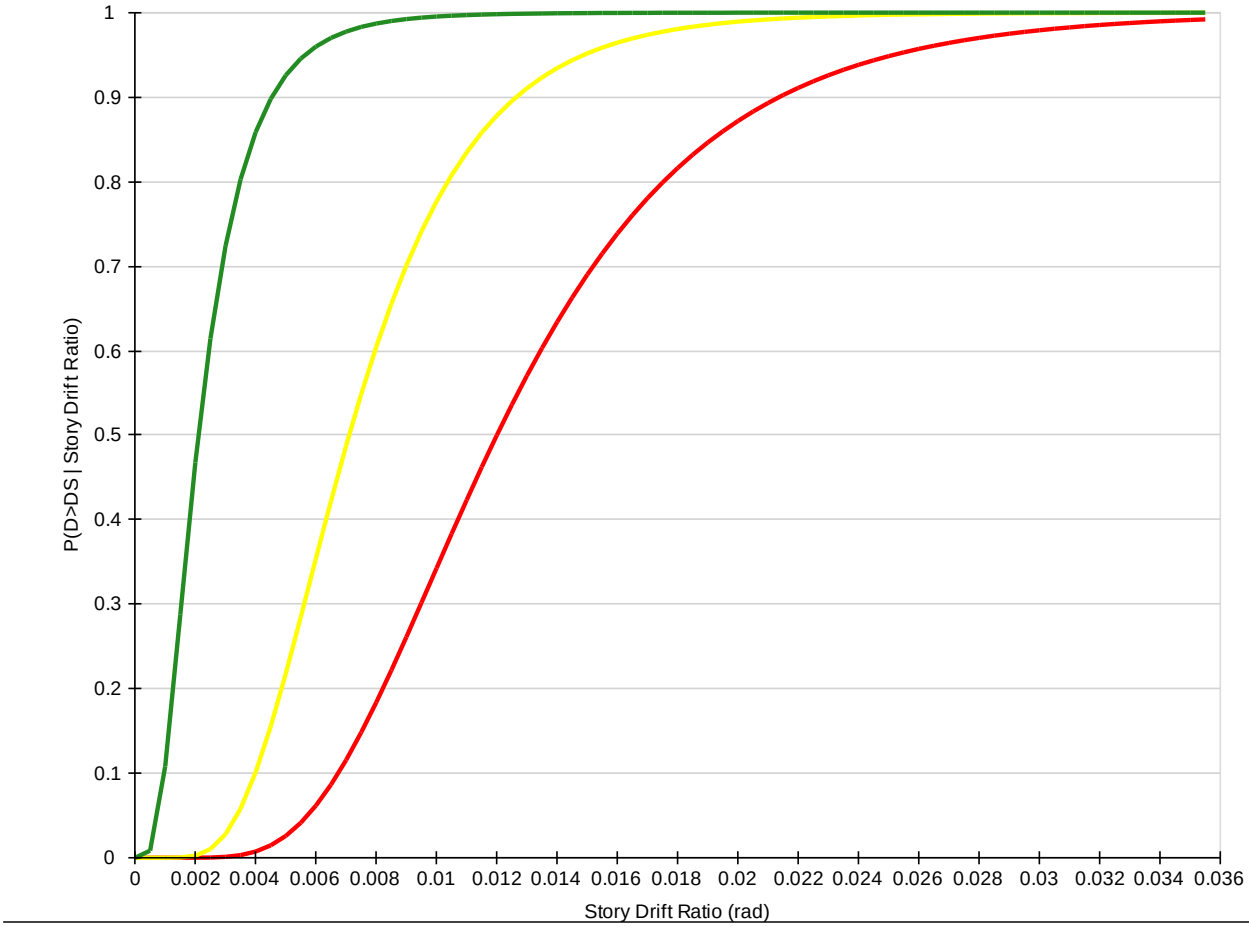

Figure 2-3. Gypsum Wall Board Fragility Curve (PACT)

2.3.3.1 Performance Based Earthquake Engineering

The most common current application of fragility curves within the field of structural engineering is Performance Based Earthquake Engineering (PBEE). Interest in PBEE began in the 1980s, and today the state-of-the-art is being developed by the Applied Technology Council in a project called FEMA P-58 (FEMA 2013a). PBEE is currently embedded in several other design methodologies, including ASCE 41 (ASCE 2013) and the PEER guidelines for the seismic design of tall buildings (PEER 2010). The basic intent behind PBEE is to establish quantifiable design objectives that can be computed on a probabilistic basis and compared to a structural model to determine if the objectives have been met. The performance objectives are intended to be easily understood by decision makers (e.g. owners, architects, officials, etc.). FEMA P-58 has narrowed down the performance objectives to three: loss of life, cost to repair or replace the structure, and loss of use of the structure (Hamburger 2006).

The Pacific Earthquake Engineering Research Center (PEER) formalized the PBEE approach. In general, there are four steps that comprise PBEE (Moehle and Deierlein 2004): hazard analysis, structural analysis, damage analysis, and loss analysis. These four steps lead to four outcomes, which are, respectively, intensity measure (IM), engineering demand parameter (EDP), damage measure (DM), and decision variable (DV). The IM relates to the hazard in question (e.g. for an earthquake, peak ground acceleration could be used). The EDP is commonly interstory drift or floor accelerations. The DM is a representation of physical damage. The DV is a meaningful value used by the decision maker. It can be expressed in terms of casualties (lives lost), cost (dollars), or downtime (days). These variables are the subject of much research by PEER, ATC,

and others. Fragility curves are employed as a useful link between EDPs and DMs (FEMA 2013b).

2.3.3.2 Performance Based Wind Engineering

Performance Based Wing Engineering (PBWE) has not gained as much traction as PBEE. The concepts used in seismic design, however, can be extended for use in wind design. Wen (2001) calls for performance based design for both earthquake and wind engineering. The phrase 'Performance Based Wind Engineering' was first coined by Paulotto et al. (2004). The authors describe a method that makes use of the PEER framework, applied to wind engineering. Historically, wind fragility curves were expressed in terms of probability of damage due to a wind speed, p(DM|IM). This runs counter to PEER's framework, which calls for probability of damage due to a particular engineering demand parameter, p(DM|EDP). The authors cite this discrepancy and call for fragility curves which express the probability of exceeding a certain damage state expressed as a function of an EDP (such as peak roof displacement).

Ciampoli et al. (2011) describe a general PBWE procedure and provide an example of a performance based analysis of a bridge across the Messina Straight in Italy. This analysis considered a dynamic model of the bridge, where the limit states were based on rotational velocities and accelerations. A simple Monte Carlo simulation was performed to account for the uncertainty in the mean wind velocity. Separate analyses were performed to investigate the impact of uncertainties related to the roughness length, the aerodynamic coefficients, and the wind-action model. The authors did not consider drifts or deflections as limit states in the example. Griffis et al. (2012) propose a PBWE procedure which explicitly includes nonlinear

dynamic effects. Controlled inelastic response is allowed, and the building is analyzed at different performance levels with actual wind pressure histories recorded from wind tunnel tests. It is recommended that the nonlinear model be analyzed with the same software used in PBEE, including Perform3D and OpenSees.

2.3.3.3 Fragility Curve Theory

For the purposes of preventing damage to non-structural components, the most useful fragility curves typically contain interstory drift (or another EDP such as shear strain) on the horizontal axis and percent chance of exceeding a particular damage measure on the vertical axis. The curves are created based on a data set which contains test data on a material. Table 2-4 contains an example (hypothetical) data set. There are ten specimens. For this hypothetical example, each specimen was loaded in the same manner, increasing the interstory drift until a particular damage state (DS) occurred. The interstory drift ratio was noted, and then the process repeated for the next specimen.

Table 2-4. Hypothetical Fragility Curve Data Set

Spec. #	Interstory Drift Ratio at Which DS Occurs
1	0.00209
2	0.00199
3	0.00212
4	0.00206
5	0.00201
6	0.00223
7	0.00221
8	0.00202
9	0.00217
10	0.00208

The following mathematical expressions for fragility curves are taken from Porter et al. (2006), Porter et al. (2007), FEMA P-58 FEMA (2013a), and Ang and Tang (2007). First, the mean and standard deviation of the data set should be calculated with the following equations.

$$\mu = \frac{1}{M}\Sigma r_i \qquad (2.2)$$

$$\sigma = \sqrt{\frac{1}{M}\Sigma\left(r_i - \mu\right)^2} \qquad (2.3)$$

where:

μ = mean of the EDP values (e.g. interstory drift ratios)
σ = standard deviation of the EDP values
M = number of specimens tested
r_i = EDP at which the DS occurred

The above mean and standard deviation would be used for a normal (Gaussian) distribution. However, fragility curves are typically constructed using a lognormal distribution because most data sets used in structural engineering form a better fit to this type of distribution. For this reason, the following fragility curve parameters must be calculated. The following equations are derived for what Porter et al. (2006) call "Method A," which is the method to use when all tested specimens failed at an observed EDP.

$$x_m = \exp\left(\frac{1}{M}\sum_{i=1}^{M}\ln r_i\right) \qquad (2.4)$$

$$\beta = \sqrt{\left(\frac{1}{M-1}\sum_{i=1}^{M}\left(\ln\left(r_i / x_m\right)\right)^2\right)} \qquad (2.5)$$

The fragility function $F_{dm}(edp)$ is defined generically by the following equation.

$$F_{dm}(edp) = P\left[DM \geq dm \mid EDP = edp\right] \qquad (2.6)$$

This fragility function, then, can be expressed as "the probability that the damage measure (*DM*) will equal or exceed a specified value (*dm*) given that the engineering demand parameter (*EDP*) equals a specified value (*edp*)." Mathematically, the fragility function is defined with a lognormal distribution as a function of the above variables x_m and β.

$$F_{dm}(edp) = \Phi\left(\frac{\ln(edp / x_m)}{\beta}\right) \quad (2.7)$$

where:

Φ = standard normal (Gaussian) cumulative distribution function

The standard normal distribution function is included in most spreadsheet programs, including Microsoft Excel. If only the normal mean and standard deviation are known (μ and σ) then the logarithmic mean and logarithmic standard deviation (x_m and β) can be estimated with the following conversion equations.

$$\beta = \sqrt{\ln\left(1 + (\sigma / \mu)^2\right)} \quad (2.8)$$

$$x_m = \mu / \sqrt{1 + (\sigma / \mu)^2} \quad (2.9)$$

An example is presented in Figure 2-4 using the hypothetical values given in Table 2-4. The resulting fragility curve is plotted in Figure 2-5. Note that one point on the curve is approximately (0.00198, 0.50), indicating that at the mean value there is a 50% chance of exceeding the damage state, as expected. The ten hypothetical interstory drift values are included in the plot to illustrate the fit of the fragility curve.

Data set			Calculations	
Spec. No.	Interstory Drift Ratio at Which DS Occurs	Probability of Exceedance	$\ln(r_i)$	$\ln(r_i / x_m)^2$
7	0.00179	0.05	-6.33	0.0104
1	0.00183	0.15	-6.30	0.0061
10	0.00184	0.25	-6.30	0.0054
5	0.00191	0.35	-6.26	0.0015
2	0.00194	0.45	-6.24	0.0004
4	0.00208	0.55	-6.18	0.0022
3	0.00208	0.65	-6.18	0.0022
9	0.00211	0.75	-6.16	0.0037
6	0.00213	0.85	-6.15	0.0052
8	0.00216	0.95	-6.14	0.0076
		Sum =	-62.23	0.0447

x_m =	0.00198
β =	0.06684

Figure 2-4. Example Fragility Curve Parameter Calculations

The probability of exceedance for a specific data point (see calculations in the above figure) can be determined with the following formula, after the data points have been sorted in ascending order by the engineering demand parameter.

$$p_i = \frac{i - 0.5}{M} \qquad (2.10)$$

where:

p_i = probability of exceedance
i = rank of the data point in the sorted set
M = number of sample point in the data set

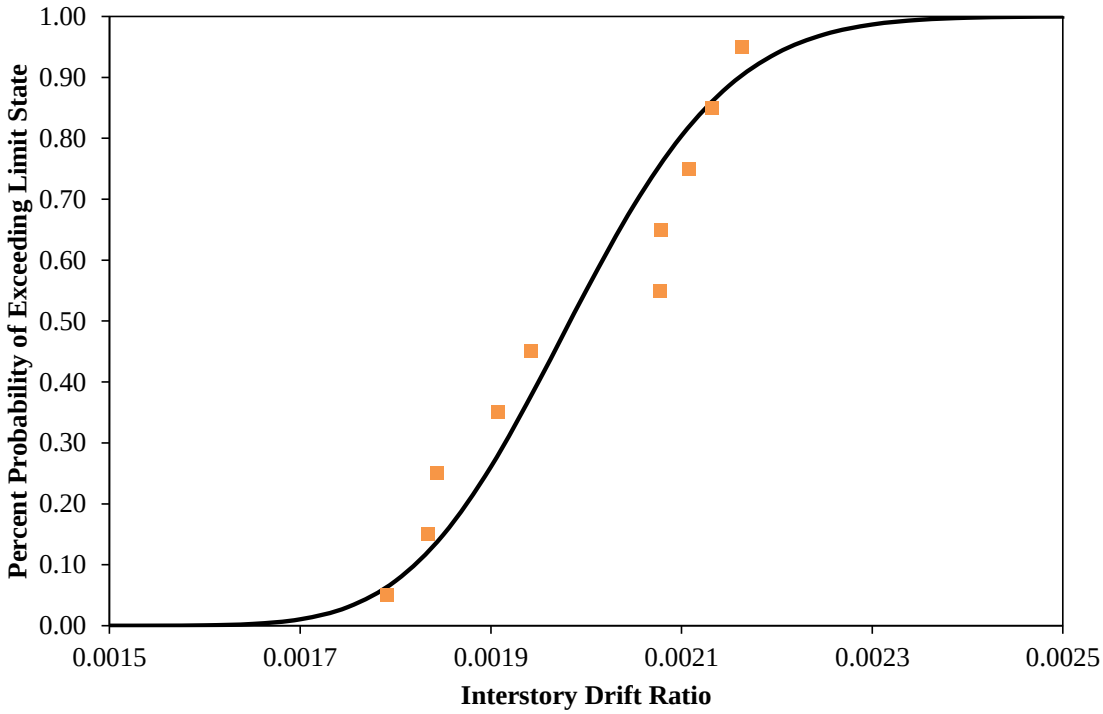

Figure 2-5. Hypothetical Fragility Curve

Examples of fragility curve parameters developed for the FEMA P-58 project (FEMA 2013a) and the PACT program (FEMA 2013b) can be found in Miranda (2013) and O'Brien Jr et al. (2012).

2.4 Wind Loads

2.4.1 Mean Recurrence Interval

When designing for wind drift one of the most important decisions to be made is the selection of an appropriate mean recurrence interval (MRI). The mean recurrence interval is the return period for a wind event. For example, a 10-year MRI corresponds to a wind event that occurs once, on average, every 10 years.

In the United States the wind loads for the strength design of buildings are determined in accordance with ASCE 7. The current edition is ASCE 7-10, which departs from previous editions in that the wind speeds provided are the ultimate wind speeds. The wind load factor for most cases is 1.0, where it was previously 1.6 (ASCE 2010). Chapter 26.5 of ASCE 7-10 provides basic wind speeds for the US. There are three maps; one for Risk Category II, one for Risk Categories III and IV, and one for Risk Category I. Table 2-5 shows the Risk Categories, probability of exceedance in 50 years, and the MRI given by ASCE 7-10, Section 26.5. For locations where the wind speed cannot be determined through inspection of the ASCE 7 maps, the Applied Technology Council (2012) has provided a wind speed by location calculator (http://www.atcouncil.org/windspeed/index.php).

Table 2-5. Ultimate Level Wind Speeds in ASCE 7-10

Risk Category	Probability of Exceedance in 50 Years	MRI (yrs)
I	15%	300
II	7%	700
III and IV	3%	1700

It can be seen from the table that the MRI for strength design varies between 300 years and 1700 years. Typical buildings (those whose failure would not pose a significant risk for economic loss or to human life) are classified as Risk Category II, with an MRI of 700 years. This is a high MRI, and is appropriate for strength design. However, in the context of serviceability design, the 700-year MRI is excessively conservative.

ASCE 7 provides no guidance on loads to be used in serviceability design. However, other codes or methodologies have attempted to standardize loads and their associated return intervals, especially in the context of serviceability design for seismic events and performance based

earthquake engineering. For example, the PEER tall building guidelines (PEER 2010) specify an MRI of 43 years, and the ICC performance code (ICC 2012) gives an MRI of 72 years.

There is a general consensus in the literature that it is appropriate to use wind loads for serviceability design that are lower than wind loads for strength design. Various sources give different MRIs for serviceability, but a commonly suggested return period is 10 years. The 10-year MRI is reasonable in part due to the fact that it roughly equates to the average length of one tenancy, which is approximately 8 years (Tallin and Ellingwood 1984). Charney (1990b), Griffis (1993), and the ASCE Task Committee on Drift Control of Steel Building Structures (1988) also recommend a 10-year MRI for wind drift serviceability design. Furthermore, AISC Design Guide 3 suggests using the 10-year wind speed "due to the non-catastrophic nature of serviceability issues" (West et al. 2003). Despite the various 10-year MRI recommendations, many design engineers continue to use longer return periods. Only 47% of respondents to the latest wind drift survey reported using a 10-year MRI for wind loads, and the rest used either a 50- or 100-year MRI (Charney and Berding 2007).

After the return interval is selected the wind speeds associated with that return interval must be determined. There are different methods for accomplishing this task. The 2005 edition of ASCE 7 included a table (Table C6-7) with factors to convert between return periods. For example, to convert a wind speed from a 50-year MRI to a 10-year MRI, the table provides a factor of 0.84. Using this factor, a 50-year wind speed of 90 mph becomes a 10-year wind speed of 76 mph. Because the wind pressures are proportional to the square of the wind speeds, this conversion results in a 10-year wind pressure equal to 71% of the 50-year wind pressure (i.e. $0.84^2 = 0.706$).

The table contains separate conversion factors for hurricane wind speeds and for Alaska. The values given in the table are based on Eq. 2.11 (Peterka and Shahid 1998):

$$f_R = 0.36 + 0.10\ln(12R) \qquad (2.11)$$

where:

f_R = conversion factor from MRI = 50 years to MRI = R

R = desired MRI (e.g. 10 years)

Rosowsky (1995) presents a different set of factors for converting from a 50-year MRI. Table 2-6 presents Rosowsky's factors beside the factors given in ASCE 7-05 (note that for MRIs below 5 years, Eq. 2.11 is used to calculate the ASCE 7-05 MRI conversion factors).

Table 2-6. Non-hurricane MRI Conversion Factors

MRI (yrs)	Rosowsky	ASCE 7-05
0.5	0.62	0.54
1	0.67	0.61
2	0.72	0.68
5	0.80	0.78
10	-	0.84
25	0.94	0.93
50	1.00	1.00
100	1.07	1.07

The 2010 edition of ASCE 7 eliminates the 2005 approach of using conversion factors and instead provides wind speed maps (Figures CC-1 through CC-4) for potential serviceability MRIs (10-, 25-, 50-, and 100-year). Using Fig. CC-1 (the US wind speed map for a 10-year MRI) yields a 10-year wind speed of 76 mph for the same region of the country associated with a 50-year wind speed of 90 mph. This 76 mph wind speed is the same as the wind speed calculated using the conversion factor of 0.84. The conversion factors can still be utilized for MRIs not included in Figures CC-1 through CC-4.

2.4.2 Wind Hazard Curves

A hazard curve presents information about the likelihood of some hazard occurring. For example, a typical wind hazard curve will plot wind pressure against the return period (the inverse of the frequency of occurrence). In Figure 2-6 five wind hazard curves are shown for five different US cities. The plots were generated using the ASCE 7-10 wind speeds with the pressures calculated for select MRIs (10-, 25-, 50-, 100-, 300-, and 700-year) and no modifications were made to the pressures to account for exposure, topography, or elevation. As expected due to its location on the hurricane coast, Charleston experiences the highest wind pressures. The shape of the curve should also be considered. For example, Charleston and New Orleans have similar hazard curves up to approximately the 100-year mark and then significantly diverge for higher MRI values. This would indicate similar serviceability wind pressures (e.g. 10-year MRI) for the two cities, but considerably different ultimate wind pressures.

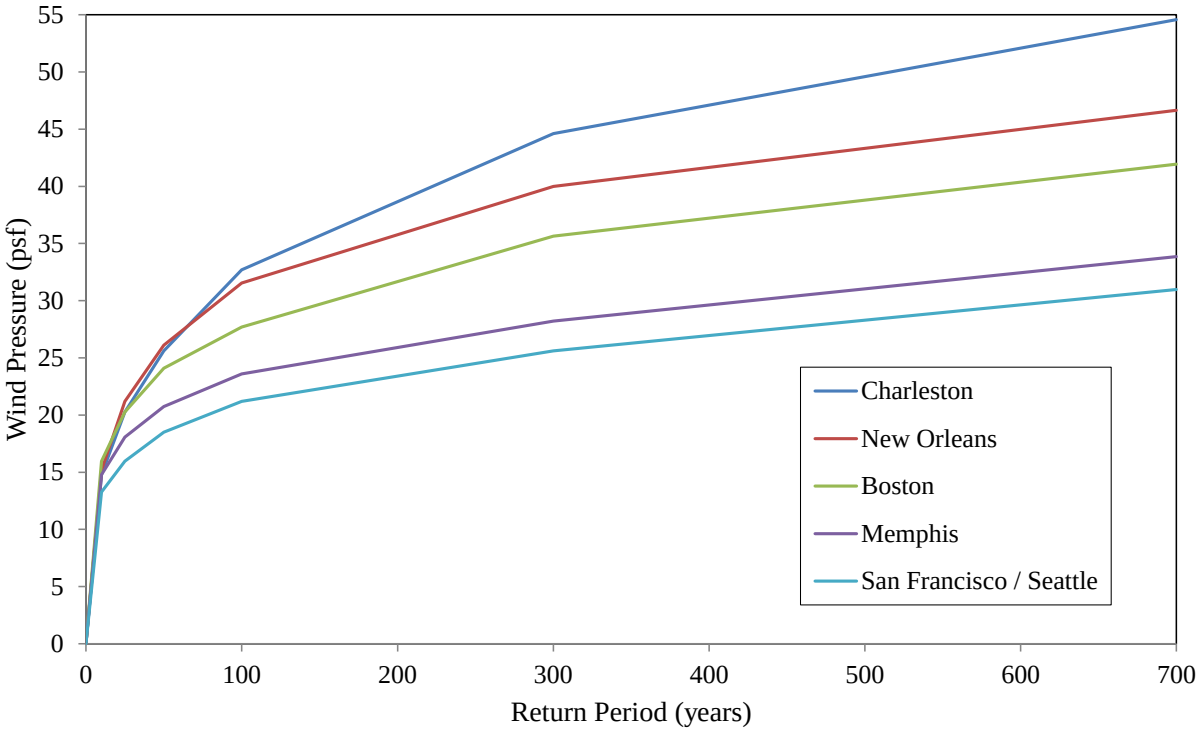

Figure 2-6. Wind Hazard Curves for Five US Cities

2.4.3 Hurricane and Non-hurricane Regions

The commentary of ASCE 7 (2010) provides an explanation of the development of wind speeds for hurricane regions. Wind speeds and mean recurrence intervals between hurricane and non-hurricane regions can vary dramatically. A consequence of this is that the MRI conversion factors are not the same between the two regions. ASCE 7-05 accounts for this by providing different factors for hurricane and non-hurricane regions. ASCE 7-10 builds the factors into the wind speed maps.

The hurricane wind speeds (for areas along the coast from Texas to Maine) were developed based on a Monte Carlo simulation (ASCE 2010). Compared to the hurricane wind speeds in ASCE 7-05, the newer wind speeds are lower, although the intense storm frequency actually increased. The Commentary of ASCE 7-10 describes the correlation between the wind speed map and the Saffir-Simpson Scale. The Saffir-Simpson scale, commonly cited in both research and the media, classifies a storm on a scale of Category 1 through Category 5, with the determining classification factor being wind speed. In order to better explain the relationship, ASCE 7-10 provides Table C26.5-4, which shows the equivalent design hurricane for Risk Category II structures in hurricane prone areas. For example, the basic wind speed in Galveston, Texas, correlates to a Category 4 hurricane. The basic wind speed in Key West, Florida, correlates to a Category 5.

Due to the fact that hurricane and non-hurricane regions have wind events of vastly different natures, it may be appropriate for a designer to select different MRIs and drift limits. Smith (2011) suggests using a lower return period with a tighter drift limit in hurricane regions. For

example, he suggests a 10- or 20-year MRI with a limit of H/600 for hurricane regions, and a 50- or 100-year MRI with a limit between H/500 and H/300 for non-hurricane regions.

2.5 Structural Modeling

2.5.1 Lateral Stiffness

Accurately determining the lateral stiffness of a building is essential to determining the deformation. The following generic equation (Charney 1990b) represents the different contributors to the overall lateral stiffness, K_S.

$$K_S = K_{SL} + K_{SG} + K_{SN} + K_G \qquad (2.12)$$

where:

K_{SL} = stiffness from the lateral load resisting system

K_{SG} = stiffness from the rest of the structural system (e.g. the gravity system)

K_{SN} = stiffness from the non-structural components (e.g. partitions)

K_G = stiffness from the P-Delta effect (usually negative).

These sources of lateral stiffness will be discussed in more detail in the following sections.

2.5.2 Sources of Deformation

It is important to account for all significant sources of deformation when calculating deformation in a structure. Studies by Charney (1990a) and Berding (2006) calculate the influence of various sources of deformation, including axial, flexural, and shear deformations of columns and beams in addition to panel zone deformations (those occurring in the beam-column joint region). These sources of deformation must be modeled appropriately in order to accurately calculate lateral

deflection. The following discussion of structural modeling, largely based on Berding's work (2006), examines methods to include various sources of deformation.

Charney (1990a) analyzed 45 steel structures, varying the number of bays, bay width, and number of stories. The structural systems were plane frames (10, 20, and 30 stories) and framed tubes (40 and 50 stories). The joint deformations alone made up 30.5%, on average, of the overall drift. Shear deformations made up 15.6%. Flexural deformations were most influential for shorter structures, while axial deformations were most influential for taller structures. In general, it was concluded that shear, axial, flexural, and joint deformations should *always* be included in calculations. It was recommended that code committees develop guidelines related to accurate drift calculations, because underestimating drift can lead to an underestimation of P-Delta effects.

The study conducted by Berding (2006) examined 27 planar frames and 18 framed tube structures. The story heights were held constant at 12.5 ft, and the number of stories, size and number of bays, and method of joint modeling were varied for each structure. All structural members were commonly used W sections. The applied lateral loads were calculated using Method 2 of ASCE 7-05 with a 10-year MRI (wind speed of 76 mph) and no load factor. Berding determined the relative contribution from flexural, axial, shear, and panel zone deformations. He concluded that each of these sources of deformation should always be included, for all building heights and widths. In general, drift in slender buildings tends to be more influenced by axial deformations, while stockier buildings are more influenced by flexural deformations. The influence of shear deformations held relatively constant, between

approximately 9% and 16%. Shear deformations were slightly higher in the framed tube structures than the planar frame structures. The contribution from panel zone deformations was shown to be very significant, varying between approximately 16% and 39%. These sources of deformation will be discussed in more depth later.

From these studies it is recommended that in order to accurately model a structure to calculate drift all significant sources of deformation should be included. Given the quickness with which the state of the practice is increasing alongside computing power, this is a reasonable recommendation. In fact, Berding and Charney (2007) point out that with many current structural analysis programs all sources of deformation are included by default. For example, SAP 2000 requires a property modifier to be used in order to effectively eliminate a particular source of deformation (such as artificially increasing the cross-sectional area to eliminate axial deformations). In this case, the full stiffness matrix will still be constructed and so no computational time is saved.

2.5.3 Shear Deformations

Axial and flexural deformations are generally well understood. Axial deformations are relatively easy to calculate, and flexural deformations are included in simple beam theory, which ignores shear deformations. As demonstrated above, shear deformations are a significant source of overall deflection and should always be included in a structural model.

When modeling frame structures, the shear area used to calculate deformations can be defined in multiple ways. The most common definition for effective shear area is the gross cross-sectional

area divided by κ, the form factor. For a rectangle the form factor is typically taken as 1.2. For a wide flange shape loaded about its strong axis, the form factor is typically defined as follows:

$$\kappa = \frac{A_g}{(d - t_f)t_w} \qquad (2.13)$$

where:

A_g = gross cross-sectional area

d = total depth of the cross-section

t_f = flange thickness

t_w = web thickness

The above equation defines the effective shear area as the web thickness times the distance between the centers of the flanges. This is a reasonable definition and is recommended by Charney et al. (2005) to be used to determine shear deformations in all sections except the stockiest (e.g. heavy W14s). Many computers program use this definition, or a variant of it. SAP2000 (Computers and Structures 2009a) defines the effective shear area in major axis bending as the *total depth* times the web thickness (i.e. $t_w d$). In weak axis bending, SAP2000 uses an effective shear area of five-thirds times the area of one flange (i.e. $5/3 t_f b_f$).

For stocky sections Eq. 2.12 breaks down. For these shapes it is recommended that the following equation be used (Cowper 1966):

$$\kappa = \frac{(12 + 72m + 150m^2 + 90m^3) + 30n^2(m + m^2)}{10(1 + 3m)^2} \qquad (2.14)$$

where:

$$m = \frac{2b_f t_f}{dt_w}$$

$$n = \frac{b_f}{d}$$

d = distance between the centers of the flanges

In Cowper's original paper he described d as the total depth of the cross-section. However, it is defined here as the center-to-center flange distance based upon the recommendation of Charney et al. (2005). Furthermore, Cowper's original equation also contained Poisson's ratio, ν. Setting Poisson's ratio equal to zero yields Eq. 2.13 and the effect is found to be negligible (compared to ν = 0.30). Given these recommendations, it is not unreasonable for commercial software to include Cowper's equation for determining the form factor.

2.5.4 Connection Deformations

Deformations within the beam-column connection region (also called panel zone deformations) contribute a significant amount to the overall drift of a structure (Berding found that panel zone deformations constitute between 16% and 39% of the total drift). There are essentially five panel zone models (Berding 2006):

- clearspan (rigid joint)
- centerline model (flexible joint)
- partial rigid model (some flexibility)
- mechanical joint model
- frame model.

Various researchers have documented the significance of panel zone deformations, and have compared and developed models to represent these deformations. An accurate model will be able to capture the complex behavior within the panel zone: axial, flexural, and shear deformations.

Léger et al. (1991) compared five models and developed a three-DOF frame joint element to represent the panel zone. Charney and Pathak (2008a) compare two mechanical joint models (Krawinkler Joint, Scissors Joint), a frame model (Fictitious Joint), and a detailed 3D finite element model. Lui and Wai-Fah (1986) developed a simple model and compared it to experimental results, as well as analyzing a simple frame to illustrate the importance of properly accounting for panel-zone deformations. Kato et al. (1988) summarize much of the research up to the time of their paper and present a model that accounts for shear deformations, but not axial or flexural.

In general, the consensus is that the clearspan model is unconservative and unfit as a representation of the behavior of the connection. It assumes that there is no deformation within the panel zone (i.e. the panel zone is infinitely rigid). The centerline model, on the other hand, assumes the joint is flexible. It will overestimate flexural deformations, but ignore shear deformations. The two will somewhat offset each other, resulting in a more accurate model than the clearspan model. The centerline model is recommended for use when the knowledge or resources are not available for a more robust approach (Charney and Pathak 2008a), although it can be unconservative in some circumstances.

The partial rigid model assigns some flexibility to the panel zone. This is done through the use of a rigid end zone factor, Z (Berding 2006). See Figure 2-7. The value of Z varies between zero (making it the centerline model) and one (making it the clearspan model). A value between zero and one assigns partial flexibility to the panel zone. Léger et al. (1991) suggest $Z = 0.5$ as a reasonable value for analysis. Many commercially available programs have the ability to model

partially rigid connections. However, the partially rigid model is less conservative than the centerline model and its use should be well understood before application.

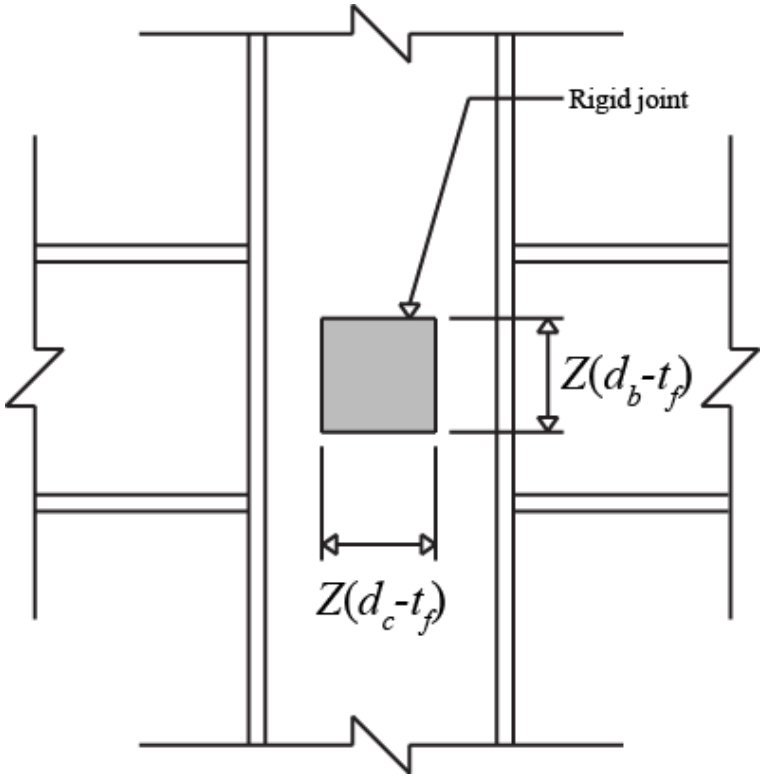

Figure 2-7. Partially Rigid Panel Zone Model

Mechanical joint models are more accurate but require more knowledge and resources to implement. Two common mechanical models are the Krawinkler Joint (KJ) and the Scissors Joint (SJ). Both models consist of rigid links and rotational springs. The models do not include the effects of flexure in the panel zone. The Krawinkler Joint model (Krawinkler 1978), shown in Figure 2-8, contains rotational springs in opposite corners. In the top left corner is a rotational spring representing panel zone shear, while in the bottom right corner the rotational spring represents column flange bending.

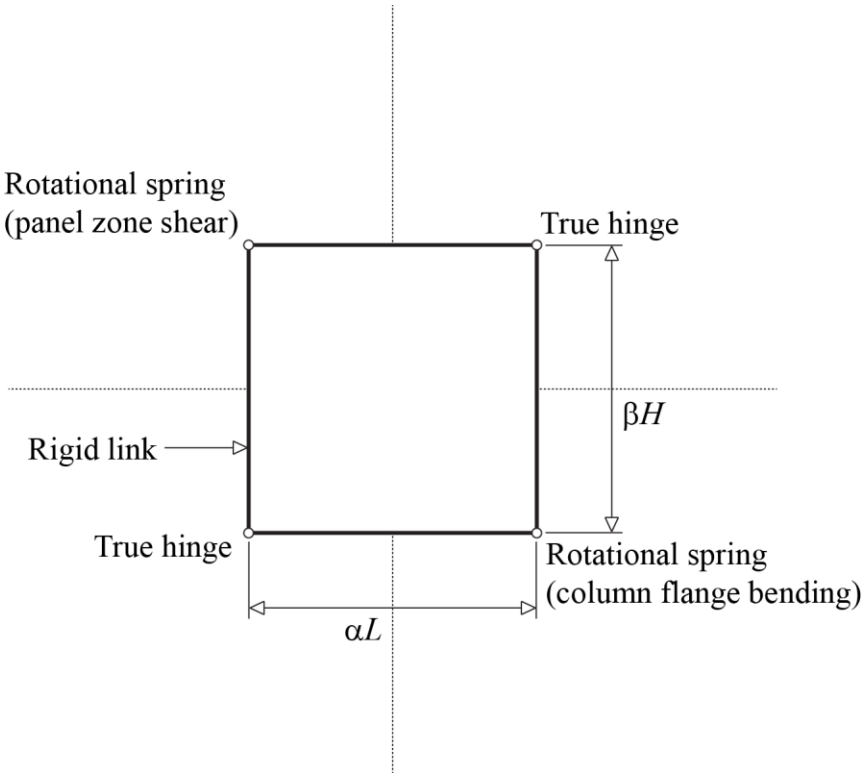

Figure 2-8. Krawinkler Joint Model

The Scissors Joint model (Figure 2-9) also uses rigid links and a rotational spring to model the panel zone. However, the Scissors Joint requires only four DOF, while the Krawinkler Joint requires twenty-eight. This is a significant computational advantage, but it should be noted that the Scissors Joint does not model true panel zone behavior as well as the Krawinkler Joint.

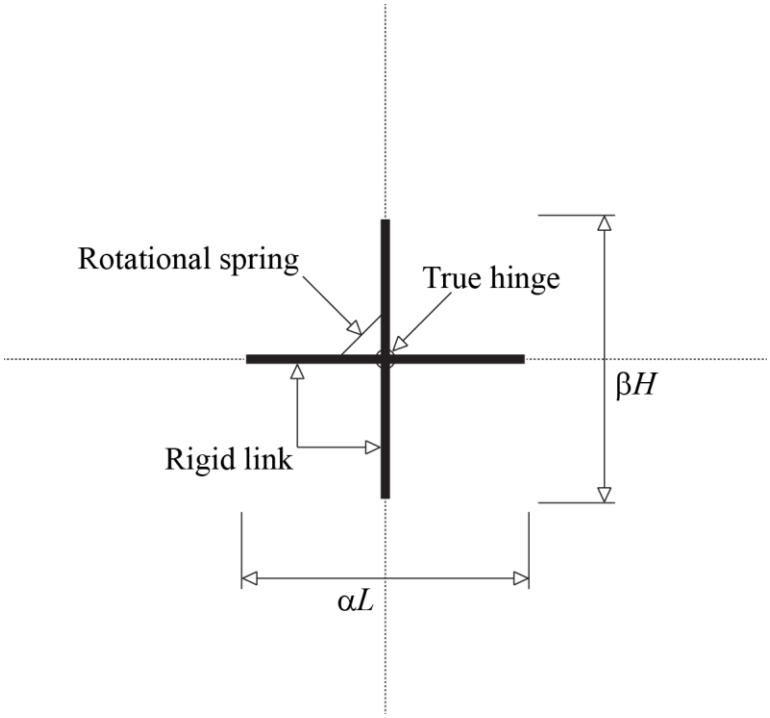

Figure 2-9. Scissors Joint Model

The following equations can be used to calculate the required stiffness of the rotational springs representing the panel zone shear in the KJ and SJ models (Charney and Pathak 2008a). For the Krawinkler Joint model:

$$K_{KJ} = \alpha L \beta H t_p G \qquad (2.15)$$

where:

K_{KJ} = required rotational spring stiffness for KJ model (shear panel stiffness only)

$$\alpha = \frac{d_{Ce}}{L}$$

$$\beta = \frac{d_{Be}}{H}$$

L = length of beam

H = height of the column

d_{Ce} = effective column depth (distance between flange centers)

d_{Be} = effective beam depth (distance between flange centers)

t_p = shear panel thickness (including doubler plates)

G = shear modulus

For the Scissors Joint model:

$$K_{SJ} = \frac{\alpha L \beta H t_p G}{(1-\alpha-\beta)^2} \qquad (2.16)$$

where:

K_{SJ} = required rotational spring stiffness for SJ model

Based on an analysis of both the KJ and SJ models, Charney and Marshall (2006) made some recommendations concerning their use. First, the rotational spring properties of the KJ model should never be used for the SJ model. Second, the KJ model is preferred over the SJ model, due to it being a better representation of the true panel zone behavior. Third, as the ductility demand increases, so too does the discrepancy between the KJ and SJ results. This means that the SJ model should only be used "for elastic structures or for systems where ductility demands are low."

The Fictitious Joint (FJ) model is a frame model. Readers interested in its derivation are directed to Charney and Pathak (2008a). Unlike the KJ and SJ models, the Fictitious Joint model includes flexural deformations in the panel zone. This is a significant advantage because flexural deformations can account for up to 15% of the total subassemblage drift. The KJ and SJ models, however, are widespread and it is useful to adapt them to include flexural deformations. This is shown in Charney and Pathak (2008b).

2.5.5 Connection Flexibility

A connection can be modeled in several ways. The two most common (and most convenient) ways are simple or fixed (e.g. infinitely flexible or infinitely rigid). In reality any connection will fall on a continuum somewhere between simple and fixed, exhibiting some qualities of each. In the 1988 ASCE survey, two-thirds of respondents reported that they do not consider connection flexibility (ASCE 1988). The task committee's opinion was that this reflected the state-of-the-art at the time (i.e. there were no rational methods to consider connection flexibility). In the 2006 update to the survey, fifty one percent of respondents used semi-rigid connections (Charney and Berding 2007).

The AISC Specification (2010) defines a simple connection as one which "transmits negligible moment." It breaks moment connections into two categories: fully restrained (FR) and partially restrained (PR). A fully restrained connection "transfers moment with negligible rotation" while a partially restrained connection also transfers moment, but with significant rotation. For a FR connection, the AISC Manual describes an alternative called a flexible moment connection (FMC), which is considered a simple connection for gravity loads and a FR connection for lateral loads (AISC 2010). Parts 11 and 12 of the Manual describe PR and FR moment connections.

2.5.6 Gravity System

The gravity load resisting system contributes some amount of stiffness to the lateral load resisting system. The structural engineer may separate the systems for design purposes, but in reality the two behave together. In some cases the contribution of the gravity system is small and can be ignored, but in other cases it is significant. It is up for debate whether the gravity system

should always be included in lateral load analysis. Charney and Berding (2007) emphasize that the gravity system's contribution to lateral stiffness may be negligible "for taller stiffer structures, but may be important in low rise buildings. For low rise buildings in particular, the rotational stiffness of the simple framing connections may contribute significantly to the lateral stiffness of the structure." In general, the stiffness contribution from the gravity resisting system should be included whenever the engineer believes it may be significant.

AISC Design Guide 8 (Leon et al. 1996) and ASCE 41 (ASCE 2013) can be used to determine the moment-rotation relationship of a steel connection. The guide should be employed to calculate the stiffness of components of the structural system which are not included in the main lateral force resisting system.

2.5.7 Floor Diaphragms

A floor diaphragm can be modeled in a number of ways. In the simplest sense a floor diaphragm is classified as either rigid or flexible. A rigid diaphragm is computationally the easiest approach because it eliminates a number of degrees of freedom. It also allows the lateral load to be proportioned based on stiffness (e.g. a wall that is twice as stiff as another wall will receive twice the load). A flexible diaphragm, on the other hand, distributes the lateral load based on tributary area. ASCE 7 Chapter 12 (Seismic Design Requirements) gives definitions for flexible and rigid diaphragms. A flexible diaphragm is untopped steel decking or wood panels (provided it meets at least one condition in Section 12.3.1.1). A rigid diaphragm is a "concrete slab or concrete filled metal deck with span-to-depth ratios of 3 or less" in structures with no horizontal irregularities (ASCE 2010).

The decision to model a diaphragm as rigid or flexible can have an important impact on the calculated lateral stiffness of a structure, because it determines the distribution of lateral load. In order to most accurately account for the effects of the diaphragm flexibility, the diaphragm should be modeled as semi-rigid, meaning it exhibits qualities of a flexible and rigid diaphragm. To do this the engineer can employ the finite element method.

2.5.8 Non-Structural Components

An often overlooked source of lateral stiffness is the contribution of non-structural components (NSC). In the 2006 ASCE wind drift survey update, only 21% of respondents sometimes include the stiffness of non-structural components (Charney and Berding 2007). Li et al. (2010) conducted a survey of fifteen high-rise structures in Australia, Taiwan, and mainland China. After speaking with the engineers of the various buildings, it was observed that there was very little effort given to incorporating the effects of NSCs on the building stiffness at service level loads. Non-structural components are ignored for a variety of reasons. Common motives include lack of experience with the materials by the engineer, lack of knowledge concerning the specifics of the NSCs design (location, quantity, etc.) as provided by the architect, and a belief that the contribution to lateral stiffness by the NSCs is negligible. There is also the rationale that at the strength limit state the non-structural components are likely to be severely damaged (meaning they have little ability to resist lateral loads). While this may be true at the strength limit state, at the serviceability limit state the influence of non-structural components should not be ignored. This is especially true for the case when the intention of the serviceability check is to prevent

damage to non-structural components. If the NSCs are designed to be undamaged, then it is logical that their stiffness contributions should be included.

There are several advantages to accounting for non-structural components. One advantage is economic gain, since including the extra source of stiffness could allow for smaller member cross-sections. A second advantage is the increased accuracy of the predicted response of the building (e.g. period of vibration) with respect to the measured response (Berding 2006).

Negro and Verzeletti (1998) conducted experiments on a four story reinforced concrete frame (bare frame and full frame). The lateral stiffness of the full frame was found to be 2.6 times higher than the lateral stiffness of the bare frame. Su et al. (2005) conducted a more realistic study, examining the influence of NSC (partition walls, external walls, parapet walls, and precast façade walls) on the lateral stiffness at service level loads. Three buildings were examined (14, 15, and 41 stories) and their natural frequencies measured (using ambient vibration tests). Finite element (FE) models were created with ETABS for each structure (for both the bare frame and the full frame). The full frame FE models included the effects of modifying the concrete elastic modulus (*E*), NSCs, secondary beams, and flexible diaphragms (using flexible slab elements). Table 2-7 summarizes the calculated periods for each of the three buildings. Note the remarkable precision with which the FE model predicts the full frame periods, relative to the measured periods. It is also important to note the large discrepancies between the bare frame and the full frame periods. This indicates the importance of including the effects of, among other things, NSCs. The lateral stiffness of the buildings was determined for the bare frames and full frames. The ratios of the full frame to bare frame stiffness were large, varying between 4.0 and 11.1,

with an average around 7.0. This means that, on average for these three buildings, the full-frame stiffness was 7 times greater than the bare frame stiffness.

Table 2-7. Influence of NSCs on Fundamental Period (Su et al. 2005). Used under fair use, 2013.

		Fundamental Period (sec)		
	Vibration Direction	Bare Frame	Full Frame	Measured
15-Story	*x*	1.22	0.58	0.60
	y	1.59	0.56	0.57
	Torsional	0.97	0.45	0.42
14-Story	*x*	1.88	0.55	0.56
	y	1.51	0.59	0.58
	Torsional	1.61	0.36	0.38
41-Story	*x*	2.61	1.25	1.28
	y	2.77	1.38	1.39
	Torsional	2.62	1.55	1.54

The two broad categories of non-structural components that are generally thought to have the greatest influence on lateral stiffness are non-structural walls and cladding.

2.5.8.1 Non-structural Walls

Non-structural walls are typically either masonry infill or veneer walls. Masonry infill walls can be constructed of a variety of materials, including concrete masonry units and brick. As previously discussed, research by Su et al. (2005) and others (Kose and Karslioglu 2011) has demonstrated the significant influence of masonry infill walls on the lateral stiffness of a structure. The ratio of the stiffness of the full frame to the bare frame varies between 1.2 and 50, according to a summary presented by Su et al. An analytical model which substitutes an equivalent diagonal compression strut (similar to a braced frame) for the infill wall was proposed by Holmes (1961). This model was used by Li et al. (2011) to construct a finite element model in

which it was determined that adding the effects of infill walls to a bare frame model increased the stiffness of the model by 60%.

Despite the apparent significance of infill walls and the ability to represent their effects with Holmes' strut model, many engineers have been reluctant to include infill walls in the structural model. This is partly due to the fact that infill wall construction is not specified by the engineer, and construction practice in the field can vary significantly from wall to wall, making the stiffness of the wall difficult to quantify. Furthermore, the location and makeup of walls can change during design, construction, and after the building's completion. These issues make it nearly impossible for the engineer to reliably determine the location or stiffness of infill walls over the lifetime of a structure. Keeping these problems in mind, it is still important that the effects of the infill walls be included in the design process. Serviceability issues are usually not life-safety related, and so excessive conservatism is not warranted in most cases.

It is also important to include veneer walls in the structural model. A veneer wall is "drywall, plywood, plaster board or other similar materials supported by wood or metal studs" (Berding 2006). There has been much research concerned with quantifying the stiffness and strength of veneer walls. Algan (1982) summarizes much of this research. More recently, Restrepo and Bersofsky (2011) conducted racking tests on gypsum sheathed metal stud walls. From these tests the lateral stiffness per unit length of wall was determined. Similar tests have been conducted on other materials. Using the stiffness parameters derived from these tests, the nonstructural partition walls can be included in the model. This can be accomplished through an equivalent diagonal element, or something similar to a shell element.

2.5.8.2 Cladding

Cladding can be a significant source of lateral stiffness for a structure, provided that it is detailed adequately. Often the engineer attempts to detail the cladding such that it will not interact with the structure. This simplifies the design process because the cladding's stiffness can be ignored. However, this is conservative, because the cladding can be utilized for lateral stiffness as well as energy dissipation (Pinelli et al. 1995). Furthermore, many times the engineer believes that the cladding is isolated from the structure when, in reality, it is not. This is especially true at the ultimate limit state when large drifts are present, but can also be true at the serviceability limit state.

Much of the research on the effects of cladding on the structural system has been conducted in the realm of earthquake engineering. In general, the research has found that cladding has a significant effect and should not be ignored, especially in terms of lateral stiffness and energy dissipation (Palsson et al. 1984, Goodno and Palsson 1986).

2.5.9 Second Order Effects

Second order (or P-Delta) effects are the effects "on shear and moments of structural members due to the action of the vertical loads induced by horizontal displacement of the structure resulting from various loading conditions" (ASCE 2010). In the 1988 ASCE wind drift survey, 72% of respondents reported considering second order effects in their designs. The task committee recommended that *all* buildings consider second order effects, despite the fact that 40% of respondents indicated that for 1-3 story buildings they would ignore second order effects.

In the recent update to the survey, 50% of respondents usually include P-Delta effects, with the majority using procedures included in commercial software (Charney and Berding 2007).

P-Delta effects can be a significant source of drift in a structure. Berding and Charney (2007) found that including P-Delta effects increased drift 17% over a model without the effects. Berding (2006) recommends that P-Delta effects always be included, given the ease with which today's software can model them. Berding suggests using the survey live loads given by ASCE 7 (2005; 2010) for P-Delta analyses, given that design live loads are unreasonable for serviceability considerations because they far exceed the actual expected live load (Ellingwood and Culver 1977). Léger et al. (1991) found that including P-Delta effects increased drift by approximately 30% on average, compared to their models without P-Delta effects.

There are two general components of second order effects: P-δ (the loadings acting through member deflections) and P-Δ (the loads acting through frame deflections). One of the most popular numerical approaches to determining second order effects is the incremental load approach. This technique divides the applied load into increments, and steps through each increment until the full load is applied. At the end of each increment the deformed geometry of the structure is calculated and becomes the undeformed geometry for the next step (Chen and Lui 1987). AISC (2010) provides three approaches in the Specification (Section C1 and Appendix 7) to provide stability. The first approach is the *direct analysis method* and is the most complete approach given. Using this method, the effective length of the members is equal to the member length (i.e. K = 1.0). A second order analysis must be performed. The second approach is the *effective length method*. This method uses effective length factors, K, with notional loads equal

to at least 0.2% of the applied gravity loads at each story. With this approach, a second order analysis must also be performed. The third approach, the *first-order analysis method*, is the simplest approach. Second order effects are accounted for by applying notional loads of at least 0.42% of the gravity loads at each story. No second order analysis is required for this approach. When it is required, AISC allows any rational method of second order analysis to be used. This includes a general analysis (computer analysis) or an amplified first order analysis (such as the B_1/B_2 approach).

2.5.10 Other Effects

There are various other sources of lateral stiffness and deformation that may need to be included in an accurate structural model. Su et al. (2005), for example, included not only non-structural components, but also secondary beams, which are usually excluded from a lateral model. Engineering judgment should be used to determine other necessary effects, such as foundation flexibility and composite floor action. Further discussion on modeling composite beams and girders can be found in Schaffhausen and Wegmuller (1977), and Vallenilla and Bjorhovode (1985).

2.6 Optimization and Redesign

If a structure is found to be deficient (either the design fails to meet the performance requirements or it is found to be overly conservative) the designer has many options for methods of redesign. Many of the most popular methods for deciding which members to modify rely on the principle of virtual work and are implemented in commercial structural analysis software (Computers and Structures 2009b, Bentley 2013).

The use of procedures based on virtual work is further discussed in Charney (1991), Baker (1990), Charney (1993), and Velivasakis and DeScenza (1983). As a general approach, these procedures calculate each member's contribution to the overall lateral drift of a frame by determining the strain energy in the member. Using this method, the members with the highest contributions can be made larger, and the members with the lowest contributions can be made smaller. Chan et al. (2010) describe the optimization of a 40-story concrete shear wall building, in which the optimization procedure converges on a design after 12 iterations. The optimization algorithm allowed for target drift limits at each story (a limit of H/500 was employed).

2.7 References

Wind Speed by Location. Applied Technology Council 2012. Available from http://www.atcouncil.org/windspeed/index.php.

AISC. 2010. Steel Construction Manual (Fourteenth Edition). American Institute of Steel Construction.

Algan, Bekir Bulent. 1982. *DRIFT AND DAMAGE CONSIDERATIONS IN EARTHQUAKE-RESISTANT DESIGN OF REINFORCED CONCRETE BUILDINGS*. 8302791, University of Illinois at Urbana-Champaign, United States -- Illinois.

Ang, Alfredo Hua-Sing, and Wilson H Tang. 2007. *Probability concepts in engineering: emphasis on applications in civil & environmental engineering*: John Wiley & Sons Inc.

ANSI/AISC. 2010. Specification for Structural Steel Buildings (ANSI/AISC 360-10). American Institute of Steel Construction.

ASCE. 1988. "Wind Drift Design of Steel‐framed Buildings: State‐of‐the‐art Report." *Journal of structural engineering (New York, N.Y.)* no. 114 (9):2085-2108.

ASCE. 2005. Minimum design loads for buildings and other structures. Reston, VA: American Society of Civil Engineers.

ASCE. 2010. Minimum design loads for buildings and other structures. Reston, VA: American Society of Civil Engineers.

ASCE. 2013. Seismic Evaluation and Retrofit of Existing Buildings. Reston, VA: American Society of Civil Engineers.

Baker, William F. 1990. Sizing techniques for lateral systems in multi-story steel buildings. Paper read at Proceedings of 4th World Congress on Tall Building: 2000 and Beyond.

RAM Frame, Exton, PA.

Berding, D., and F.A. Charney. 2007. The Effect of Modeling Parameters on the Wind Drift of Steel Frame Buildings. Paper read at New Horizons and Better Practices.

Berding, Daniel Christopher. 2006. *Wind drift design of steel framed buildings an analytical study and a survey of the practice*. M s, Civil & Environmental Engineering, Virginia Polytechnic Institute and State University, Blacksburg, Va.

Chan, C. M., and M. F. Huang. 2010. Optimal wind resistant performance-based design of tall buildings. Paper read at Structures Congress 2010: 19th Analysis and Computation Specialty Conference, at Orlando, Florida.

Chan, CM, MF Huang, and KCS Kwok. 2010. "Integrated wind load analysis and stiffness optimization of tall buildings with 3D modes." *Engineering Structures* no. 32 (5):1252-1261.

Charney, FA. 1990a. Sources of elastic deformation in laterally loaded steel frame and tube structures. Paper read at Proceedings of the World Congress on Tall Buildings.

Charney, FA. 1991. The use of displacement participation factors in the optimization of drift controlled buildings. Paper read at Proceedings of 2nd conference on Tall Buildings in Seismic Regions, 55th Regional Conference, Los Angeles, CA.

Charney, FA, and J. Marshall. 2006. "A comparison of the Krawinkler and scissors models for including beam-column joint deformations in the analysis of moment-resisting steel frames." *ENGINEERING JOURNAL-AMERICAN INSTITUTE OF STEEL CONSTRUCTION* no. 43 (1):31.

Charney, Finley A. 1993. Economy of steel frame buildings through identification of structural behavior. Paper read at Proceedings of the Spring 1993 AISC Steel Construction Conference.

Charney, Finley A. 1990b. "Wind drift serviceability limit state design of multistory buildings." *Journal of Wind Engineering & Industrial Aerodynamics* no. 36 (1-3):203-212.

Charney, Finley A., and Daniel C. Berding. 2007. "Analysis and Commentary on the Results of a Nationwide State-of-the-Practice Survey on Wind Drift Analysis and Design." In *New Horizons and Better Practices*, 1-10.

Charney, Finley A., Hariharan Iyer, and Paul W. Spears. 2005. "Computation of major axis shear deformations in wide flange steel girders and columns." *Journal of Constructional Steel Research* no. 61 (11):1525-1558.

Charney, Finley A., and Rakesh Pathak. 2008a. "Sources of elastic deformation in steel frame and framed-tube structures: Part 1: Simplified subassemblage models." *Journal of Constructional Steel Research* no. 64 (1):87-100.

Charney, Finley A., and Rakesh Pathak. 2008b. "Sources of elastic deformations in steel frame and framed-tube structures: Part 2: Detailed subassemblage models." *Journal of Constructional Steel Research* no. 64 (1):101-117.

Chen, Wai-Fah, and E. M. Lui. 1987. *Structural stability: theory and implementation*. New York: Elsevier.

Ciampoli, M, F Petrini, and G Augusti. 2011. "Performance-based wind engineering: towards a general procedure." *Structural Safety* no. 33 (6):367-378.

Computers and Structures, Inc. 2009a. CSI Analysis Reference Manual. Berkeley, CA.

SAP2000 14.0.0. CSI, Berkeley, CA.

Cowper, G. R. 1966. "The Shear Coefficient in Timoshenko's Beam Theory." *Journal of Applied Mechanics* no. 33:335-340.

Dymiotis-Wellington, Christiana, and Chrysoula Vlachaki. 2004. "SERVICEABILITY LIMIT STATE CRITERIA FOR THE SEISMIC ASSESSMENT OF R/C BUILDINGS."

Ellingwood, B., Allen, D., Elnimeri, M., Galambos, T., Iyengar, H., Robertson, L., Stockbridge, J., Turkstra, C. 1986. "Structural Serviceability: A Critical Appraisal and Research Needs." *Journal of Structural Engineering* no. 112 (12):2646-2664.

Ellingwood, Bruce R., and Charles G. Culver. 1977. "Analysis of Live Loads in Office Buildings." *Journal of the Structural Division* no. 103 (8):1551-1560.

FEMA. 2013a. Seismic Performance Assessment of Buildings: Volume 1 – Methodology. In *FEMA P-58-1*. Washington, D.C.

FEMA. 2013b. Seismic Performance Assessment of Buildings: Volume 3 – Supporting Electronic Materials and Background Documentation. In *FEMA P-58-3*. Washington, D.C.

Galambos, Theodore V., and Bruce Ellingwood. 1986. "Serviceability Limit States: Deflection." *Journal of Structural Engineering* no. 112 (1):67-84.

Goodno, B.J., and H. Palsson. 1986. "Analytical studies of building cladding." *Journal of structural engineering* no. 112 (4):665-676.

Griffis, L. G. 1993. "Serviceability limit states under wind loads." *Engineering Journal* no. 30 (1):1-16.

Griffis, Lawrence, Viral Patel, Susendar Muthukumar, and Sridhar Baldava. 2012. A framework for performance-based wind engineering. Paper read at Proceedings of the ATC-SEI Advances in Hurricane Engineering Conference.

Hamburger, Ronald O. 2006. "The ATC-58 project: development of next-generation performance-based earthquake engineering design criteria for buildings."

Holmes, M. 1961. Steel frames with brickwork and concrete infilling. Paper read at ICE Proceedings.

ICC. 2012. ICC Performance Code for Buildings and Facilities. Washington, D.C.: International Code Council.

Kato, B., W. F. Chen, and M. Nakao. 1988. "Effects of joint-panel shear deformation on frames." *Journal of Constructional Steel Research* no. 10 (0):269-320.

Kose, M. Metin, and Ozge Karslioglu. 2011. "Effects of infill walls on base responses and roof drift of reinforced concrete buildings under time-history loading." *The Structural Design of Tall and Special Buildings* no. 20 (3):402-417.

Krawinkler, H. 1978. "Shear in beam-column joints in seismic design of steel frames." *Engineering Journal* no. 15 (3).

Léger, P., P. Paultre, and R. Nuggihalli. 1991. "Elastic analysis of frames considering panel zones deformations." *Computers & Structures* no. 39 (6):689-697.

Leon, Roberto T., Jerod J. Hoffman, and Tony Staegar. 1996. *AISC Design Guide 8: Partially Restrained Composite Connections*. Chicago, IL: American Institute of Steel Construction.

Li, Bing, Graham L. Hutchinson, and Colin F. Duffield. 2011. "The influence of non-structural components on tall building stiffness." *The Structural Design of Tall and Special Buildings* no. 20 (7):853-870.

Li, Bing, Graham Leighton Hutchinson, and Colin Fraser Duffield. 2010. "Contribution of typical non-structural components to the performance of high-rise buildings based on field reconnaissance." *Journal of Building Appraisal* no. 6 (2):129-151.

Lui, Eric M., and Chen Wai-Fah. 1986. "Frame analysis with panel zone deformation." *International Journal of Solids and Structures* no. 22 (12):1599-1627.

Miranda, E. 2006. "Use of probability ‐ based measures for automated damage assessment." *The Structural Design of Tall and Special Buildings* no. 15 (1):35-50.

Miranda, E., Mosqueda, G. 2013. Seismic Fragility of Building Interior Cold-Formed Steel Framed Gypsum Partition Walls. Redwood City, CA: Applied Technology Council.

Moehle, J., and G.G. Deierlein. 2004. A framework methodology for performance-based earthquake engineering. Paper read at Proc. of 13th World Conference on Earthquake Engineering, at Vancouver, CA.

Negro, P., and G. Verzeletti. 1998. "Effect of infills on the global behaviour of R/C frames: energy considerations from pseudodynamic tests." *Earthquake engineering & structural dynamics* no. 25 (8):753-773.

NRCC. 2010a. National Building Code of Canada. Ottawa, Canada: National Research Council of Canada.

NRCC. 2010b. User's Guide - NBC 2010 Structural Commentaries (Part 4 of Division B). Ottawa, Canada: National Research Council of Canada.

O'Brien Jr, William C, Ali M Memari, Paul A Kremer, and Richard A Behr. 2012. "Fragility Curves for Architectural Glass in Stick-Built Glazing Systems." *Earthquake Spectra* no. 28 (2):639-665.

Palsson, H., B.J. Goodno, J.I. Craig, and K.M. Will. 1984. "Cladding influence on dynamics response of tall buildings." *Earthquake engineering & structural dynamics* no. 12 (2):215-228.

Paulotto, C., M. Ciampoli, and G. Augusti. 2004. Some proposals for a first step towards a Performance Based Wind Engineering. Paper read at Proc. First IFED-Int. Forum in Engineering Decision Making, Stoos, CH, www. ifed. ethz. ch.

PEER. 2010. Guidelines for Performance-Based Seismic Design of Tall Buildings. In *Report 2010/05*. Berkeley, CA: Pacific Earthquake Engineering Research Center.

Peterka, J.A., and S. Shahid. 1998. "Design gust wind speeds in the United States." *Journal of Structural Engineering* no. 124 (2):207-214.

Pinelli, J.P., J.I. Craig, and B.J. Goodno. 1995. "Energy-based seismic design of ductile cladding systems." *Journal of Structural Engineering* no. 121 (3):567-578.

Porter, K., R. Kennedy, and R. Bachman. 2007. "Creating fragility functions for performance-based earthquake engineering." *Earthquake Spectra* no. 23 (2):471-489.

Porter, KA, RP Kennedy, and RE Bachman. 2006. "Developing Fragility Functions for Building Components." *Report to ATC-58, Applied Technology Council, Redwood City, CA*.

Restrepo, José I., and Andrew M. Bersofsky. 2011. "Performance characteristics of light gage steel stud partition walls." *Thin-Walled Structures* no. 49 (2):317-324.

Rosowsky, David V. 1995. "Estimation of design loads for reduced reference periods." *Structural Safety* no. 17 (1):17-32.

Schaffhausen, R, and A Wegmuller. 1977. "Multistory rigid frames with composite girders under gravity and lateral forces." *AISC Engineering Journal, 2nd Quarter*:68-77.

Smith, Rob. 2011. Deflection limits in tall buildings-are they useful? Paper read at Structures Congress 2011, at Las Vegas, Nevada.

Su, R. K. L., A. M. Chandler, M. N. Sheikh, and N. T. K. Lam. 2005. "Influence of non-structural components on lateral stiffness of tall buildings." *The Structural Design of Tall and Special Buildings* no. 14 (2):143-164.

Tallin, Andrew, and Bruce Ellingwood. 1984. "Serviceability Limit States: Wind Induced Vibrations." *Journal of Structural Engineering* no. 110 (10):2424-2437.

Vallenilla, C, and R Bjorhovode. 1985. "Effective width criteria for composite beams." *Engineering Journal* no. 22 (4).

Velivasakis, Emmanuel E, and Robert DeScenza. 1983. Design optimization of lateral load resisting frameworks. Paper read at Electronic Computation (1983).

Wen, YK. 2001. "Reliability and performance-based design." *Structural safety* no. 23 (4):407-428.

West, Michael, James Fisher, and Lawrence Griffis. 2003. *Steel design guide 3: Serviceability design considerations for steel buildings*. 2nd ed: American Institute of Steel Construction.

3 Journal Article (Engineering Journal)

The preceding literature review is in support of the journal article submitted for publication to AISC's *Engineering Journal* titled "Recommended Procedures for Damage Based Serviceability Design of Steel Buildings."

Recommended Procedures for Damage Based Serviceability Design of Steel Buildings under Wind Loads

Kevin Aswegan[a], Finley A. Charney, Ph.D., P.E.[b], and Jordan Jarrett[a]

ABSTRACT

This paper provides a recommended procedure for nonstructural damage control of steel buildings under serviceability level wind loads. Unlike traditional procedures that provide a single drift limit under a given reference load, the recommended procedure provides a decision space that spans a range of wind hazards and associated damage states. Central to the procedure are the use of shear strain in nonstructural components as the engineering demand parameter and the use of component fragility as a reference for limiting damage.

Keywords: Wind, Drift, Serviceability; Damage, Fragility, Performance Based Engineering

BACKGROUND

During the design of a building the structural engineer is typically concerned with both strength and serviceability limit states. Design and detailing requirements for the strength limit states such as yielding, fracture, and buckling are prescribed in the applicable building codes. However, the same building codes do not provide prescriptive requirements for the serviceability limit states. This is largely due to the non-catastrophic nature of serviceability failures.

Instead of providing serviceability requirements, the codes take a performance-based approach wherein only the expectations of a successful design are provided. The AISC Specification (AISC, 2010) defines serviceability as "a state in which the function of a building, its appearance, maintenance, durability, and comfort of its occupants are preserved under normal usage." On the topic of drift, the specification states that drift "shall be evaluated under service loads to provide for serviceability of the structure, including the integrity of interior partitions and exterior cladding." ASCE 7-10 (ASCE, 2010) contains similar language, stating that "sufficient stiffness must be provided such that deflection, drift, and vibrations are limited to an acceptable level".

[a] Structural Engineering Graduate Student, Dept. of Civil Engineering, Virginia Tech, Blacksburg, VA
[b] Professor of Structural Engineering, Dept. of Civil Engineering, Virginia Tech, Blacksburg, VA

The lack of wind serviceability design standards has led to a wide variation in design practices across the United States. To assess the state of the practice, ASCE created, in 1984, the Task Committee on Drift Control of Steel Building Structures. The committee surveyed structural engineering firms and released its results in 1988 (ASCE, 1988). In general, the results from the survey showed that there was little consistency in terms of the selection of service level wind loads, the development of mathematical models of the structural system, the selection of appropriate drift measures, and the establishment of drift limits. A more recent survey, conducted in 2006 by the ASCE/SEI Committee on the Design of Steel Building Structures, found similar results (Charney and Berding, 2007). When asked to list the primary motivation for limiting drift, the respondents to the most recent survey reported, in the following order: to prevent structural damage (most common response), to prevent nonstructural damage, to control second order (P-Delta) effects, and to limit lateral accelerations. With the possible exception of P-Delta effects (which contribute to drift), these motivations are all serviceability considerations.

One approach to improving wind drift serviceability design would be to borrow from the concepts of performance based earthquake engineering, commonly referred to as PBEE, that are already in use for existing buildings through the provisions of ASCE 41-13 (ASCE, 2013) and that have been recommended for tall buildings (PEER, 2010). The PBEE concept is built around quantifying hazard intensity measures, engineering demand parameters, damage measures, and decision variables (cost, downtime, or casualties) at multiple limit states. In order to account for inherent uncertainties in the process, the PBEE methodology is supported by a probabilistic framework (Moehle and Deierlein, 2004). Various government supported efforts to develop a comprehensive PBEE procedure recently cumulated with the publication of the FEMA P-58 report (FEMA, 2013a) and related materials, including software.

The development and advancement of performance based wind engineering (PBWE) would logically follow closely that of PBEE. However, there are significant differences related to the wind and seismic hazards, the limit states that need to be considered, and the necessity (in seismic design) to explicitly include inelastic behavior associated with life-safety and collapse-prevention limit states. Paulotto, et al. (2004), Ciampoli, et al. (2011), and Griffis et al. (2012) proposed the adaptation of the PBEE framework to wind. Paulotto, et al. and Ciampoli, et al. provide probabilistic frameworks that incorporate the concepts of fragility. Fragility is also central to the FEMA P-58 PBEE procedure, as well as the procedure recommended in this paper.

Griffis, et al. propose multiple wind-related performance levels, dynamic nonlinear analysis of structures under wind loading, and the concept of allowing inelastic behavior at more severe wind limit states. Despite the various proposals, without a coordinated government-supported effort to develop PBWE, it has not gained, nor is it likely to achieve, the same level of usage as PBEE.

The purpose of this paper is to describe a damage-based method for the evaluation and design of steel structures subjected to serviceability level wind loads. While the proposed method falls short of PBWE as envisioned by the authors cited above, it does address three key issues: selection of appropriate wind loads, accurate definition and calculation of the damage measure, and selection of rational damage limits. Unlike other methodologies that rely on a single wind return period or a set of established drift limits, the procedure described in the remainder of this paper follows the basic principles on serviceability that were published in 1986 (Committee on Serviceability, 1986), which states:

> "*Serviceability guidelines need to be flexible and adaptable to different occupancies, use requirements, and techniques for integrating nonstructural components. The guidelines ought to be negotiable, within limits, between the engineer, architect, and building owner.*"

OVERVIEW OF PROCEDURE

The procedure is based on the computation and limitation of shear deformations in nonstructural components. Features of the procedure, described in much more detail later, are as follows:

1. The procedure is developed explicitly for the serviceability assessment of tier-type structures. This limitation is applicable because such buildings have numerous interior architectural partitions and exterior finishes that need to be protected from damage.
2. A broad wind hazard basis is used, wherein a range of mean recurrence intervals are considered.
3. The deformation that is controlled is shear strain in nonstructural components.
4. A 3-Dimensional mathematical model of the building is used to perform the structural analysis, and is calibrated to provide the best possible estimate of the damaging shear

strain deformations in the nonstructural components. A different model would likely be used to address strength limit states.

5. The limiting shear strain is based on the concept of structural fragility and the use of fragility curves. Such curves are based on laboratory testing of nonstructural components, and provide the probability of exceeding a given damage state (e.g. minor cracking of drywall partitions) given the computed shear strain.
6. The results of the serviceability analysis provide a broad basis for making decisions about controlling damage in nonstructural components, but fall short of providing quantitative information on the consequences of accepting some damage.

While the procedure could be expanded to consider other wind related serviceability limit states such as perception of motion, and to include structural damage, the current focus is on the control of damage in nonstructural components, such as interior walls and exterior walls and finishes. Damage under seismic loads could also be controlled using the same general procedure.

WIND LOADS

Current Wind Load Design Provisions

Buildings in the United States are designed for wind loads according to the provisions of ASCE 7. The current edition, ASCE 7-10 (ASCE, 2010), provides three methods for determining wind loads for the main wind-force resisting system of a building: the directional procedure, the envelope procedure, and the wind tunnel procedure. The wind tunnel procedure is generally the most accurate but also the most time-consuming and expensive. For the serviceability level wind loads, any of the allowed procedures is suitable, provided that an appropriate mean recurrence interval (MRI) is selected.

Mean Recurrence Interval (MRI)

The mean recurrence interval is the return period for a wind event. A 10-year MRI refers to a wind event that occurs, on average, once every 10 years. A shorter MRI corresponds to lower intensity wind loads, while a longer MRI corresponds to higher intensity wind loads. For Risk Category II buildings designed according to the provisions of ASCE 7-10, the MRI is 700 years. Risk Category I and III-IV buildings are designed using 300 and 1700 year MRIs, respectively.

Each of these risk-related MRIs represents ultimate strength level loading, and as such, the load factor on wind loads is 1.0. Service level wind speeds (as used in previous editions of ASCE 7) are generally in the range of 50 to 100 years. The wind loads based on these service level wind speeds must be factored up to strength level for the design of the main lateral load resisting system. It is important to note that "service" level wind speeds and "serviceability" are not synonymous. It was never the intent in ASCE 7 to use service-level loads for serviceability.

Various authors have recognized that the service level and particularly the ultimate level wind loads are overly conservative for serviceability considerations when traditional drift limits (in the range of $H/500$, where H is the story height) are used. For this reason, Tallin and Ellingwood (1984), Charney (1990b), and Griffis (1993) proposed serviceability MRIs of 8 to 10 years. This particular MRI range is approximately the length of the average tenancy in the US and the UK (Ellingwood and Culver, 1977). Additionally, AISC Design Guide 3 (West, et al., 2003) recommends a 10-year wind event for interstory drift checks.

Although many sources have suggested a 10-year MRI, it is recommended that a designer select a wind serviceability MRI based on the specific needs of the owner or other stakeholders relative to the use (risk category) of the building and the probability of and potential consequences of exceeding a particular damage limit state. Another factor in determining the appropriate MRI is the range and resolution of test data that has been used to establish damage limits. This important concept is discussed later in the paper in association with the use of component fragility as a damage indicator.

Recognizing the need to use a lower MRI for serviceability considerations, the commentary to Appendix C of ASCE 7-10 provides wind speed maps for 10-, 25-, 50-, and 100-year MRIs. Using the 10, 25, 50, and 100 year wind speed maps, a designer can select the appropriate wind speed and use the provisions of ASCE 7 to determine the serviceability wind loads. When a building site is located such that it is difficult to manually determine the wind speed with the ASCE 7 maps, an online tool developed by the Applied Technology Council (ATC, 2013) can be used. This tool, using the same data that was used to generate the ASCE 7 maps, will provide wind speeds for various MRIs given a physical address or latitude and longitude.

Wind and Seismic Hazard Curves

A hazard curve is a plot showing the relationship between a hazard measure (such as wind speed or wind pressure) and likelihood of occurrence. Figure 1 shows wind hazard curves for select cities across the United States. The vertical axis shows the velocity pressure (q_z in ASCE 7-10), assuming that the wind directionality factor (K_d), the velocity pressure exposure coefficient (K_z), and the topographic factor (K_{zt}) are each equal to 1.0. The likelihood of occurrence is represented by MRI on the horizontal axis.

The wind hazard curves contain valuable information relating to service and ultimate level wind loads. For the 10-year MRI the wind pressures are similar for the six cities shown, varying between 13.3 psf and 16.0 psf. Examining the wind pressures for one particular MRI, however, can be misleading. For example, in the cities of Charleston and Memphis the wind pressures due to the 10-year MRI are equal (14.8 psf). This is not the case, however, for higher MRIs. For the 700-year MRI (ultimate level wind loads), the wind pressure in Charleston significantly diverges from the wind pressure in Memphis. The difference is due to the fact that Charleston is located in the hurricane region of the United States. It should also be noted that due to the location of Charleston, New Orleans, and Boston along the hurricane-prone coast, where the mapped wind speed contours are tightly spaced, seemingly small changes in latitude or longitude between locations can lead to significant differences in speeds and wind pressures.

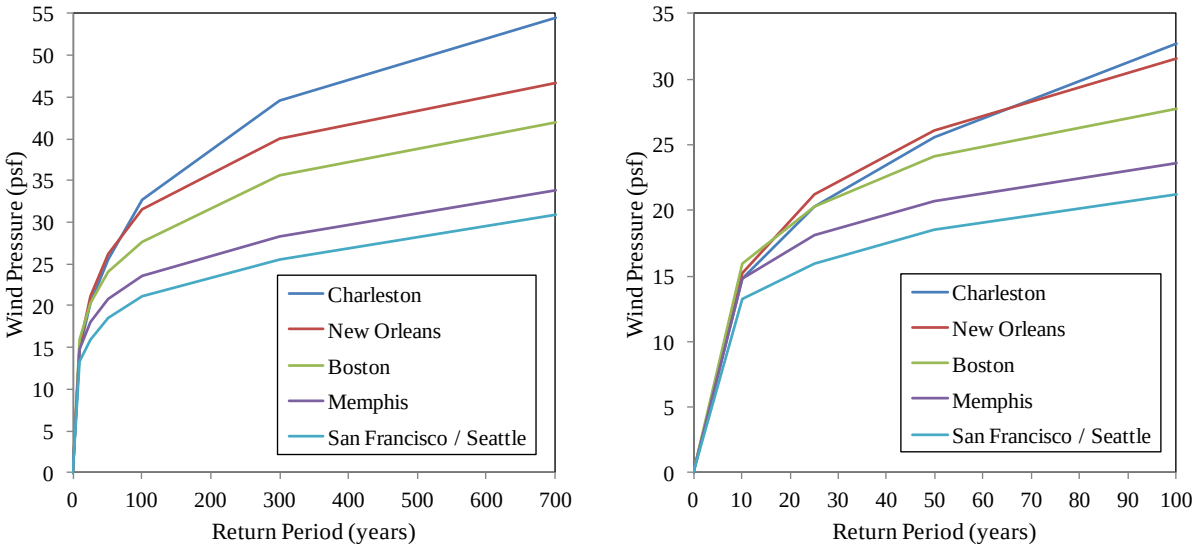

(a) Return Periods between 0 and 700 yrs (b) Return Periods between 0 and 100 yrs

Figure 1. Wind Hazard Curves for Select United States Cities

It is of some interest to compare the wind and seismic hazards, as well as to discuss the MRIs typically used for seismic serviceability. Figure 2 presents seismic hazard curves for the same six U.S. cities shown in Figure 1. These curves show 5% damped Site Class B-C boundary one-second spectral acceleration, plotted against MRI.

While the shapes of the wind hazard curves are similar for the cities indicated, the shapes of the seismic hazard curves are quite different. The difference is most noticeable when one distinguishes between Pacific west coast and the central and eastern U.S. locations. For example, in Charleston the 50-year spectral acceleration is only 4.5% of the 500-year value, while in San Francisco the 50-year acceleration value is much higher at 28% of the 500-year spectral acceleration. A general conclusion from the wind and the seismic hazard curves is that seismic serviceability is not likely to be a controlling issue in the central and eastern U.S., and that wind serviceability is probably not a controlling issue along the Pacific west coast.

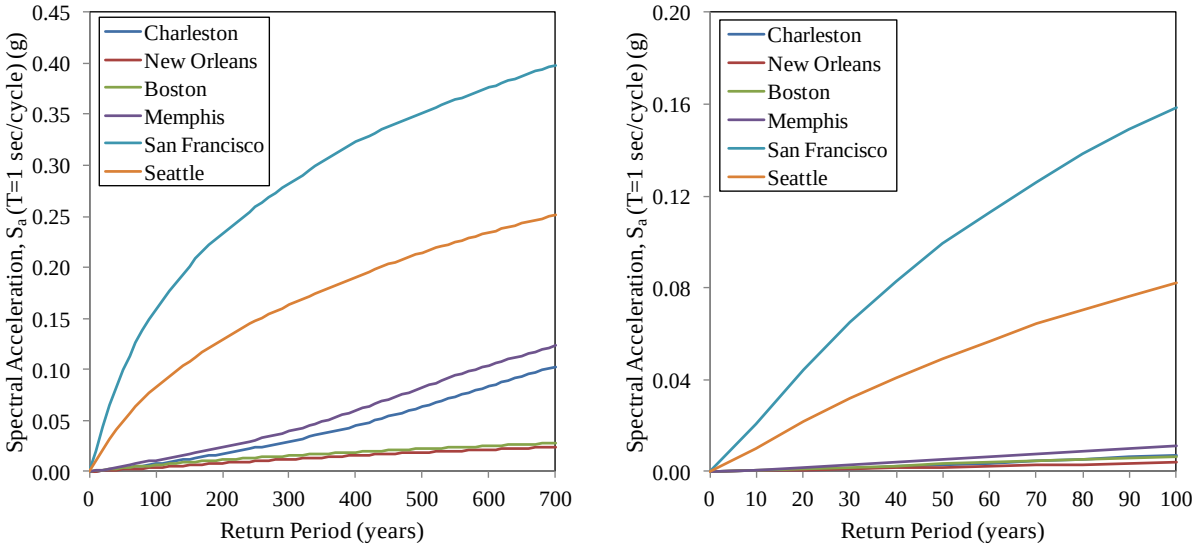

(a) Return Periods between 0 and 700 yrs (b) Return Periods between 0 and 100 yrs

Figure 2. Seismic Hazard Curves for Select United States Cities

In performance based earthquake engineering, "serviceability" level drifts are determined for events with an MRI in the range of 43 years (PEER, 2010) to 72 years (ICC, 2012). One factor in selecting these MRIs is the fact that the probabilistic data used to develop the hazard does not provide information sufficient to assess the hazards at MRIs less than 43 years. It is also important to note that nonstructural and some degree of structural damage (including minor yielding of steel) is *expected* under the 43 to 72 year shaking in the western U.S. For example, the PEER Tall Building Guidelines limit interstory drift to 0.5% of the story height (H/200)

when the structure is subjected to the 43 year MRI. Other seismic serviceability drift limits are summarized by Dymiotis-Wellington and Vlachaki (2004).

For wind-based serviceability, MRIs in the range of 10 to 50 years are appropriate, as it is in this range of wind loads that nonstructural components will first experience damage. As described later, it is recommended that a 25-year MRI be used as the "basic wind speed" for wind damage serviceability because it is in this range of loading that the test-based fragility data is likely to be most reliable. Deformation demands for different wind MRIs can be estimated from those determined by the 25-year MRI as follows:

$$\delta_{Mx} = \delta_{M25} \frac{V_{Mx}^2 G_{Mx}}{V_{M25}^2 G_{M25}} \tag{1}$$

where δ_{Mx} is the deformation demand under an x MRI wind, δ_{M25} is the same deformation demand under the 25 year MRI wind, V is the basic wind velocity, and G is the gust factor for the indicated MRIs. The gust factors are computed in accordance with Section 26.9 of ASCE 7-10. Torsional effects are calculated by applying the ASCE 7 design wind loads cases, which require 75% of the load be applied at an eccentricity of 15% of the width of the building.

PREDICTING DAMAGE IN STRUCTURES

Drift as a Damage Measure

Given that the purpose of the serviceability analysis is to prevent or control damage, the response quantity used to predict damage and the associated damage limits must be consistent with the physical mechanism that causes damage. Borrowing from the field of performance based earthquake engineering, the following terms are used in this paper:

Engineering Demand Parameter (EDP) is the computed quantity that is used as a predictor of damage. Traditional serviceability analysis uses interstory drift as the EDP. The procedure presented herein uses shear strain as the EDP.

Damage State (DS) is a physical description of the expected damage. An example is first observation of cracking in a brick masonry veneer.

Damage Measure (DM) is the value of the EDP at which a certain damage is expected to occur. Traditional serviceability analysis used an interstory drift limit as the DM. The

procedure outlined in this paper does not provide a specific limit, and instead uses fragility curves to estimate the probability of exceeding a given Damage State.

The concept of the EDP is discussed in this section of the paper. The Damage Measure and Damage States are discussed in later sections.

Traditional EDPs include total drift, roof drift, and interstory drift (and for other applications, floor acceleration and plastic hinge rotations are also used). Total drift is the lateral displacement of a frame at a given level with respect to a chosen datum (typically the ground). Roof drift is simply the total drift measured at the roof level. Interstory drift is the relative lateral displacement between two adjacent levels. The drift index is the total, roof, or interstory drift divided by the height over which the drift applies. For example, the interstory drift index (IDI) is the interstory drift divided by the height of the story. This same quantity is also referred to as the interstory drift ratio. Based on the surveys cited earlier, most engineers attempt to control drift by providing limiting values on the computed interstory drift or the interstory drift ratio.

The interstory drift and the interstory drift ratio are not, however, accurate measures of damage in a nonstructural component, and are therefore not the most suitable EDPs if the purpose of the analysis is to limit damage in the nonstructural components. This is because interstory drift tracks only lateral displacement (not necessarily equal to deformation) and does not account for vertical racking or rigid body rotation. A true damage measure for nonstructural components, accounting for both horizontal and vertical racking, but excluding rigid body rotation, would be mathematically equivalent to the in-plane shear strain in the component.

Another reason for using shear strain as the EDP is that it is the best quantity to correlate with laboratory tests on nonstructural components. These tests are typically performed by loading the specimens in pure shear, and then correlating the damage, as it occurs, to the shear strain imposed on the specimen at the time the damage is observed. As described later in this paper the same laboratory tests may produce sufficient information to establish the fragility of the tested component. The use of fragility in wind damage serviceability analysis allows the engineer not only to establish damage limits, but also to determine the probability that damage will occur if the imposed limits are reached or exceeded.

Using Shear Strain as the Engineering Demand Parameter

To alleviate the shortcoming of interstory drift as a damage measure, Charney (1990b) developed a revised damage measure, called the Drift Damage Index, which in this paper is renamed the Deformation Damage Index (DDI) to eliminate the reliance on horizontal drift as a damage measure. In accordance with the terminology adopted in the previous section, the DDI can be used as the EDP for the proposed method. The DDI is mathematically equal to the shear strain in a vertical rectangular panel of the structure, called a Drift Damageable Zone, here renamed a Deformation Damageable Zone (DDZ). A DDZ spans between floors in the vertical direction and between column lines (real or imaginary) in the horizontal direction. For two-dimensional analysis only the horizontal and vertical displacements are needed at the four corners (nodes) of the DDZ. For three-dimensional analysis the two horizontal displacement components would need to be transformed into the plane of the DDZ. As shown later, this procedure can be automated by the use of special finite elements, called "Damage Gages".

Conceptually, the DDZ can represent interior non-structural partitions (such as a gypsum wall), exterior walls, or any other damageable element in a building model. When a building model is created and loaded with the appropriate wind loads, each DDZ will have an associated DDI, defined by the following equation:

$$DDI = 0.5\left[\frac{X_A - X_C}{H} + \frac{X_B - X_D}{H} + \frac{Y_D - Y_C}{L} + \frac{Y_B - Y_A}{L}\right] \quad (2)$$

where X_N is the lateral deflection at node N, Y_N is the vertical deflection at node N, H is the story height, and L is the width of the DDZ (usually the bay width). These variables are shown in Figure 3. Note that the terms in Equation 2 containing X-direction lateral deflection values represent the interstory drift index. If the terms representing vertical deflection were set to zero, the DDI would be equal to the IDI.

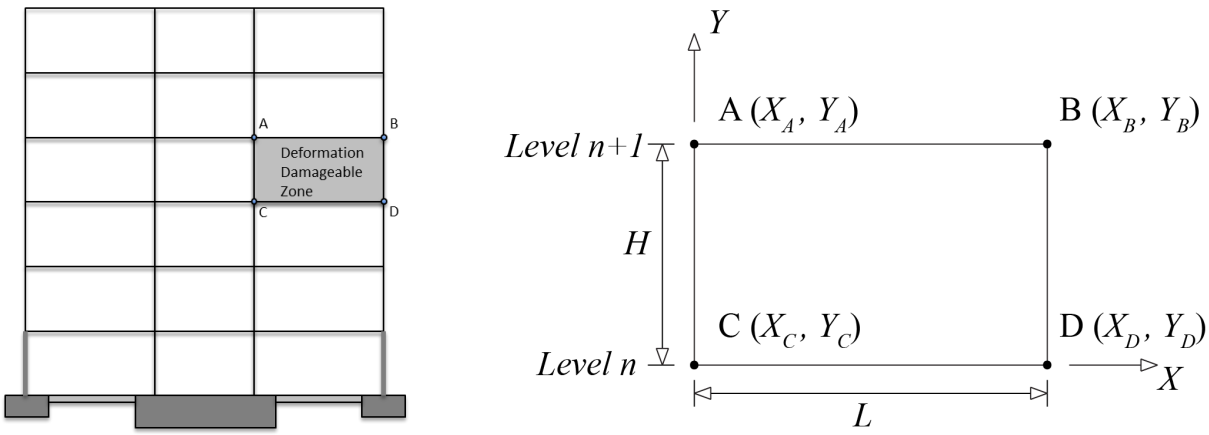

(a) Location in Frame (b) Details for Calculation

Figure 3. Deformation Damageable Zone

Damage Gages

Computation of the Deformation Damage Index can be cumbersome, particularly for three-dimensional analysis. When using a finite element analysis program, the DDI can easily be computed by placing membrane or shell elements in the desired location. For example, the DDZ shown in Figure 3(a) can be represented by a 4-node element. When specifying the properties of this element, it is necessary to use a very low thickness and/or modulus of elasticity such that the element does not significantly contribute to the stiffness of the structure. If a shear modulus of 1.0 is used, then the reported shear stress is identical to the shear strain, and thus the DDI is automatically determined. In general, it is preferable to average the shear strains at the four corners of the element to obtain the best estimate of the DDI. It is noted that when finite elements are used to represent the DDZ, the elements can be placed in any orientation, are not restricted to vertical planes, and need not be rectangular in shape.

An example of the analysis of a 10-story X-braced planar frame is provided to clarify the concepts of computing DDIs using Damage Gages. This example will also be used later in the paper to demonstrate the use of fragility in wind damage analysis. A more detailed analysis of a 12-Story Building is provided in Appendix A.

The example frame has three 30 ft wide bays, and the story height is constant at 12.5 ft. The building is located in Dallas, Texas, and is designed for the ultimate level wind speeds for that location. The column sections are W14s, and the beams range from W24s to W30s. The lateral force resisting system is an X-braced frame in the center bays in which the members are W12s. For this example, a service level wind loading corresponding to a 25-year MRI is applied

to the structure. The 25-year MRI was selected due to the hypothetical owner's preference that the serviceability design be based on a 25 year time period.

The structure is modeled in SAP2000 (Computers and Structures, Inc., 2009). All connections and column bases are modeled as pinned. To calculate the DDI a "Damage Gage" (DG) shell element is inserted into each bay, representing an interior partition wall. The elements are connected to the frame only at the four corners of each bay. The shear modulus of the DG element is assigned a unit value so that the calculated shear stress in the element is numerically equal to the shear strain. After the shear strains have been calculated for the elements, the DDI will be equal to the average of the shear strain values at the four corners of the element.

The analysis is run for the applied loads, and the nodal displacements and DDIs in the elements are determined. Table 1 contains the displacements and shear strains for the top left bay of the structure. The DDI, average shear strain, and conventional interstory drift index are calculated based on the values at the nodes. Figure 4 shows the 10-story braced frame with the applied loading. The shear strain contours are plotted on each element, with the DDI labeled at the center of the element and the conventional interstory drift index labeled in parentheses. Equation 2 can also be used to calculate the DDI given the calculated nodal displacements. However, for the example, the DDI for each bay is calculated by averaging the values of the shear strain at the corners of the element.

Table 1. DDI Calculations for Top Left Bay in Example 1

Node	Lateral Disp. (ft.)	Vertical Disp. (ft.)	Shear Strain
A	0.1920	0.0000	0.00315
B	0.1911	0.0270	0.00236
C	0.1686	0.0000	0.00315
D	0.1679	0.0267	0.00235
		DDI =	0.00275
		Average Shear Strain =	0.00275
		Conventional Interstory Drift Index =	0.00186

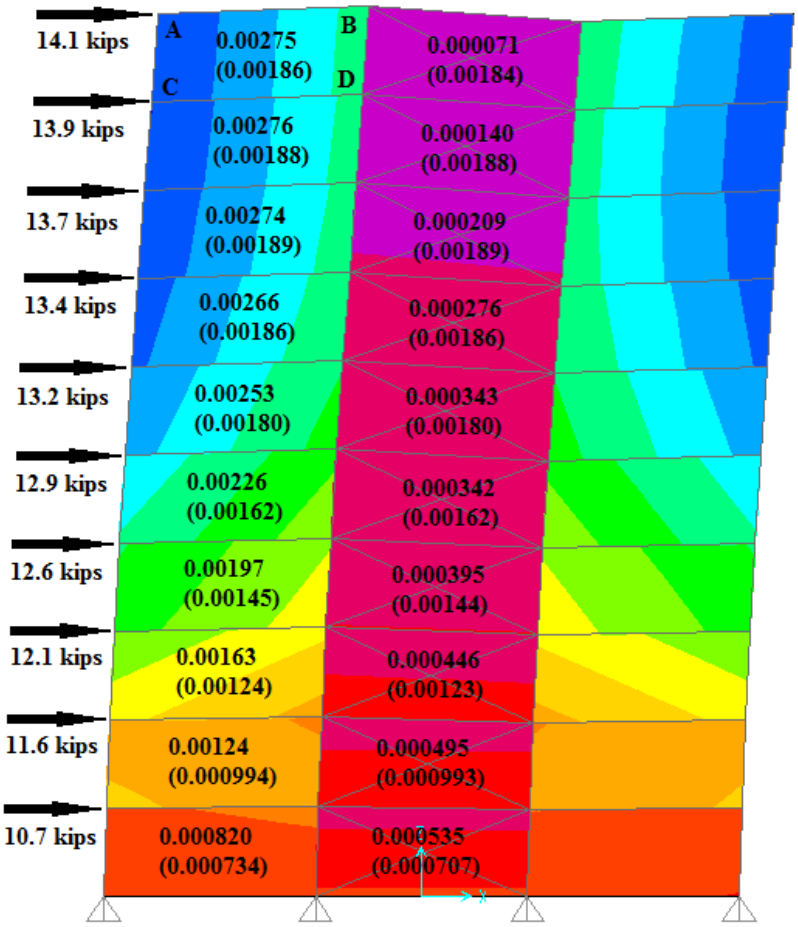

Figure 4. Shear Strains and Interstory Drift Indices in a Ten Story Braced Frame Under Serviceability Level Wind Loads

Some important observations can be made based on the results shown in Figure 4. The first is that the DDIs in the outer bays are very different than the DDIs in the inner bay, even for the same story. For example, the DDI in the top left bay is equal to 0.00275, while the DDI in the adjacent braced bay is 0.000071 (only 2.6% of the value for the unbraced bay), despite having nearly equal conventional interstory drift indices. This difference is present, but less pronounced, at lower levels as well. A second observation is that the DDIs are significantly different from the conventional interstory drift indices (which only account for horizontal racking). For the top left bay the conventional interstory drift index is 0.00186, which is 68% of the DDI. In the adjacent braced bay, the conventional interstory drift index is 26 times the DDI. This wide discrepancy is due to the fact that the conventional interstory drift index does not include vertical racking, and

does not remove the influence of rigid body rotation. For this example the nodes comprising the inner braced bays experience significant vertical deflections, particularly in the upper stories.

STRUCTURAL MODELING

Accurate computation of the EDP requires a mathematical model that can account for any source of deformation that contributes to the EDP. Thus, *any part* of the building-foundation system that is stressed under the wind load should, theoretically, be included in the mathematical model. This includes components of the main lateral load resisting system, components of the gravity load resisting system, architectural components, diaphragms, the soil-foundation system, and all connections. Additionally, second order (P-Delta) effects should be included. For example, for steel moment frames, the modeling of the columns and (possibly composite) beams should allow for unrestricted axial, flexural, shear, and torsional deformation. Additionally, deformations in the panel-zone of the beam-column joints must be considered.

The importance of including all appropriate deformation sources in the structural components was illustrated in a study performed by Charney (1990a), which quantified the relative influence of the various deformation sources on the overall lateral deflection of a frame. Using the principle of virtual work and the concept of displacement participation factors (Charney, 1991; Charney, 1993), 45 different steel structures were analyzed, ranging from 10 to 50 stories. It was found that flexural deformations are very influential in shorter, stockier structures and that axial deformations are influential in taller slender structures. Shear deformations contributed, on average, 15.6% to the overall lateral deflection. Panel zone deformations were found to constitute an average of 30.5% of the drift in a structure. A study by Berding (2006) found similar results, with panel zone deformations comprising as much as 39% of the total deformation. Based on the results of these studies it is recommended that any structural model used to calculate deformation include the effects of axial, flexural, shear, and panel zone deformations. The exclusion of any of these effects could result in the underestimation of component deformations.

Given that most commercial programs are designed to develop 3-Dimensional models of building structures, it is recommended that a 3-D model be used for all wind damage serviceability analyses. There are several advantages to utilizing a 3-D building model, such as modeling the interaction of orthogonal building frames, and the automatic inclusion of inherent

torsional response. Torsion can increase the computed shear strain in some parts of a building, while decreasing the shear strain in others. The torsional response is difficult, if not impossible, to model in 2D.

Additional modeling considerations are briefly provided below. More detailed recommendations can be found in Berding (2006).

Panel Zone Deformations

As previously discussed, panel zone deformations can constitute a significant contribution to the overall drift of a steel moment resisting frame. There are several methods to model panel zone deformations, including the clearspan model, the centerline model, and more sophisticated mechanical joint models, such as the Krawinkler Joint (KJ) and Scissors Joint (SJ) models (Charney and Marshall, 2006). The clearspan model unconservatively assumes the panel zone is infinitely rigid and should never be used. The centerline model uses center-to-center dimensions and will tend to overestimate flexural deformations and underestimate shear deformations within the beam-column joint. These effects partially offset each other, leading the centerline model to be sufficiently accurate in most situations (as long as there is no yielding in the panel zone). The KJ and SJ models are the most accurate, and incorporate rigid links and rotational springs and explicitly represent both shear and flexural deformation within the beam-column joint. However, these models are somewhat difficult to implement. It is recommended that the centerline model be used when the mechanical joint models are not feasible (Charney and Pathak, 2008).

Floor and Roof Diaphragms

In most circumstances the floor and roof diaphragms may be modeled as rigid in their own plane and flexible out of plane. However, for certain structures the out-of-plane stiffness of the diaphragms may act to couple the lateral load resisting elements, thereby having a significant influence on lateral displacements and damage prediction.

Composite Beams

For serviceability analysis it is generally acceptable to include some contribution from slabs, even if the beams are not designed as fully composite. The main concerns are related to the effective width of slabs to use in analysis, and to the effectiveness of the slab if it is likely to be cracked in tension under serviceability wind loads. The slab can generally be broken into four moment regions under lateral loads (Schaffhausen and Wegmuller, 1977): (1) positive bending

moment region – slab is located away from column (2) positive bending moment region – slab is adjacent to a column, (3) negative bending moment – slab is adjacent to interior column and may have compression reinforcement, and (4) negative bending moment region – slab is adjacent to exterior column and is not likely to have compression reinforcement. In general, for regions (1) and (2) the full effective slab width should be used. In a strict sense the effective slab width should reduce to the width of the column for region (2). For regions (3) and (4) the girder properties alone should be used. In the determination of the composite moment of inertia for regions (1) and (2), the compressive strength of the concrete and the composite percentage based on the number of shear connectors should be considered. For a discussion on effective width, the reader is directed to Vallenilla and Bjorhovde (1985).

Gravity System

In some cases it may be worthwhile to include the additional lateral stiffness of the gravity system in the structural model. To do so, the engineer must estimate realistic moment-rotation relationships for the connections. *Design Guide 8* (Leon, et al., 1996) provides guidance on the calculation of the connection's rotational stiffness, as does the ASCE Standard 41-13 (ASCE, 2013). An example of the possible influence of the stiffness and strength of the gravity connections is shown in Figure 5, which is taken from analyses of a 4-Story Steel Moment Frame (Flores and Charney, 2013). The different curves from nonlinear static pushover analysis represent different assumptions regarding the effective strength and stiffness of the connections from the beams to the columns. The curve marked "4Story+PDelta" represents the lateral system only, and the curve marked "4Story+35GS" assumes that the gravity connections have 35% of the stiffness of the full beam section. As may be seen, there is a considerable increase in system stiffness and strength when the gravity system is considered.

While it is recommended that the gravity system be included in the wind serviceability analysis, it is recognized that neglecting the gravity system will be conservative.

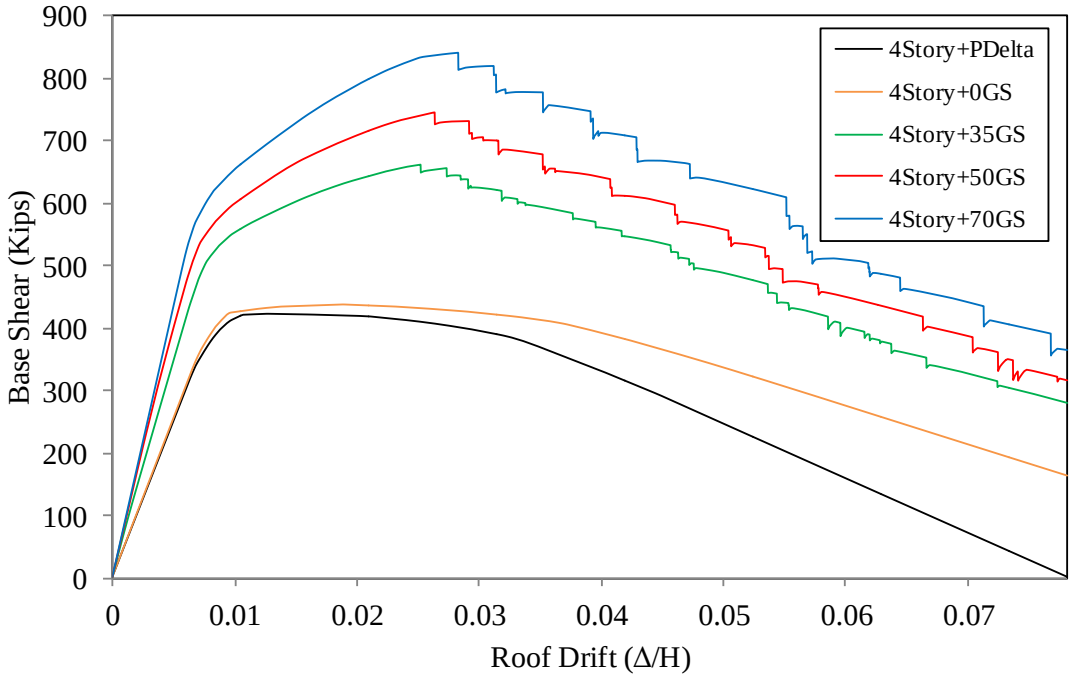

Figure 5. Nonlinear Static Pushover Curves for a 4-Story Frame

Architectural Components

The influence of architectural components on the response of a building under serviceability wind loads depends on the number of components, the location and orientation of the components, the basic in-plane unit stiffness of the component, the method of attachment, and the total contributing stiffness of components relative to the overall stiffness of the lateral load resisting system. In this sense, an infill masonry wall in a 3-story building would significantly influence the computed response, but drywall partitions in a 30-story office building would likely provide negligible stiffness. Due to uncertainties in establishing component location and to estimating the component stiffness, it is recommended that architectural components not be included in wind drift serviceability analysis.

Second Order (P-Delta) Effects

Second order effects typically increase lateral deflection and should always be included in the model. When modeling second order effects a decision must be made concerning gravity loads. Actual live load values are typically much less than design values (Ellingwood and Culver, 1977), making it unreasonable to use design live loads in a serviceability-based P-Delta analysis. It is recommended that unfactored dead loads be used with the mean expected live loads, taken

from live load surveys. Table C4-2 of ASCE 7 (2010) contains survey loads for office buildings, residences, hotels, and schools.

Foundation

The significance of the flexibility of the foundation on nonstructural deformations depends on several factors, including the composition of the soil and the characteristics of the foundation itself. Consider, for example, the simple structure shown in Figure 6. Here, slight rotation of the mat foundation under the X-Braced frame would contribute to the vertical racking in the adjacent bays, as would the axial elongation in the basement columns. Additionally, the P-Delta effects would be more significant if the foundation and subgrade structure were included in the model. Thus, the shear strains, when used as the EDP, could be significantly underestimated if the mat rotation and the basement columns were not included in the mathematical model.

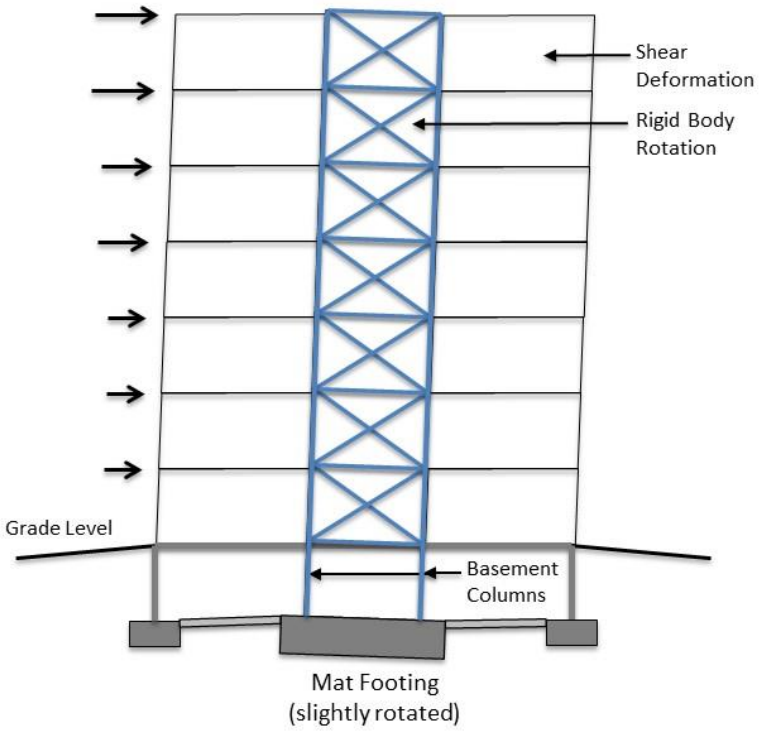

Figure 6. Foundation Modeling Concerns

DAMAGE MEASURES

As already discussed in this paper, the Engineering Demand Parameter (EDP) that is recommended for controlling damage in nonstructural components is shear strain. Such strains develop from the three-dimensional displacements that occur at the attachment points between the structure and the nonstructural component. Given a structural model, the shear strains can be

computed with relative ease, either manually or by use of the Damage Gages described previously.

To control damage, the Damage Measure (DM) must be compatible with the EDP. Thus, it is logical that those levels of shear strain that cause some level of observable damage in nonstructural components be used as the limiting damage measure. As already mentioned, interstory drift or interstory drift ratios are not suitable as damage measures because they include rigid body rotations (which do not cause damage) and exclude vertical racking (which does cause damage).

Conventional Drift Limits

Interstory drift limits have historically been based on rules-of-thumb, and ASCE (1988) reported structural engineers to be employing drift limits ranging from *H*/600 to *H*/200, where *H* is the story height. A review of the literature reveals a commonly suggested interstory drift limit of *H*/500, which is also recommended in *Design Guide 3* (West, et al., 2003). However, it should be noted that these limits are generally invariant across material type. Galambos and Ellingwood (1986) provide a broad set of interstory drift limits that are tied to specific serviceability problems that can arise. These limits range from *H*/1000 (cracking of brickwork) to *H*/100 (damage to lightweight partitions, impaired operation of windows and doors, etc.). Within this range, the limit of *H*/500 is associated with the cracking of partition walls. The limits provided by Galambos and Ellingwood, however, are not connected to any specific structural or nonstructural material.

The preceding discussion illustrates the wide range of applied interstory drift limits in historical use. However, these limits are typically not modified by engineers to account for specific structural or nonstructural materials, as limits on shear strain would be. Rather, a designer may indiscriminately employ the same interstory drift limit for each bay in the building, or even for two or more buildings with different owner preferences, functions, and material makeup. For a more accurate measure of component damage, rational shear strain limits intended to control damage to a particular material should be defined on the basis of the material's properties. For example, if the goal is to prevent damage to interior gypsum wall partitions, then the damage limit should be defined based on test data of gypsum wall board. Using rational damage limits will likely lead to a separate shear strain damage limit for each damageable material in a building.

Griffis (1993) recognized this problem, and recommended limiting shear strains in a variety of nonstructural components. Selected values are repeated in Table 2. The recommended limits are those which are expected to be at the threshold of causing observable damage in the given building element, and recommended for use in association with a 10-year MRI. The use of limiting strains as shown in Table 2 is a step in the right direction, but there is no information provided as to the type of damage that could be expected, nor is any information provided as to the likelihood that the damage would occur if the recommended drift limit were to be achieved under the designated wind load.

Table 2. Selected Recommended Shear Strain Limits (Griffis 1993). Used under fair use, 2013.

Building Element	Supporting Structural Element	Deformation Type	Recommended Limit
Brick Veneer	Wind Frame	Shear Strain	H/400
Concrete Masonry Unreinforced (Exterior)	Wind Frame (1 story)	Shear Strain	H/600
	Wind Frame (2 story)	Shear Strain	H/400
Concrete Masonry Reinforced (Exterior)	Wind Frame (1 story)	Shear Strain	H/200
	Wind Frame (2 story)	Shear Strain	H/400
Gypsum Drywall, Plaster	Wind Frame	Shear Strain	H/400
Brick (Interior Partition)	Wind Frame	Shear Strain	H/1250

Fragility

A more rational approach for damage control is based on the concept of *fragility*, and specifically *fragility curves*. A fragility curve is a mathematical relationship between an engineering demand parameter (e.g. shear strain in nonstructural components) and the probability of attaining some observable damage measure. The curves are based on laboratory test data, usually from a number of sources. Figure 7 contains three sample fragility curves for gypsum wall boards, obtained from the Performance Assessment Calculation Tool (PACT) developed by the Applied Technology Council (FEMA, 2013b) as a part of FEMA P-58. The horizontal axis shows the EDP of Deformation Damage Index (or shear strain), and the vertical axis contains the probability of exceeding one of the three damage states shown. Note that many of the fragilities found in PACT use interstory drift ratio as the EDP. As long as racking tests were performed on the individual component to develop the fragilities, the interstory drift ratio will be equal to shear strain, and therefore, those fragilities can be used in this procedure where the EDP is shear strain.

The blue curve in Figure 7 represents Damage State 1 (DS1), which is screws popping out and minor cracking. The orange curve (DS2) is DS1 plus moderate cracking or gypsum crushing, and the maroon curve (DS3) is DS2 plus significant cracking or crushing. From Figure 7, it may be seen that for a deformation damage index of 0.005 (1/200) corresponding to a hypothetical 10-year MRI, there is a 93% probability of DS1 occurring, a 22% probability of DS2 occurring, a 2.6% Probability of DS3 occurring, and a 7.0% probability of no damage.

One of the advantages of the fragility approach is that a *design space* of information is provided, instead of information on just one specific damage limit or wind speed. In this sense, the entire plot represents the design space, and the DDIs that could occur under several MRIs can be examined. In addition to the 10-year MRI previously discussed, Figure 7 also contains vertical lines representing the DDIs under the loads corresponding to the 25- and 50-year wind loads. Note that the location of the wind speed MRI lines will shift laterally on the plot when different geographic locations are chosen. Using this design space the engineer can gather probabilistic information for a range of MRIs.

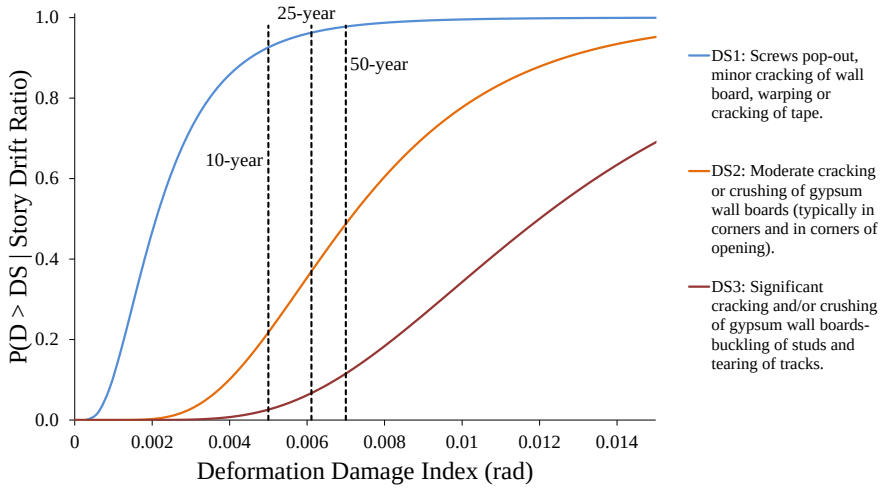

Figure 7. Gypsum Wall Board Fragility Curves (PACT)

Fragility Curve Theory

There are many different methods used to develop fragility curves (FEMA 2013a; Porter, et al., 2007). If the objective of the fragility curve is to obtain rational damage measures, the most useful method is experimental testing. A typical test might involve fixing the base of the component (e.g. a sheet of gypsum wall board) and applying an in-plane load in order to induce a

shear strain. In the ideal testing procedure, there will be no vertical racking and no rigid body rotation, thus the shear strain and the interstory drift ratio in the component will be equal. As the test progresses the load is incrementally increased until a particular damage state is observed (e.g. screws popping out, cracking, or crushing). The shear strain at which the damage state occurs is noted, and the test is repeated on a new specimen.

Table 3 shows data obtained from tests performed on gypsum wall partitions (Miranda and Mosqueda, 2013). The data is collected from six different sources, dating between 1966 and 2010. The values represent the shear strain (in this case equivalent to the interstory drift ratio, due to the absence of vertical deformation) at which damage state 1 (minor damage such as cracking of drywall or warping of tape) was first observed.

Table 3. Gypsum Partition Wall Data Set (Miranda and Mosqueda, 2013). Used under fair use, 2013.

Source	DS1
JAB	0.0026
	0.0026
	0.0026
	0.0052
	0.0026
	0.0052
	0.0026
	0.0026
	0.0007
	0.0026
	0.0013
	0.0026
Japan	0.0020

Source	DS1
NEESR	0.0040
	0.0020
	0.0040
	0.0020
	0.0040
	0.0020
	0.0020
	0.0040
	0.0040
	0.0040
	0.0040
	0.0040
	0.0040

Source	DS1
Rihal	0.0039
	0.0039
	0.0026
	0.0046
	0.0052
	0.0046
	0.0039
	0.0033
	0.0039
	0.0039
	0.0039
Lang	0.0025
	0.0028

Source	DS1
AMB	0.0030
	0.0030
	0.0005
	0.0005
	0.0030
	0.0030
	0.0050
	0.0050
	0.0010
	0.0010
	0.0010
	0.0010
	0.0010
	0.0010

The "raw" fragility data is plotted as solid symbols in Figure 8. Such a plot is created by first sorting the fragility data in ascending order, and then assigning a probability to each data point as follows:

$$p_i = \frac{i - 0.5}{M} \tag{3}$$

where M is the number of sample points and i is the rank of the sorted data point.

Table 4 shows some of the data from Table 3 that is used to plot the symbols in Figure 8, where column (2) of the table are the X-axis values, and column (4) of the table are the Y-axis values.

Table 4. Reduced Fragility Data

(1)	(2)	(3)	(4)
Data Point	**Sorted Value**	**Ln(Sorted Value)**	**Probability**
1	0.0005	-7.6	0.0094
2	0.0005	-7.6	0.0283
3	0.0007	-7.264	0.0471
4	0.001	-6.908	0.066
5	0.001	-6.908	0.0948
…	…	…	…
51	0.0052	-5.259	0.9527
52	0.0052	-5.259	0.9716
53	0.0052	-5.259	0.9905
Mean	**0.00297**	**-5.950 = ζ**	-
Standard Deviation	**0.00132**	**0.602 = λ**	-

The mathematical fragility curve is simply the integral of a probability distribution function (PDF). In most cases, a lognormal PDF is used, as follows:

$$f_X(x) = \frac{1}{(x\zeta)\sqrt{2\pi}} \exp\left[-\frac{1}{2}\left(\frac{\ln x - \lambda}{\zeta}\right)^2\right] \quad x \geq 0 \tag{4}$$

where λ is the mean of the natural log of the set (ln x) and ζ is the standard deviation of the natural log of the data set. For example, for the gypsum partition wall data shown in Table 3, λ = -5.95 and ζ = 0.602. These values are computed as shown in column (3) of Table 4.

The smooth mathematical fragility function is given by:

$$P(X \leq x) = \int_0^x f_X(x)dx \tag{5}$$

The fitted curve in Figure 8 represents the mathematical fragility function given by Equation 5.

Note that before using a curve developed from test data for design purposes, a goodness of fit test should also be performed (Porter, et al., 2007). Additional caution should be exercised when using shear strains that correspond to sections of a fragility curve where there is little data resolution. To avoid this problem it may be appropriate to select an MRI such that the

corresponding shear strains from the fragility curve falls within a segment of the curve with a high resolution of tested data points.

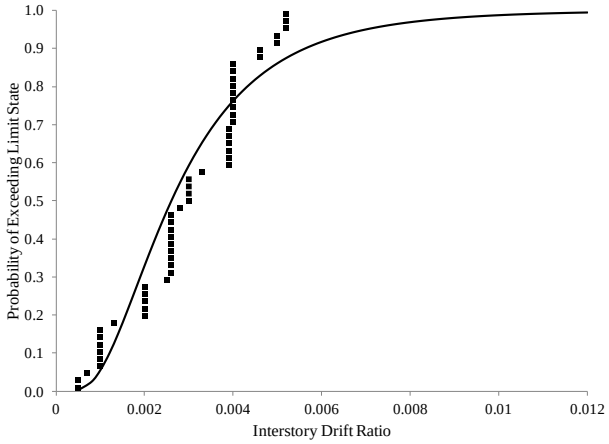

Figure 8. Fragility Curve Construction

Tables 5 through 8 contain λ values (mean of the natural log of the data), dispersion ζ values (standard deviation of the natural log of the data), and the descriptions of the associated damage states for a variety of nonstructural and structural components. The values in the tables were taken from the Performance Assessment Calculation Tool (FEMA, 2013b), which contains the same type of information for hundreds of structural and nonstructural components. PACT also contains useful data on the cost of repairing or replacing the building elements. When the cost data is combined with the probability of damage occurring, the engineer can estimate an expected repair cost over the time period in question. This aspect of the serviceability design is discussed later in regards to the potential adaptation and application of PACT to PBWE. More information on component testing and fragility development for specific components can be found in Miranda and Mosqueda (2013), Lee, et al. (2006), O'Brien, et al. (2012), and Algan (1982). Additionally, if the fragility parameters for a particular component cannot be found, fragility curves can be developed by the engineer, using the FEMA P-58 Appendix H procedures (FEMA, 2013a). If actual test data is available, the engineer should use the mean and dispersion (appropriately adjusted for testing procedures) to create a fragility curve. In the absence of test data, other procedures may be used, including Monte Carlo simulation, "Expert Opinion," and the "Single Calculation" procedure. The "Single Calculation" procedure consists of determining a best estimate for the average capacity (*Q)* of the component and setting the mean value equal to 0.92*Q*, with a dispersion equal to 0.40. This procedure can be applied when damage state means are known, but dispersions are unknown or difficult to quantify.

Table 5. Fragility Information for Gypsum Drywall Building Elements (PACT)

Building Element	Damage State	Mean Demand	λ	Dispersion (ζ)
Fixed Below, Fixed Above[1,2,3]	DS1	0.0021	-6.166	0.60
	DS2	0.0071	-4.948	0.45
Fixed Below, Slip Track Above w/ Returns[1,2,3]	DS1	0.002	-6.215	0.70
	DS2	0.0050	-5.298	0.40
Fixed Below, Slip Track Above w/o Returns[1,2,3]	DS1	0.0035	-5.655	0.70
	DS2	0.0093	-4.678	0.45

Notes:

1. DS1 is screw pop-out, minor cracking of wall board, warping or cracking of tape. DS2 corresponds to moderate cracking or crushing.

2. Full height wall with gypsum on metal studs.

3. These fragilities also apply to gypsum + wallpaper, gypsum + ceramic tile, and high end marble or wood panel, provided that the fixities (below and above) are equivalent. See PACT for more information

Table 6. Fragility Information for Exterior Enclosure Building Elements (PACT)

Building Element	Damage State	Mean Demand	λ	Dispersion (ζ)
Glass Curtain Wall (Monolithic)[1]	DS1	0.0338	-3.387	0.40
	DS2	0.0383	-3.262	0.40
Glass Curtain Wall (Insulating Glass Units)[1]	DS1	0.021	-3.863	0.45
	DS2	0.024	-3.730	0.45
Generic Storefront (Monolithic)[2]	DS1	0.029	-3.540	0.50
	DS2	0.0473	-3.051	0.25
Generic Storefront (Insulating Glass Units)[2]	DS1	0.059	-2.830	0.25
	DS2	0.0665	-2.711	0.35

Notes:

1. Generic midrise stick-built curtain wall. Aspect ratio = 6:5. DS1 corresponds to glass cracking. DS2 corresponds to glass falling from frame. For fragility information relating to other glass types, aspect ratios, and installation details see PACT.

2. Aspect ratio 6:5. DS1 corresponds to a gasket seal failure. DS2 corresponds to glass cracking.

Table 7. Fragility Information for Concrete and Masonry Building Elements (PACT)

Building Element	Damage State	Mean Demand	λ	Dispersion (ζ)
Reinforced Concrete Wall (Low Aspect Ratio)[1]	DS1	0.0055	-5.203	0.36
	DS2	0.0109	-4.519	0.30
Low-rise Reinforced Concrete Wall[2]	DS1	0.0076	-4.880	0.35
	DS2	0.0134	-4.313	0.45
Slender Concrete Wall[3]	DS1	0.0076	-4.880	0.35
	DS2	0.0134	-4.313	0.45
Ordinary Reinforced Masonry Walls[4]	DS1	0.002	-6.215	0.86
	DS2	0.0033	-5.714	0.77
Special Reinforced Masonry Walls[5]	DS1	0.0036	-5.627	0.59
	DS2	0.0059	-5.133	0.51

Notes:
1. DS1 corresponds to cracks of width between 0.04 and 0.12 in. DS2 represents crushed concrete core, localized concrete cracking (width > 0.12 in.), and buckling of vertical rebar.
2. Wall with return flanges. DS1 is crushed concrete core, localized concrete cracking (widths > 0.12 in.), and buckling of vertical rebar. DS2 is sliding of the wall resulting in distributed cracking.
3. DS1 corresponds to spalling of cover and vertical cracks. DS2 is exposed longitudinal reinforcing and buckling of vertical rebar. DS2 is sliding of the wall resulting in distributed cracking.
4. Partially grouted cells, shear dominated. DS1 is first occurrence of major diagonal cracks. DS2 is wide diagonal cracks in each direction, crushing or spalling at wall toes.
5. Fully grouted cells, shear dominated. DS1 is first occurrence of major diagonal cracks. DS2 is wide diagonal cracks in each direction, crushing or spalling at wall toes.

Table 8. Fragility Information for Structural Steel Building Elements (PACT)

Building Element	Damage State	Mean Demand	λ	Dispersion (ζ)
Braced Frame (No Seismic Detailing)[1]	DS1	0.0042	-5.473	0.25
Ordinary Steel Concentric Braced Frame[2]	DS1	0.00159	-6.444	0.70
	DS2	0.010	-4.605	0.30
Special Steel Concentric Braced Frame[3]	DS1	0.0035	-5.655	0.46
	DS2	0.0058	-5.150	0.65

Notes:
1. Design for factored loads, no additional seismic detailing. DS1 corresponds to the fracture of brace or gusset plate, gusset buckling, and significant decrease in lateral stiffness.
2. DS1 is minor damage, including some buckling of the brace and initial yielding of the gusset. DS2 is moderate damage, including additional brace buckling, gusset yielding, and yielding of members.
3. WF braces, balanced design criteria. DS1 corresponds to initial brace buckling, yielding of the gusset, slight residual drift. DS2 is moderate damage, significant buckling of brace, initiation of yielding and out-of-plane deformation of the gusset, initiation of cracking of welds of gusset, and yielding of members.

Example of 10 Story Frame, Continued

The example of the 10-story frame is now continued to illustrate the use of fragility in the context of Engineering Demand Parameters, Damage Measures, and Damage States.

After the MRI is selected, the wind loads are determined, the building is modeled, and the DDIs are calculated (see Figure 4), the next step is to select damage limits and then compare the DDIs to these limits. For this example, the Deformation Damageable Zones represent interior gypsum wall partitions with metal studs. It is the owner's preference that there is no greater than a 30% chance of minor damage (DS1) to each partition under the 25-year wind loads. Using the fragility information from Table 5 (median demand = 0.0021, dispersion = 0.6), it is determined that a DDI of 0.00153 corresponds to a probability of exceedance of DS1 of 30%. (See Appendix B for details on computing such probabilities.) Based on the DDIs shown in Figure 4, the outside bays in the top eight levels exceed the limit, while none of the interior (braced) bays do so.

An alternative to comparing the maximum DDI to some limit from the fragility curve is to look at the range of the DDIs in all of the bays of interest. Figure 9 shows the fragility curve for DS1 for gypsum drywall. The middle 50% range of DDIs is shown on the figure, along with the mean of the DDIs for the 10-, 25-, and 50-year wind loads. This figure provides information concerning multiple MRIs. For the 10-year wind loads, the average DDI corresponds to a 10.5% probability of exceeding DS1; for the 25-year MRI, this probability is 18.7%; for the 50-year MRI, it is 26.2%. This constitutes a design space with which the engineer can make a decision based on performance at multiple MRIs.

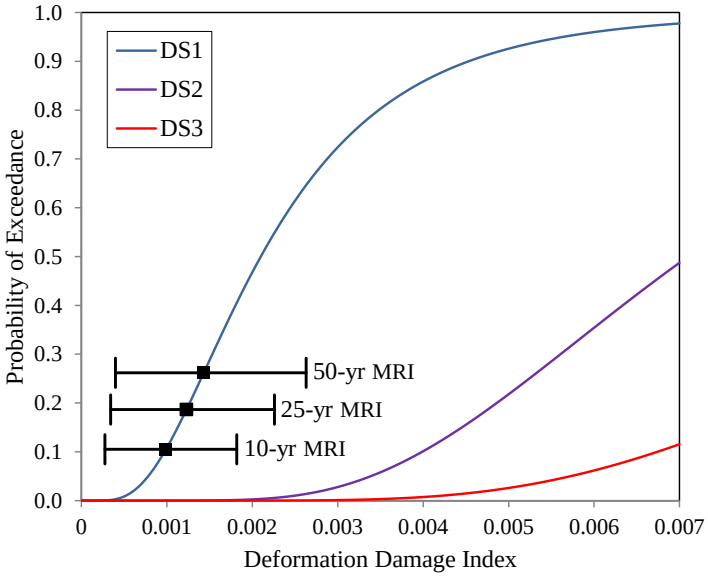

Figure 9. Middle Range of DDIs for the 10-Story Building

PERFORMANCE ASSESSMENT AND DECISION MAKING

One of the most challenging aspects of the recommended methodology is making design decisions based on the results of the damage assessment. After the damage assessment has been conducted, the designer must come to a decision concerning the acceptability of the design (either it is adequate or it is not). The decision space (probabilities of damage relative to deformation levels due to various MRIs) aids in this decision making process, but it is the responsibility of the engineer to set acceptability thresholds (for example, no more than a 30% probability of exceedance due to the 25-year MRI) in coordination with the architect, building owner, and other stakeholders. As discussed later, it will likely be helpful to connect the probability of damage to cost of repair or replacement, thus providing a decision variable in terms of cost, which is typically more useful to a building owner than shear strain or damage probabilities.

OPTIONS FOR REDESIGN IF PERFORMANCE TARGETS ARE NOT MET

In many cases the designer will find that the structure does not meet the required serviceability requirements and that the system must be re-proportioned to meet such requirements. Unfortunately, it may be difficult to determine which members of the main lateral load resisting system to modify (make stiffer or more flexible). Virtual Work based procedures (Velivasakas and DeScenza, 1983; Baker, 1990, Charney, 1991; Charney, 1993) have been developed to simplify this task, and are included in some commercial analysis programs such as SAP2000 (Computers and Structures, 2009), and RAM Frame (Bentley, 2013). These procedures can provide information as to which elements to modify, and even further, to recommend which section properties within these elements (axial area, shear area, moment of inertia) to modify. These simple virtual work methods are the basis of much more complex automated optimization procedures that have been used in tall building design (Chan, et al., 2010).

APPLICATION TO THE FEMA P-58 METHODOLOGY

While the FEMA P-58 (FEMA, 2013a) methodology was developed for seismic response of structures, the procedure and its four goals could easily be adapted to the wind serviceability

procedure discussed previously. The FEMA P-58 methodology provides a PBEE framework with four major goals: (1) to include the behavior of non-structural components; (2) to investigate response at a global level; (3) to relate damages to more meaningful consequences, such as repair time, repair costs, casualties and injuries, and potential for unsafe placards; and (4) to account for uncertainties and variations within structural analysis.

The first goal, to include the effects of nonstructural components, is already a crucial part of the wind serviceability procedure presented in this paper, as well as the P-58 procedure. However, the other three P-58 goals could be added to the previous procedure to provide more robust solutions. The P-58 process gives its final solution in terms of the global consequences, using the idea of a Building Performance Model. This model is a collection of information about the structure needed to determine the consequences of a structure under loading. This information includes, among other things, a list of all the structural and nonstructural components in the structure and their potential damage states and consequences. Each individual component will have a set of fragility curves developed for a discrete number of damage states, as discussed previously in this paper. For each of these damage states, the time and cost needed to repair that component under the particular level of damage will be known as well.

The wind serviceability procedure developed above describes how to relate structural response to component damage through the use of fragility. The FEMA P-58 methodology can be used to take this process one step further and relate the component damages to the global consequences. The P-58 methodology includes hundreds of fragilities for both structural and nonstructural components, as well as their corresponding consequences. By using these fragilities along with their corresponding consequences, the end result will describe the global response and be significantly more meaningful to decision makers, because the results will be in terms of dollars and downtime (time that the structure must be vacated to allow for repair).

This seismic-based methodology could be applied to the wind serviceability procedure, because the main input is building information and response. The building information (i.e. shear strains) will be the same regardless of what loads are applied to it, and instead of using the structural response from ground motions, the user could input structural response from wind loads. Traditionally, the P-58 procedure finds the building response under a suite of ground motions and then expands the data using a determined level of dispersion and Monte Carlo simulation (in order to account for variability in seismic analyses). For the wind serviceability

procedure, this process could be applied to account for uncertainty in selecting an appropriate serviceability MRI, as discussed earlier. A number of MRIs could be analyzed (for example, from 10 to 50 years), and a range of possible behaviors could be determined. This range of responses would be converted into potential damages, which will be converted into a distribution of probable consequences.

The P-58 procedure will also be useful if initial targets are not met, as an alternative option to the virtual work methods described in the previous section. When the results are displayed in the corresponding software, the PACT program (FEMA, 2013b), the consequences are broken down by component. The program determines which components are causing the most problems and have the highest influence on repair cost and time. Along with the global consequences, this methodology could provide valuable information for the engineer to decide which components should be the focus of the redesign.

SUMMARY AND CONCLUSIONS

In this paper a rational method for the wind serviceability design of steel structures is described. The process includes the calculation of appropriate service loads, accurately modeling all significant sources of deformation and stiffness, and the determination of rational shear strain limits based on material test data and fragility curves.

The use of fragility curves combined with an accurate structural model allows the structural engineer more confidence with respect to the building's performance under serviceability level wind loads. Using the recommended procedure, the engineer can estimate probabilities of damage and potentially link these probabilities to cost and repair time, which are meaningful decision variables for owners and decision makers.

Recommended Procedure

The following is a summary of the steps in the procedure recommended in this paper. The proposed method is general and can be adapted for different applications.

1. *Select an appropriate mean recurrence interval*.

   Various MRIs have been suggested, typically ranging between 10 and 50 years. While the length of the MRI could be adjusted after collaboration with the building owner or decision maker, it is recommended that a basic 25-year wind speed be used as a standard, so that the DDIs calculated are generally in the range of the test data used to develop fragility

curves for common nonstructural components. Different MRIs may be used for different levels of nonstructural component protection, as appropriate.

2. *Determine wind speed and loading.*

The wind speed corresponding to selected MRIs can be found in ASCE 7-10. Alternatively, there are equations available in the literature to convert between wind speeds associated with a 50-year MRI to wind speeds associated with other MRIs (Peterka and Shahid, 1998). The service wind loads can be determined using the applicable building code.

3. *Accurately model the structure.*

The structural model should include all significant sources of deformation and lateral stiffness. The deformation source should include axial, shear, flexural, and panel zone deformations, when appropriate. Engineering judgment should be used to determine sources of lateral stiffness to include with the bare frame stiffness. Possible additional lateral stiffness sources include connection flexibility, diaphragm stiffness, and gravity frame stiffness. Direct modeling of the soil-foundation interface should also be considered.

4. *Calculate the Deformation Damage Index.*

The damage measure for nonstructural components should include vertical racking deformation as well as horizontal racking. For this reason, the DDI should be used instead of the conventional interstory drift index (measuring only horizontal racking). The use of Damage Gages is recommended as they are easily implemented in most commercial software.

5. *Select rational damage limits.*

The Deformation Damage Index should be compared to damage limits which are determined on a rational and consistent basis. In this paper fragility curves are recommended as the source of information regarding damage to nonstructural components due to shear strain (DDI).

6. *Compare the DDIs to the damage limits.*

The calculated DDIs for each bay should be compared to the damage limits determined with fragility curves. Stiffness can be added or subtracted from the structure at locations determined by the engineer.

7. *Repeat steps 1-7 until an economical design is achieved or other loading cases control.*

ACKNOWLEDGMENTS

The authors acknowledge the comments and contributions of the ASCE/SEI Committee on Design of Steel Building Structures. The authors also acknowledge the work of Virginia Tech graduate student Johnn Judd for his work on the wind hazard curves presented in this paper. Funding for authors K. Aswegan and J. Jarrett was partially provided by the Charles E. Via Endowment of the Virginia Tech Department of Civil and Environmental Engineering, and by a grant from the National Institute of Standards and Technology (NIST).

APPENDIX A: Example of a 12-Story Perimeter Moment Resisting Frame

In this example a twelve story unsymmetrical steel-framed office building located in Charleston, South Carolina is analyzed. This building, with slightly different properties, is also used in the Analysis chapter of FEMA P-751 (2012a). The first story is 18 ft tall, and the remaining stories are 12.5 ft. The building contains setbacks at levels 5 and 9. At the lower levels of the building there are 7 bays spaced at 30 ft in the east-west direction and 7 bays spaced at 25 ft in the north-south direction. The lateral system is composed of perimeter steel moment resisting frames.

The wind loads are calculated using the ASCE 7 Directional Procedure (2010). After consultation with the owner of the building, it was determined that a 10-year wind event would be the basis for the serviceability design, due to the fact that this is approximately the length of the average tenancy. For completeness, however, results for a 25 year MRI are also provided at the owner's request. The design wind speed of 146 mph and the 10-year MRI serviceability wind speed of 76 mph are determined with the aid of the Applied Technology Council's Wind Speed Calculator. The structure is modeled in SAP2000 and the loads are applied at the nodes. Damage gage elements were added to the exterior corners of the building to represent glazing (glass curtain wall) or drywall, and around the interior core (elevator and stairs) to represent ordinary masonry walls or drywall. While the use of drywall on the exterior is not likely for any building, the DDIs computed for these damage gages could be used to represent drywall in unknown or arbitrary locations. Figure 10 shows two views of the structural model. The vertical shaded elements represent the Damage Gages located at the perimeter and in the interior of the structure.

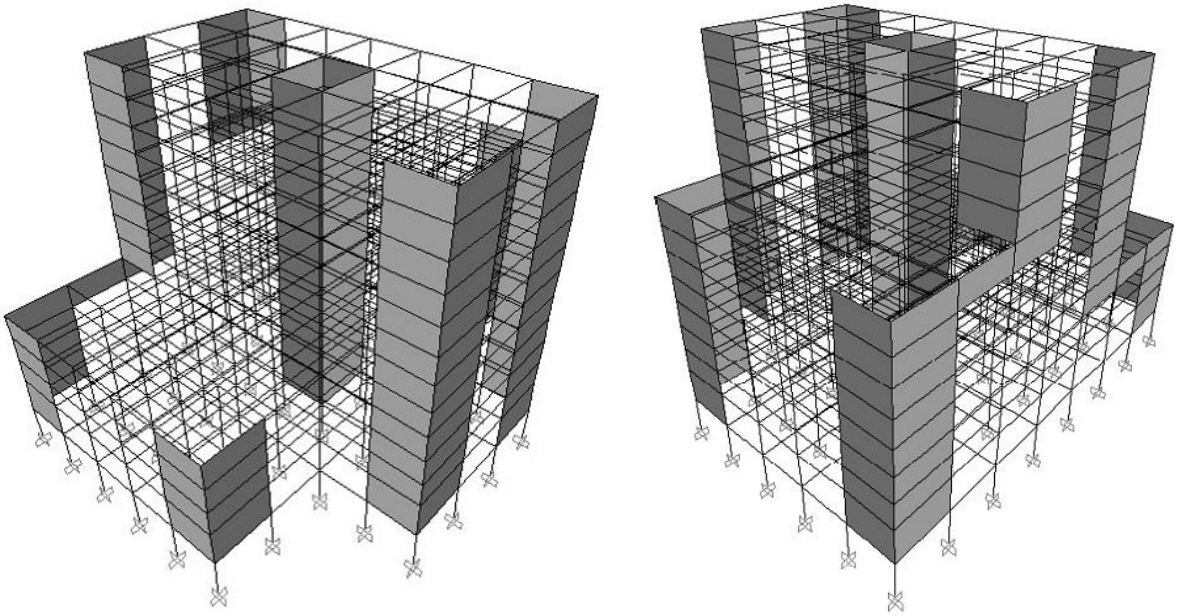

(a) From the South-West (b) From the North-East

Figure 10. Model of Twelve Story Building

Figure 11 shows the building model with the perimeter DDIs labeled on each damage gage. As expected, the highest DDIs (0.00276, or 1/362) are found in the first story. Figure 12(a) shows the drywall fragilities for DS1 and DS2, together with the maximum DDIs for the 10- and 25-year MRIs. There is approximately a 65% probability of exceeding DSI, given the 10-year maximum DDI of 0.00276. Figure 12(b) shows the DS1 fragility curve for the glass curtain wall, along with a vertical line at the maximum DDI, computed using the 10-year MRI. The curve illustrates the fact that a DDI of 0.00276 is not an issue for the glass curtain wall, due to the fact that the probability of exceedance of DS1 is negligible.

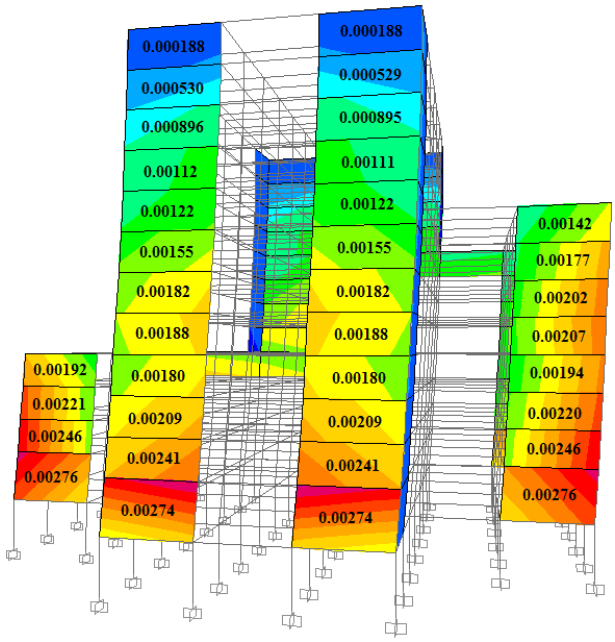

Figure 11. Computed DDIs on Perimeter of Building

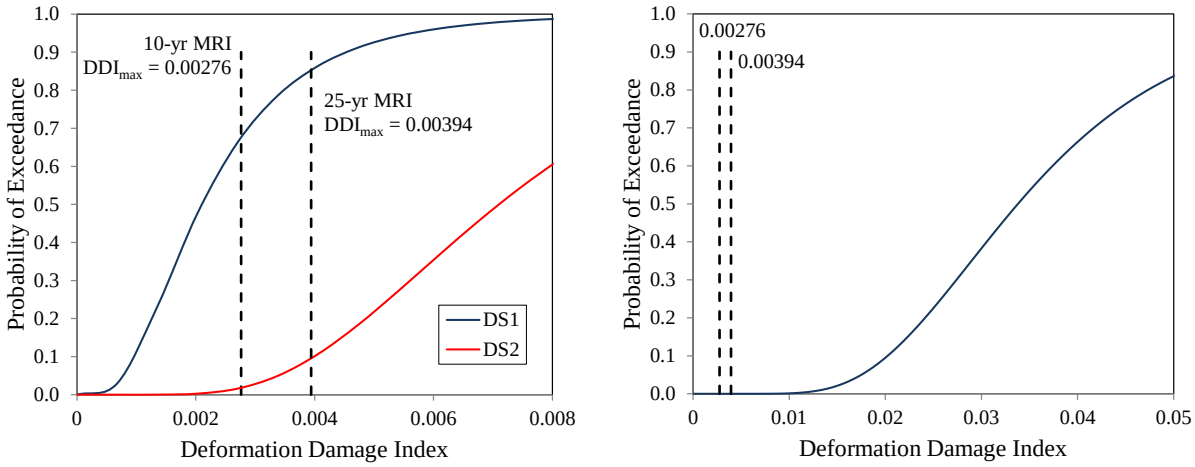

(a) Drywall (b) Curtain Wall for 10 year MRI

Figure 12. Decision Spaces for Exterior Drywall and for Exterior Curtain Wall

The interior core masonry walls present a greater issue than the exterior curtain wall. Figure 13 shows a cross-section of the model under the 10-year wind load, with the DDIs for the interior core labeled. The maximum DDI of 0.00274 occurs at the first story, and the minimum of 0.000478 occurs at the top story. Figure 14(a) shows two fragility curves for drywall. The minimum, mean, maximum, and full range of computed DDI values are illustrated in the figure for the 10-year and 25-year wind loads. Figure 14(b) shows the DS1 and DS2 fragility curves for ordinary masonry walls as well as the DDI ranges. The 25-year DDIs were calculated with

Equation 1 for a wind speed of 89 mph. The hypothetical building owner has indicated that the average wall in the core (gypsum wallboard or masonry) should have no more than a 30% chance of minor damage (DS1) under the 10-year wind loads, and no more than a 70% chance of minor damage under the 25-year wind loads. From Figure 14 (a) and (b), the designer can see that the average DDI (0.00171) under the 10-year wind loads has a probability of exceedance for DS1 greater than 30%, thus failing the owner's requirement. However, the average DDI under the 25-year wind loads is approximately 60%, thus meeting the owner's requirement that it be less than 70%. The DDIs corresponding to other MRIs (such as 50- or 100-year) could also be determined with Equation 1 and incorporated into the decision making process, provided that the owner has selected an allowable probability of damage corresponding to those MRIs.

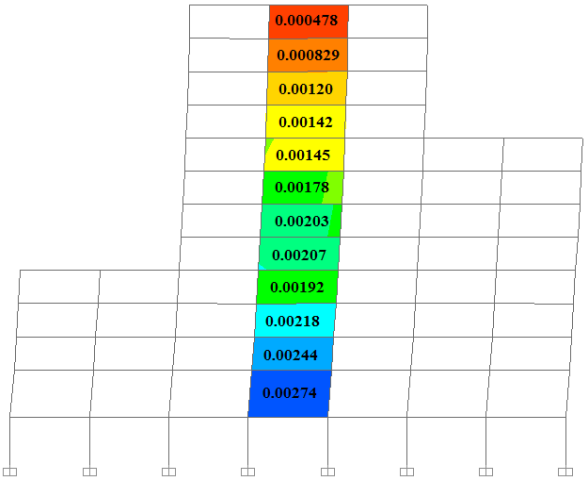

Figure 13. Computed 10-Year DDIs in Core of Building

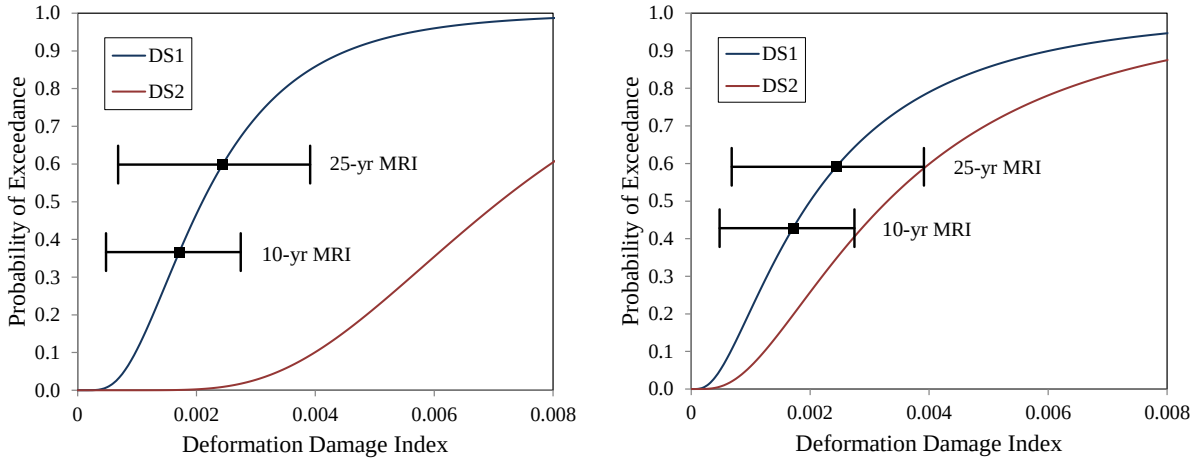

(a) Drywall (b) Masonry Wall

Figure 14. Decision Spaces for Interior Drywall and for Interior Curtain Wall

A final issue to consider is torsional wind loading. It is prudent to examine the effects of torsional loads, although due to the nature of the lateral load resisting system (perimeter moment frame) in this building, torsional loading requirements are not likely to control. For this building, torsion was examined according to the provisions of ASCE 7-10, which require that 75% of the lateral wind load be applied in combination with a torsional moment corresponding to 15% eccentricity. Figure 15 shows the structure under the 10-year torsional load specified in ASCE 7-10. From Figure 15 it can be seen that the torsional loading case does not control; the calculated DDIs are lower for this case than for the case in which 100% of the load is applied at no eccentricity (see Figure 11).

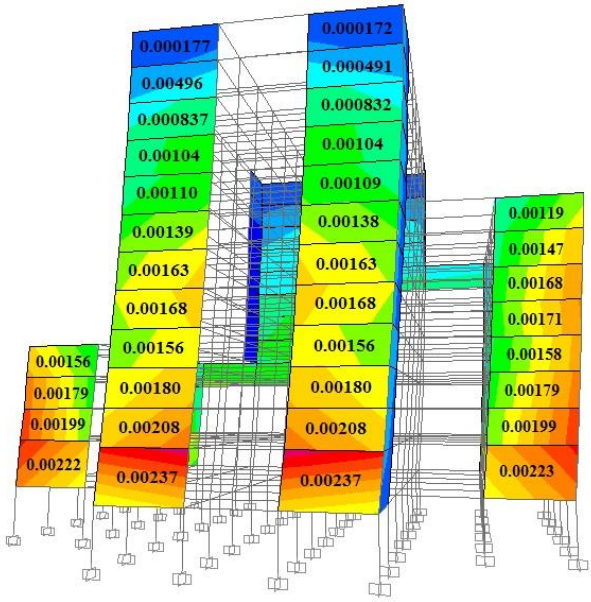

Figure 15. Computed DDIs on Perimeter of Building for Torsional Loading

APPENDIX B: Creating Fragility Curves with Software Programs

Although the Performance Assessment Calculation Tool (PACT) can be used to create and view fragility curves, the engineer may wish to create and manipulate the curves with the use of commercial software such as Microsoft Excel, Mathcad, or some other program. Many software programs contain built-in functions capable of producing fragility curves through the use of lognormal distribution functions.

In Microsoft Excel (Microsoft Corporation, 2013) the fragility curve can be plotted using the `LOGNORM.DIST` function. This function takes the following form:

`LOGNORM.DIST(x,mean,dispersion,cumulative)`, where x is the engineering demand parameter at which the probability of exceedance is to be evaluated, mean is λ, dispersion is ζ, and cumulative is true or false (if true, the cumulative distribution function is returned; if false, the probability density function is returned). Referring to the 10-story example, it was determined that a DDI of 0.00153 represents a 30% probability of exceedance of DS1 (mean demand = 0.0021, dispersion = 0.6). This can be calculated using `LOGNORM.DIST(0.00153,ln(0.0021),0.6,TRUE)=0.30`.

In Mathcad (Parametric Technology Corporation, 2007) the fragility curve is created with the `plnorm` function, of the form `plnorm(x,mean,dispersion)`, where the required inputs are defined in the same manner as the Excel function.

NOMENCLATURE

Abbreviations

DDI	Deformation damage index
DDZ	Deformation damageable zone
DG	Damage gage
DM	Damage measure
DS	Damage state
EDP	Engineering demand parameter
IDI	Interstory drift index
MRI	Mean recurrence interval
PACT	Performance Assessment Calculation Tool
PBEE	Performance Based Earthquake Engineering
PBWE	Performance Based Wind Engineering

Symbols

δ_{M25}	Deformation parameter under *25*-year MRI
δ_{Mx}	Deformation parameter under *x*-year MRI
λ	Mean of the natural log of the data set
ζ	Standard deviation of the natural log of the data set (dispersion)
G	Shear modulus
G_{M25}	Wind gust factor under *25*-year MRI
G_{Mx}	Wind gust factor under *x*-year MRI
H	Interstory height
L	Width of Deformation Damage Zone
i	Rank of sorted set of test data
K_d	Wind directionality factor (ASCE 7)
K_z	Velocity pressure exposure factor (ASCE 7)
K_{zt}	Topographic factor (ASCE 7)
M	Number of specimens in a set of test data
$P(Z > z)$	Probability of exceedance during time period, T
p_i	Probability of exceedance associated with data point i

q_z	Wind velocity pressure (ASCE 7)
T	Time period if interest for computing probability of exceedence
V_{M25}	Wind speed under *25*-year MRI
V_{Mx}	Wind speed under *x*-year MRI
X_i	*X*-coordinate of node *i*=A,B,C, or D of Drift Damage Zone
Y_i	*Y*-coordinate of node *i*=A,B,C, or D of Drift Damage Zone

REFERENCES

Ang, A.H.S., Tang, W.H. (2007), *Probability Concepts in Engineering: Emphasis on Applications in Civil & Environmental Engineering*, John Wiley & Sons, Inc., Hoboken, NJ.

Applied Technology Council (2013), "Wind Speed Web Site," < www.atcouncil.org/windspeed>

AISC (2010), *Specification for Structural Steel Buildings*, ANSI/AISC 360-10, American Institute of Steel Construction, Chicago, IL.

Algan, B. (1982), *Drift and Damage Considerations in Earthquake-Resistant Design of Reinforced Concrete Buildings*, PhD Dissertation, Department of Civil Engineering, University of Illinois, Urbana-Champaign, IL.

ASCE (1988), "Wind Drift Design of Steel-framed Buildings: State-of-the-art Report," *Journal of Structural Engineering*, Vol. 114, No. 9, pp. 2085-2108.

ASCE (2010), *Minimum Design Loads for Buildings and Other Structures*, ASCE 7, American Society of Civil Engineers, Reston, VA.

ASCE (2013), *Seismic Evaluation and Retrofit of Existing Buildings*, ASCE 41, American Society of Civil Engineers, Reston, VA.

Baker, W.D., (1990), "Sizing Techniques for Lateral Systems in Multi-Story Buildings," *Proceedings of the 4th World Congress on Tall Buildings*, Council on Tall Buildings and Urban Habitat, pp 857-868.

Bentley (2013), http://www.bentley.com/en-US/Products/RAM+Frame/

Berding, D.C. (2006), *Wind Drift Design of Steel Framed Buildings: An Analytical Study and a Survey of the Practice*, M.S. Thesis, Department of Civil and Environmental Engineering, Virginia Tech, Blacksburg, VA.

Chan, C.M., Huang, M.F., and Kwok, K.C.S. (2010), "Integrated Wind Load Analysis and Stiffness Optimization of Tall Buildings with 3D Modes", Engineering Structures, 31:1252-1261.

Charney, F.A. (1990a), "Sources of Elastic Deformation in Laterally Loaded Steel Frame and Tube Structures," *Proceedings of the Fourth World Congress on Tall Buildings*, Council on Tall Buildings and Urban Habitat, Bethlehem, PA, pp. 893–915.

Charney, F.A. (1990b), "Wind Drift Serviceability Limit State Design of Multistory Buildings," *Journal of Wind Engineering & Industrial Aerodynamics*, Vol. 36, No. 1-3, pp. 203-212.

Charney, F.A. (1991), "The Use of Displacement Participation Factors in the Optimization of Drift Controlled Buildings," *Proceedings of the Second Conference on Tall Buildings in Seismic Regions*, Los Angeles, Council on Tall Buildings and Urban Habitat, pp. 91-98.

Charney, F.A. (1993), "Economy of Steel Framed Buildings through Identification of Structural Behavior," *Proceedings of the Spring 1993 AISC Steel Construction Conference*, Orlando, FL.

Charney, F.A., Berding, D.C. (2007), "Analysis and Commentary on the Results of a Nationwide State-of-the-Practice Survey on Wind Drift Analysis and Design," *Proceedings of the 2007 Structures Congress*, Long Beach, CA, pp. 1-10.

Charney, F.A., Marshall, J. (2006), "A Comparison of the Krawinkler and Scissors Models for Including Beam-Column Joint Deformations in the Analysis of Moment-Resisting Steel Frames," *Engineering Journal*, Vol. 43, No. 1, pp. 31-48.

Charney, F.A., Pathak, R. (2008), "Sources of Elastic Deformation in Steel Frame and Framed-tube Structures: Part 1: Simplified Subassemblage Models," *Journal of Constructional Steel Research*, Vol. 64, No. 1, pp. 87-100.

Ciampoli, M., Petrine, F,. and Augusti, G. (2011), "Performance Based Wind Engineering – Towards a General Procedure", *Structural Safety*, 33:367-378.

Committee on Serviceability Research (1986), "Structural Serviceability: A Critical Appraisal and Research Needs," *Journal of Structural Engineering*, Vol. 112, No. 12, pp. 2646-2664.

Computers and Structures, Inc. (2009), *SAP2000* (version 14.0.0), CSI, Berkeley, CA.

Dymiotis-Wellington, C., and Vlachaka, C. (2004), "Serviceability Limit State Criteria for the Seismic Assessment of R/C Buildings", 13th World Congress on Earthquake Engineering, Vancouver, BC.

Ellingwood, B.R., Culver, C.G. (1977), "Analysis of Living Loads in Office Buildings," *Journal of the Structural Division*, Vol. 103, No. 8, pp. 1551-1560.

FEMA (2012a), "2009 NEHRP Recommended Seismic Provisions: Design Examples," FEMA P-751, prepared by the Building Seismic Safety Council for FEMA, Washington, D.C.

FEMA (2013a), "Seismic Performance Assessment of Buildings: Volume 1 – Methodology," FEMA P-58-1, prepared by the Applied Technology Council for FEMA, Washington, D.C.

FEMA (2013b), “Seismic Performance Assessment of Buildings: Volume 3 – Supporting Electronic Materials and Background Documentation,” FEMA P-58-3, prepared by the Applied Technology Council for FEMA, Washington, D.C.

Flores, F., and Charney, F.A. (2013), “Influence of Gravity Framing on the Seismic Peformance of Steel Moment Frames”. *Journal of Constructional Research* (submitted).

Galambos, T.V., Ellingwood, B.R. (1986), “Serviceability Limit States: Deflection,” *Journal of Structural Engineering*, Vol. 112, No. 1, pp. 67-84.

Griffis, L.G. (1993), “Serviceability Limit States Under Wind Loads,” *Engineering Journal*, Vol. 30, No. 1, pp. 1-16.

Griffis, L.G., Patel, V., Muthukumar, S., Baldava, S. (2012), “A Framework for Performance-Based Wind Engineering,” *Proceedings of the ATC-SEI Advances in Hurricane Engineering Conference*, Miami, FL.

ICC (2012), *ICC Performance Code for Buildings and Facilities*, International Code Council, Washington, D.C.

Lee, T., Kato, M., Matsumiya, T., Suita, K., Nakashima, M. (2006), “Seismic Performance Evaluation of Non-structural Components: Drywall Partitions,” *Earthquake Engng Struct Dyn*, Vol. 36, No. 3, pp. 367-382.

Leon, R.T., Hoffman, J.J., Staegar, T. (1996), *AISC Design Guide 8: Partially Restrained Composite Connections*, American Institute of Steel Construction, Chicago, IL.

Microsoft Corporation, (2013). *Microsoft Excel*, Microsoft, Redmond, WA.

Miranda, E., Mosqueda, G. (2013), “Seismic Fragility of Building Interior Cold-Formed Steel Framed Gypsum Partition Walls,” *Background Document, FEMA P-58/BD-3.9.2*, Applied Technology Council, Redwood City, CA

Moehle, J., Deierlein, G.G. (2004), “A Framework Methodology for Performance-based Earthquake Engineering,” *Proceedings of the 13th World Conference on Earthquake Engineering*, Vancouver, CA.

O'Brien, W., Memari, A., Kremer, P., Behr, R. (2012), "Fragility Curves for Architectural Glass in Stick-Built Glazing Systems," *Earthquake Spectra*, Vol. 2, No. 28, pp. 639-665.

Parametric Technology Corporation, (2007). *Mathcad*, PTC, Needham, MA.

Paulotto, C., Ciampoli, M., Augusti, G. (2004), "Some Proposals for a First Step Towards a Performance Based Wind Engineering," *Proceeding of First International Forum in Engineering Decision Making*, Stoos, CH.

PEER (2010), *Guidelines for performance-based seismic design of tall buildings*. Report 2010/05, November 2010, prepared by the TBI Guidelines Working Group, Pacific Earthquake Engineering Research Center, University of California, Berkeley, California.

Peterka, J.A., Shahid, S. (1998), "Design Gust Wind Speeds in the United States," *Journal of Structural Engineering*, Vol. 124, No. 2, pp. 207-214.

Porter, K., Kennedy, R., Bachman, R. (2007), "Creating Fragility Functions for Performance-based Earthquake Engineering," *Earthquake Spectra*, Vol. 23, No.2, pp. 471-489.

Reiter, L. (1990), *Earthquake Hazard Analysis: Issues and Insights*, Columbia University Press, New York, NY.

Schaffhausen, R., Wegmuller, A. (1977), "Multistory Rigid Frames with Composite Girders Under Gravity and Lateral Forces," *Engineering Journal*, 2nd Quarter, pp. 68-77.

Tallin, A., Ellingwod, B.R. (1984), "Serviceability Limit States: Wind Induced Vibrations," *Journal of Structural Engineering*, Vol. 110, No. 10, pp. 2424-2437.

Vallenilla, C., Bjorhovde, R. (1985), "Effective Width Criteria for Composite Beams," *Engineering Journal*, 4th Quarter.

Velivasakis,E., and DeScenza, R. (1983), "Design Optimization of Lateral Load Resisting Frameworks," *Proceedings of the 8th Conference on Electronic Computation*, ASCE, pp 130-143.

West, M., Fisher, J., Griffis, L. (2003), *AISC Design Guide 3: Serviceability Design Considerations for Steel Buildings*, American Institute of Steel Construction, Chicago, IL.

4 Linear Response History Analysis – Literature Review

Linear response history analysis (LRHA) is one of several methods allowed in the current edition of ASCE 7 (ASCE 2010). It can be used as either a design method or a performance assessment method. Like the other permitted methods, it has its own advantages and drawbacks. Chief among its advantages are its explicit handling of dynamic behavior and its ability to preserve the signs and directions of forces, moments, and displacements (as opposed to the modal response spectrum analysis procedure which loses the signs of the results due to its combination rules). Disadvantages of the LRHA include the ambiguity of the ground motion selection and scaling requirements and its treatment of inelastic behavior through the use of the response modification (*R*) factor. Further possible disadvantages of LRHA are discussed in the Commentary to the National Building Code of Canada (NRCC 2010b): "i) such analyses produce voluminous amounts of data to be interpreted and, ii) the results depend greatly on the characteristics of the individual ground shaking accelerograms so that the analyses need to be done using a number of different time-histories." The effects of these disadvantages identified by the National Building Code of Canada can be reduced through the use of spectral matched ground motions, which allow for fewer ground motions to be used thus reducing the large amounts of data produced.

The following literature review covers the pertinent aspects of LRHA, including ground motion selection and scaling, the use of the *R*-factor, structural modeling, and LRHA guidelines and procedures in current building codes. This literature review is in support Chapter 5, which

contains a paper and proposed code language for the 2014 NEHRP Recommended Seismic Provisions and, ultimately, the 2016 edition of ASCE 7.

4.1 Response History Analysis

Response history analysis (RHA) is the calculation of the response of a structural model at various points in time to a ground motion. The procedure inherently considers the dynamics of the structure. The calculated response can be many different values with the most common being displacement and its time derivatives (velocity and acceleration). There are two methods for performing LRHA: modal analysis and direct integration. The modal LRHA is the most efficient method because it decomposes the multi degree of freedom (MDOF) system into modes, determines the response of each mode to the excitation, and then combines the modes to arrive at a final response. Using this method the engineer can specify the number of modes to include. The more modes that are included, the more accurate the solution becomes. Generally speaking, only a fraction of the complete set of elastic modes are sufficient to achieve a solution that is reasonably accurate. The direct integration method does not decompose the MDOF system, and instead directly integrates the equation of motion, inherently including all modes. This method is considered "exact" but is significantly more computationally expensive than modal analysis. Other advantages of modal response history analysis include the ability to obtain an exact solution for each mode's response using the piecewise linear approach, the ability to directly specify a damping ratio in each mode, and reduced computational storage requirements. In most cases modal analysis with a limited number of modes is sufficiently accurate, and the remainder of this text will assume that the modal LRHA procedure is employed.

4.2 Ground Motion Selection and Scaling

4.2.1 Selection

Many building codes provide some guidance on the selection of ground motions for use in response history analysis (see Section 4.6). The guidance, however, is typically relatively vague and of little real use. For example, ASCE 7 (2010) states that selected ground motions "shall be obtained from records of events having magnitudes, fault distance, and source mechanisms that are consistent with those that control the maximum considered earthquake." Simulated ground motions are permitted where recorded ones are not available. The code gives no direction relating to methods to determine the controlling magnitude, distance, and source mechanisms for a site (although there are tools available). Furthermore, it is left to the discretion of the engineer to determine if the characteristics of the earthquake are "consistent" with the controlling characteristics. For example, if the controlling magnitude is 6.7, is a ground motion recorded from a magnitude 6.1 earthquake consistent?

Considerations when selecting ground motions include the magnitude, fault distance, source mechanism, soil type, duration, spectral shape, peak ground acceleration, statistical independence of the orthogonal components of the pairs, usable period range, and time increment of the recording. Several of these considerations are included in various national building codes, with magnitude and distance being amongst the most common required considerations. For a more detailed summary of the selection requirements see Tola (2010), in which the provisions of ASCE 7-10, ASCE 4-98, the National Building Code of Canada, the New Zealand Standard, and Eurocode 8 are compared.

Much of the published literature relating to ground motion selection and scaling is related to nonlinear analysis, and indeed the parameters of the selection and scaling process are more important for nonlinear than for linear analysis. For example, duration of the earthquake is much more significant for nonlinear analysis than for linear analysis, due to the effect that yielding of the structure during the ground motion has on the response. Recent papers discussing selection of ground motions for NRHA are Kadas et al. (2011), Masi et al. (2010), Huang et al. (2011), Hines et al. (2011), and Heo et al. (2011).

A document of particular interest is NIST GCR 11-917-15, *Selecting and Scaling Earthquake Ground Motions for Performing Response-History Analyses* (NEHRP 2011). This document is intended for use in selecting and scaling ground motions for nonlinear analysis, but it contains valuable information that can be applied to LRHA as well. The document reviews relevant standards in the United States in addition to presenting "problem-focused studies." One of the problem-focused studies relates to response spectrum matching, studying (amongst other things) the precision of spectral matching and its effect on ground motions with velocity pulses.

4.2.2 Scaling Procedures

The scaling of ground motions to a target spectrum aids in the normalization of the response of various ground motions. Typically ground motions are scaled such that their acceleration response spectra exceed a certain threshold (for example the design spectrum) over a certain period range. Sources of debate include the procedures to determine the scale factors, the target spectrum itself (in some cases it is required that the mean of the individual spectra exceed 90%

of the target spectrum), and the period range. See Section 4.6 for discussion of the scaling procedures of the national building codes, as well as Tola (2010) for a more detailed review.

One useful scaling procedure will be discussed here because of its applicability to ASCE 7 (2010). The procedure is proposed by Charney (2010). It specifically addresses the fact that two engineers scaling the same set of ground motions to the same target spectrum will likely produce different scale factors for each ground motion. In fact, there are an infinite number of scale factors that satisfy scaling requirements of ASCE 7-10, which for 2D analysis simply state that the mean 5% damped spectra for the ground motion suite must equal or exceed the design spectrum over the period range of $0.2T$ to $1.5T$. This is illustrated by the following example. Figure 4-1 shows the ASCE 7-10 elastic design spectrum for S_{DS} = 1.2 g and S_{D1} = 0.6 g along with the unscaled response spectra of component "a" of each of the following three earthquakes from the FEMA P-695 Far-Field Record Set (FEMA 2009b): 1994 Northridge (Beverly Hills – Mulhol); 1995 Kobe, Japan (Nishi-Akashi); and 1989 Loma Prieta (Capitola). Table 4-1 contains five sets of different scale factors (assuming that T = 2 sec), each of which satisfy the requirements of ASCE 7-10, but which are vastly different from each other. Figure 4-2 shows the five different average spectra computed using the scale factors from Table 4-1. Note that although each of these average spectra satisfy the requirements of ASCE 7-10, there are wide variations between them. Also note that in each case, the scaling point is controlled by the upper bound of the period range (T = 3 sec). The average spectrum corresponding to Set 5 is scaled using the procedure recommended by Charney (2010), which produces a unique set of scale factors. This process is summarized in the following steps:

1. Each ground motion is multiplied by an FPS_i (fundamental period scale) factor which adjusts the ground motion so that its response spectrum matches the target spectrum at the fundamental period T. Each ground motion i will have a different FPS_i factor.
2. The average of the suite of ground motions (multiplied by their respective FPS_i factors) is multiplied by a second scale factor called the SS (suite scale) factor. This factor is calculated such that the average spectrum does not fall below the target spectrum over the period range $0.2T$ to $1.5T$ (this range is shown as vertical dotted lines in Figure 4-2).
3. The final combined scale factor CS_i is equal to $FPS_i \times SS$.

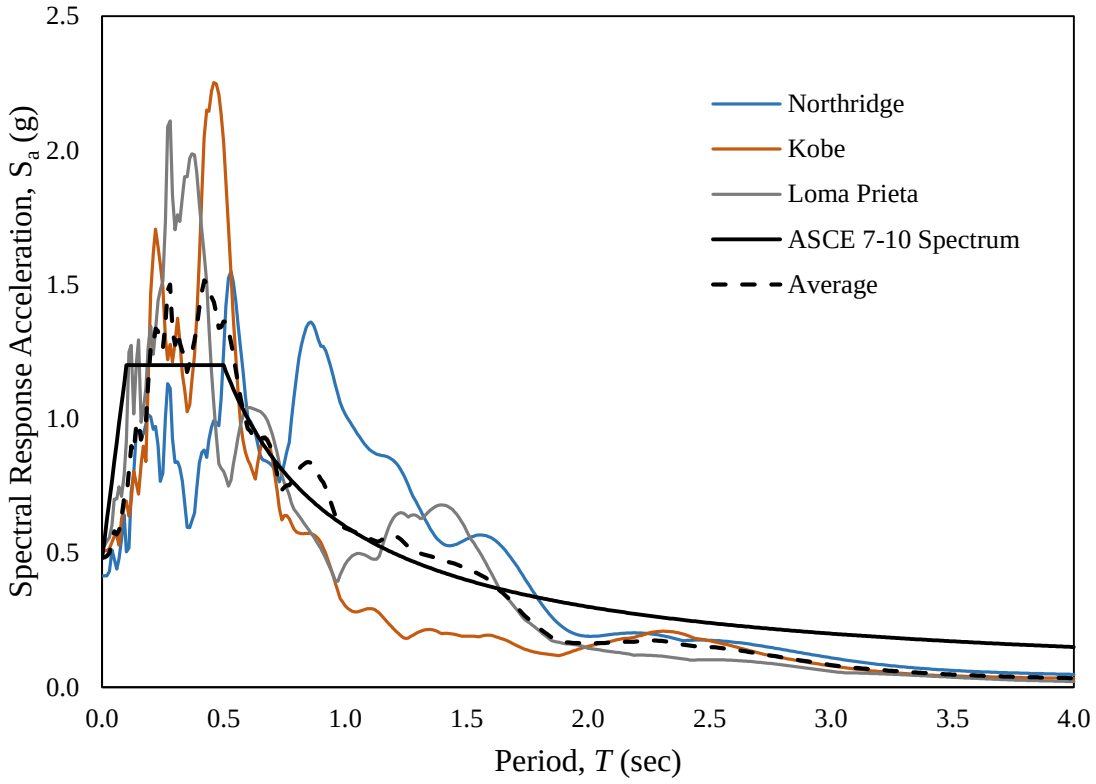

Figure 4-1. Acceleration Response Spectra for Three Earthquakes Compared to ASCE 7-10 Design Spectrum

Table 4-1. Five Sets of Scale Factors Satisfying ASCE 7-10 Scaling Requirements

	Scale Factor				
Ground Motion	Set 1	Set 2	Set 3	Set 4	Set 5
Northridge	1.00	1.00	4.18	2.40	1.42
Kobe	1.00	5.39	1.00	2.40	2.79
Loma Prieta	6.83	1.00	1.00	2.40	3.67

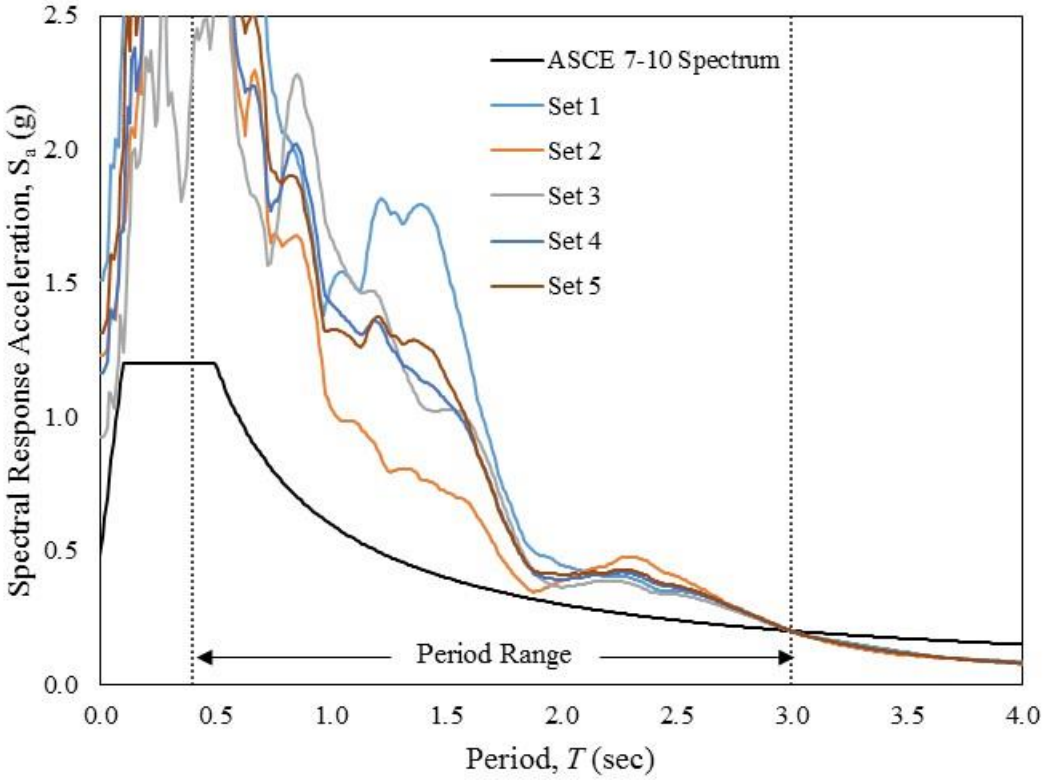

Figure 4-2. Five Average Spectra Based on Scale Factors from Table 4-1

4.2.2.1 Maximum Direction Spectrum

When two horizontal orthogonal earthquake components are used they can be rotated about a vertical axis to produce the horizontal acceleration component at any angle θ using the following formula.

$$a_\theta(t) = a_x(t)\cos(\theta) - a_y(t)\sin(\theta) \quad (4.1)$$

where:

$a_\theta(t)$ = acceleration component rotated an angle θ from the x-axis
$a_x(t)$ = recorded acceleration component in the x direction
$a_y(t)$ = recorded acceleration component in the y direction
θ = angle of rotation of the calculated component, measured counter-clockwise from the positive x-axis

A maximum-direction spectrum can be created by determining the rotation angle θ which produces the maximum response of a SDOF oscillator for each period increment in the period range. The maximum-direction spectrum, then, is an envelope of the maximum response of the oscillator to all orientation angles of the ground motion components. It is significant that the maximum-direction spectrum, unlike the SRSS or geomean spectrum, is not dependent on the orientation of the initial ground motion recordings. The orientation angle that produces the maximum response for each period in the period range can be determined by calculating the response across the entire applicable range of angles (at sufficiently small angle increments, such as 1°). A more efficient method, however, is described in Athanatopoulou (2004). This method requires the response to be calculated for only one arbitrary orientation, and from the results the critical angle (which produces the maximum oscillator response) can be determined.

The following is a description of an algorithm along with pseudo-code which could be used to generate a maximum direction response spectrum (Charney 2013). The preliminary steps are:

1. Create vector arrays of the ground motion acceleration histories. These vector arrays are referred to as *X* and *Y*. Each record has *nApoints*, and a digitization interval of *dt*. Units are in length/sec^2.
2. Create a vector array of equally spaced periods at which the response spectrum ordinates are to be computed. We will refer to this array as *T*. It will have *nTpoints* at an interval of *dT*.

3. Selecting a damping ratio, *xi*.
4. Select an angle increment *dA*. We will rotate from angle 0 to 180 degrees in this increment.
5. Use a solver (called Solveit below) that can compute the displacement history. This algorithm assumes that Solveit is a separate function, which is independent of the algorithm.
6. Use the following pseudo-code to calculate the maximum direction spectrum.

```
For i=1 to nTpoints
     T=T(i)
     w=2*pi/T
     XDir=Solveit(X,T,dt,xi)
     YDir=Solveit(Y,T,dt,xi)
     RSmax=0
For j=0,180,dA
          Ang=j*dA*pi/180
          R=(Xdir*cos(Ang)+YDir*sin(Ang))*w*w
          Rmin=Abs(min(R))
          Rmax=max(R)
          Rmax=max(Rmin,Rmax)
          RSmax=Rmax if Rmax > RSmax
Next j
Resp(i)=RSmax
Next i
```

The geomean spectrum is calculated for a specific earthquake by taking the geometric mean (the square root of the product) of the two horizontal components. The geomean spectrum is bound by the two horizontal response spectra used to create it (i.e. it is a measure of the average, and so always falls between the two component spectra). In general, it has been found that the maximum-direction spectrum for an event is approximately 1.2 to 1.35 times the geomean spectrum (Stewart et al. 2011).

4.2.3 Required Number of Ground Motions

The required number of sets of ground motions depends on the nature and purpose of the response history analysis. The following is a partial list of factors that contribute to the determination of the minimum required number of ground motion sets (NEHRP 2011):

- Desired results (mean values vs. variation in response)
- Expected extent of inelastic behavior
- Significance of higher mode effects
- Quality of the mathematical structural model
- Desired accuracy of the response

If the only the mean response is desired (as is typical for design) then fewer ground motions can be used. If the variation in a response quantity is required, many more ground motions must be used. Furthermore, increased inelastic behavior and higher mode effects lead to a higher number of required ground motions. For models with explicit modeling of inelastic behavior in which the mean response is desired, at least seven sets of ground motions should be used. For the same models in which the variation in the response is desired (e.g. if a performance based seismic analysis is being conducted) then at least 30 sets of ground motions should be used (NEHRP 2011).

ASCE 7 (2010) requires a minimum of three sets of ground motions when using the maximum computed response, and seven ground motions when using the average of the responses. Other building codes require a different number of earthquakes. As discussed in Section 4.6, the NBCC (NRCC 2010a) has no specific requirement, ASCE 4-98 (ASCE 2000) requires a minimum of only one ground motion, and Eurocode 8 (CEN 2004) requires three.

4.3 Spectral Matching

4.3.1 Introduction

Response spectrum matching (or spectral matching) is the non-uniform scaling of a ground motion such that its acceleration response spectrum closely matches some target response spectrum (Hancock et al. 2006). Figure 4-3 shows an example of spectral matching, where the response spectrum of the original ground motion is plotted alongside the response spectrum of the modified ground motion and compared to the target spectrum. The main advantage of using spectral matched ground motions is the reduction in variability of the response (NEHRP 2011). Compared to using amplitude-scaled ground motions, fewer spectral matched ground motions can be used to arrive at an estimate of mean response.

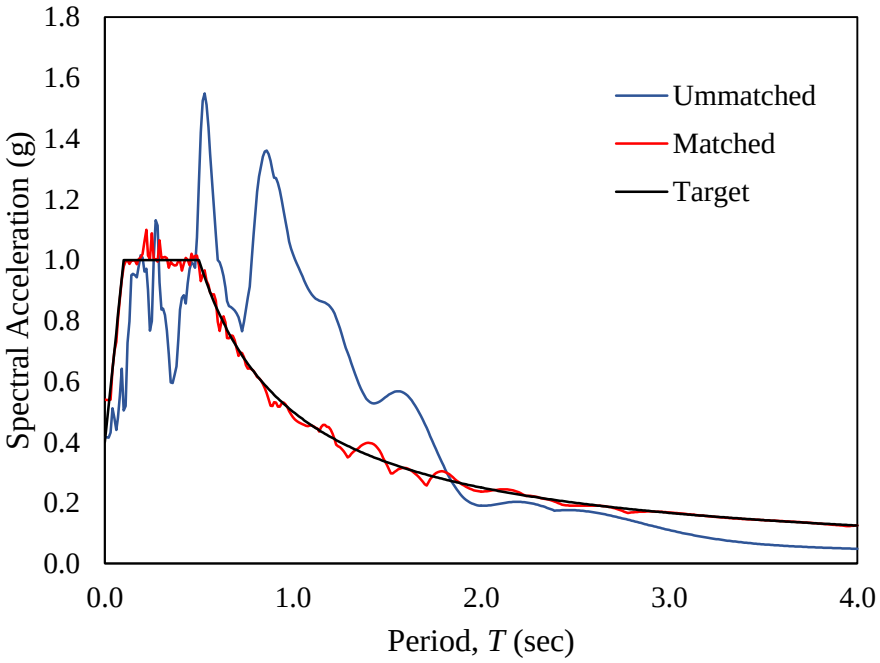

Figure 4-3. Spectral Matched and Unmatched Response Spectra vs. Target Spectrum

Disadvantages of using spectral matched ground motions include the inability to effectively calculate variance in response. The motions have been altered to produce a response spectrum

which matches a target, and therefore cannot be used to estimate anything except the mean response. For design purposes, this is often acceptable, but in certain circumstances (for example, performance based earthquake engineering), the variation in response is of interest. Other disadvantages include the fact that a spectral matched ground motion produces a response spectrum that is matched to a target spectrum, which is a smoothed envelope of the response from many different earthquakes. This may lead to a ground motion which is overly conservative (Al Atik and Abrahamson 2010). Furthermore, the smooth response spectrum of a spectral matched ground motion is unrealistic in comparison to the jagged response spectrum typical of a ground motion (Al Atik and Abrahamson 2010). Additional issues (such as overestimation of displacement demand and energy input) associated with using response spectrum matched ground motions are discussed in Naeim and Lew (1995). Several researchers have identified bias in the response of inelastic systems when using spectral matched ground motions (NEHRP 2011). The use of spectral matched ground motions for nonlinear analysis is a point of contention within the literature, and although it does not directly relate to the topic of this literature review (i.e. linear analysis), interested readers may find additional information related to the use of spectral matched ground motions for nonlinear analysis in Heo et al. (2011), Fahjan and Ozdemir (2008), Luco and Bazzurro (2007), and Hancock and Bommer (2007).

There are several methods to modify a ground motion to match a response spectrum. Preumont (1984) provides an overview of spectral matching procedures. In general, the matching is performed in either the frequency domain or the time domain. Additionally, the ground motions that are altered (i.e. the seed ground motions) are preferably actual recorded ground motions, but theoretically any ground motion will serve, even those generated as random "white noise."

Spectral matching software usually cannot be relied upon to produce certain characteristics such as velocity pulses within the time series itself. Therefore if a characteristic such as a velocity pulse is desired, the seed ground motion should exhibit the desired trait and a spectral matching algorithm should be used that best preserves the original characteristics of the ground motion. Grant et al. (2008) outlines important considerations in the selection of seed ground motions for spectral matching applications.

4.3.2 Frequency Domain Methods

Response spectrum matching methods in the frequency domain consist of modifying the Fourier amplitude spectrum (FAS) of the ground motion (Hancock et al. 2006, Rizzo et al. 1975). After the FAS is altered the matched ground motion is recovered through the inverse Fourier transform function (Bozorgnia and Bertero 2004). The process is iterative; after each iteration the response spectrum more closely matches the target spectrum. However, the procedure tends to distort the velocity and displacement records (computed by single and double integration, respectively) and result in ground motions with exaggerated energy contents. Additionally, the frequency domain methods lack strong convergence properties and can significantly alter the nonstationary characteristics of the ground motion, resulting in acceleration records that no longer resemble actual earthquake time series (Al Atik and Abrahamson 2010). A modified technique involves first making large adjustments to the FAS using random vibration theory and then making smaller adjustments using the previously described frequency domain method (Al Atik and Abrahamson 2010).

4.3.3 Time Domain Methods

Time domain methods of response spectrum matching consist altering the original acceleration series by the addition of wavelets at select times. The formal algorithm was originally proposed by Kaul (1978) and was modified by Lilhanand and Tseng (1988). The time domain method is more complex than the frequency domain method, but it possess better convergence properties and typically better conserves the nonstationary characteristics of the ground motion (Al Atik and Abrahamson 2010). Further discussion of a specific application of the time domain method of spectral matching with a program called RspMatch is provided in the next section.

4.3.4 RspMatch

Abrahamson (1992) proposed an improvement to the original Lilhanand and Tseng (1988) method in order to better preserve the characteristics of the ground motion (Al Atik and Abrahamson 2010). The method was implemented in the program RspMatch. The program has been improved and updated throughout its history; the latest version, RspMatch2009, is described in Al Atik and Abrahamson (2010).

The following discussion of RspMatch is based on Lilhanand and Tseng (1988), Al Atik and Abrahamson (2010), and Hancock et al. (2006). The program operates by adding acceleration wavelets to the original acceleration time series. One wavelet is added for each period in the matching range. A wavelet is an adjustment function $fj(t)$ with zero average and finite duration which amplifies the ground motion at the time of the peak response. For example, if it is determined that the peak response of a one second period oscillator occurs at a time 10 seconds into the ground motion, the adjustment wavelet is added to the ground motion at 10 seconds.

Figure 4-4 shows two common adjustment wavelets; Figure 4-4(a) shows the original reverse acceleration impulse response function wavelet proposed by Lilhanand and Tseng (1988) and Figure 4-4(b) shows the tapered cosine wavelet used in RspMatch2005 by Hancock et al. (2006).

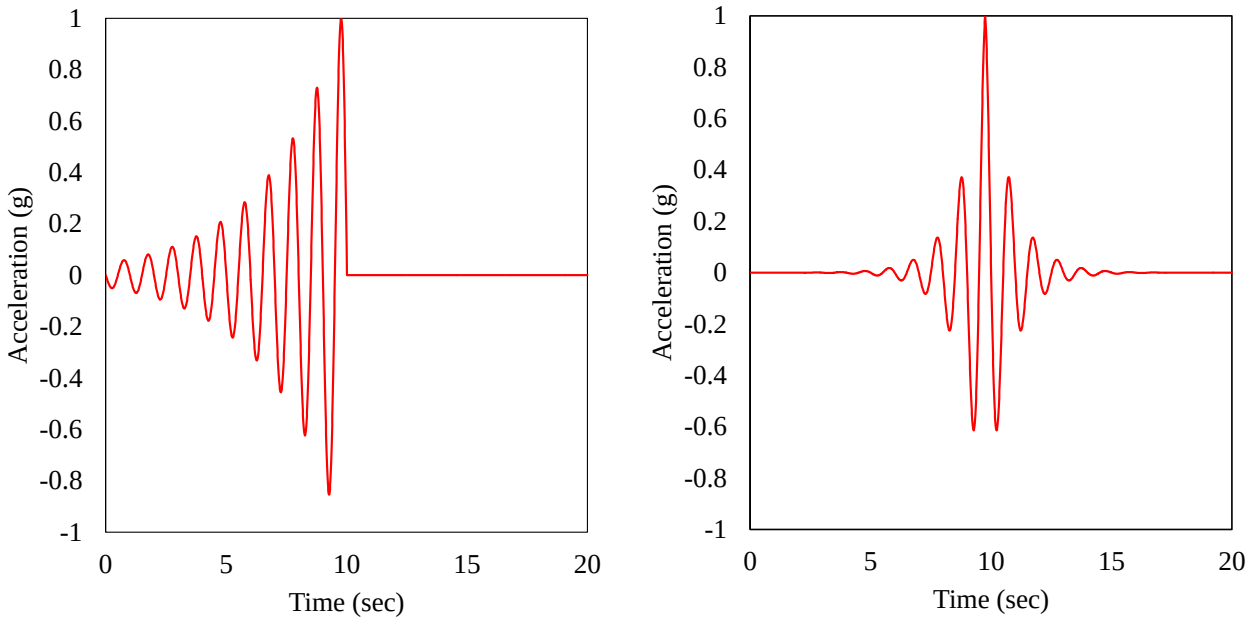

Figure 4-4. (a) Reverse Acceleration Impulse Response Function Wavelet and (b) Tapered Cosine Wavelet

RspMatch operates on the assumption that the time of peak response does not change due to the addition of the wavelets. This assumption, however, is not always valid. This is due to the effect that the wavelets have on neighboring periods. A wavelet added to alter the response of one period at one damping level affects the response of other periods and other damping levels. This can cause the peak response for each period to shift slightly in time in one of two ways: the peak response changes phase or a peak that was formerly secondary becomes critical (Hancock et al. 2006). This shifting of the peak responses renders the spectral matching problem nonlinear (if the times of peak responses were invariant with additional wavelets the problem would be linear and require only one iteration to solve). Revisions, updates, and improvements to the time domain method of spectral matching center around employing alternative wavelets and nonlinear

solving procedures. For additional information on proposed nonlinear techniques see Adekristi (2013).

The following description of the RspMatch algorithm is largely based on Al Atik and Abrahamson (2010). RspMatch functions by first calculating the spectral misfit (or mismatch) ΔR_i, which is the difference between the acceleration series' response spectrum and the target spectrum:

$$\Delta R_i = (Q_i - R_i)P_i \qquad (4.2)$$

where:

Q_i = target spectral value at period T_i
R_i = time series spectral value at period T_i
P_i = polarity of the peak response (equal to 1 if peak response is positive, -1 if peak response is negative)

The next step is to determine the adjustment time series $\delta a(t)$ to be added to $a(t)$. The adjustment function should have a response at time t_i equal to ΔR_i for all i. In this way, the combination of $a(t)$ and $\delta a(t)$ will produce an acceleration series with a response spectra R_i which matches the target spectra Q_i at all values (assuming the problem is linear, which is not truly the case). The function $\delta a(t)$ is determined with the following equation:

$$\delta a(t) = \sum_{j=1}^{N} b_j f_j(t) \qquad (4.3)$$

where:

$f_j(t)$ = set of adjustment functions (wavelets)
b_j = set of adjustment function amplitudes
N = number of points to be matched (pairs of frequency/period and damping values)

The response δR_i to the adjustment time series is:

$$\delta R_i = \int_0^\infty \delta a(\tau) h_i(t_i - \tau) d\tau \qquad (4.4)$$

where:

$h_i(t)$ = acceleration impulse response function of a SDOF oscillator with frequency ω_i and damping β_i

Inserting Eq. 4.2 into Eq. 4.3 yields:

$$\delta R_i = \sum_{j=1}^{N} b_j \int_0^\infty f_j(\tau) h_i(t_i - \tau) d\tau \qquad (4.5)$$

The acceleration impulse response function $h_i(t)$ is:

$$h_i(t) = \frac{-\omega_i}{\sqrt{1-\beta_i^2}} \exp(-\omega_i \beta_i t) \left[(2\beta_i^2 - 1) \sin(\omega_i' t) - 2\beta_i \sqrt{1-\beta_i^2} \cos(\omega_i' t) \right] \qquad (4.6)$$

where:

$$\omega_i' = \omega_i \sqrt{1-\beta_i^2}$$

and the function $h_i(t)$ is equal to zero for t less than zero. The response of a SDOF oscillator with the i^{th} frequency and damping at time t_i to the adjustment function $f_j(t)$ is:

$$c_{ij} = \int_0^{t_i} f_j(\tau) h_i(t_i - \tau) \delta\tau \qquad (4.7)$$

Inserting Eq. 4.6 into Eq. 4.4 yields:

$$\delta R_i = \sum_{j=1}^{N} b_j c_{ij} \qquad (4.8)$$

The response of the adjustment series δR_i should be close to or equal to the spectral misfit ΔR_i. The amplitude of the adjustment wavelets can be calculated with:

$$\mathbf{b} = \mathbf{C}^{-1} \delta \mathbf{R} \qquad (4.9)$$

The elements of the square matrix **C** contain the amplitudes of the SDOF oscillator response at the time of peak response t_i to each adjustment wavelet $f_j(t)$. The adjustment series $\delta a(t)$ can be recovered by summing the adjustment wavelets multiplied by their appropriate amplitudes from the **b** matrix. The new acceleration series, then, is:

$$a_1(t) = a(t) + \gamma \delta a(t) \quad (4.10)$$

where:

γ = parameter between 0 and 1 intended to damp the adjustments between iterations

Due to the nonlinearity of the problem (i.e. **C** is not a diagonal matrix) multiple iterations will be required. A target accuracy can be specified (e.g. a spectral mismatch of no more than 5%) and the solution can be repeated until the target is achieved.

A modified version of RspMatch was developed by Grant (2010). The program, called RspMatchBi, was created to simultaneously match two components of ground motion to two separate target spectra (which are the orientation-independent minor and major axis spectra).

4.3.5 Scaling of Spectral Matched Records

There are several methods to scale spectral matched records to the target spectrum. One potential option is to scale according to the 3D scaling requirements of ASCE 7 (2010), which makes use of the square root sum of the squares (SRSS) spectrum. Other methods include scaling such that the response spectra match the target only at the fundamental period of vibration (T), scaling the average of the orthogonal components independently, or scaling using the maximum direction response spectrum

Table 4-2 contains a summary of scale factors calculated for three pairs of spectral matched ground motions. The original ground motions were matched using RspMatch to a target spectrum defined by S_{DS} = 1.00g and S_{D1} = 0.50g. The eight different scaling procedures in the table are:

1) No scaling. The records are matched to the target spectrum and no additional modifications are performed. This first case is used as the reference for the remaining scale factors.
2) ASCE 7-10 SRSS. For each pair of records an SRSS spectrum is constructed. Each SRSS spectrum is scaled such that it matches the target spectrum at the fundamental period, and then the average of the SRSS spectra for the suite is scaled such that it equals or exceeds the target between T_{90} and 1.0T, where T_{90} is the period required to reach an effective mass participation of 90% of the actual mass.
3) Each individual component spectrum is scaled such that it matches the target spectrum at the fundamental period.
4) The average of the spectra for all components in each orthogonal direction is scaled such that it equals or exceeds the target spectrum over the period range 0.2T to 2.0T.
5) The same as 4), except the period range is 0.2T to 1.0T.
6) The same as 4), except the average spectra are scaled to exceed 90% of the target (instead of 100%).
7) The same as 6), except the period range is 0.2T to 1.0T.
8) For each ground motion a maximum direction spectrum is constructed. The ground motions are first scaled such that each maximum direction spectrum matches the target spectrum at the fundamental period. A second scale factor is then applied to the entire

suite of ground motions such that the average of the maximum direction spectra equals or exceeds 90% of the target spectrum over the period range 0.2*T* to 2.0*T*.

Table 4-2. Scaling of Spectral Matched Ground Motions

Scaling Procedure			Ground Motion 1		Ground Motion 2		Ground Motion 3	
No.	Scaling Description	Period Range	Comp. a	Comp. b	Comp. a	Comp. b	Comp. a	Comp. b
1	No scaling	-	1.000	1.000	1.000	1.000	1.000	1.000
2	ASCE 7-10 SRSS	T_{90} to 1.0*T*	0.714	0.714	0.729	0.729	0.737	0.737
3	Scaled to target at *T*	-	0.995	0.976	1.006	1.006	1.024	1.009
4	Spectral matched average (100% of target)	.2*T* to 2.0*T*	1.030	1.024	1.042	1.055	1.061	1.058
5	Spectral matched average (100% of target)	.2*T* to 1.0*T*	1.030	1.024	1.042	1.055	1.061	1.058
6	Spectral matched average (90% of target)	.2*T* to 2.0*T*	0.927	0.921	0.938	0.949	0.955	0.952
7	Spectral matched average (90% of target)	.2*T* to 1.0*T*	0.927	0.921	0.938	0.949	0.955	0.952
8	Maximum direction scaling (90% of target)	.2*T* to 2.0*T*	0.742	0.742	0.928	0.928	0.956	0.956

The highest scale factors belong to scaling procedures 4 and 5, in which the average spectra in each direction is scaled to 100% of the target. The reason there is no difference in the scale factors between procedures 4 and 5 (and likewise between 6 and 7) is because the controlling scaling point is between .2*T* and 1.0*T*, and thus extending the range beyond 1.0*T* does not affect the scaling results (in this particular case). The smallest scale factors belong to the SRSS scaling of ASCE 7-10. The second lowest are calculated with the maximum direction scaling procedure. The fact that the scale factors for the maximum direction scaling procedure (no. 8) are, on average, lower than those calculated for the spectral matching procedure (no. 6) can be viewed as something of a penalty on using spectral matching.

4.4 Response Modification Coefficient

4.4.1 Background

The response modification coefficient (R) is used by ASCE 7 (2010) as an approximate method to scale the seismic responses down from elastic levels to inelastic levels. The use of the response modification coefficient essentially guarantees that a structure will yield under the design bases earthquake. This is considered acceptable, and in fact some inelastic behavior is expected and even encouraged. The factor is predicated on the equal displacement rule, which assumes that elastic displacements of a structural system are approximately equal to inelastic displacements. The R factor is generally composed of system ductility and system overstrength. Overstrength is the reserve strength available to a structure from several sources, including material overstrength, design capacities higher than nominally required capacities, detailing requirements, drift requirements, structural redundancy, and force redistribution (FEMA 2009a).

4.4.2 Current Usage

The response modification coefficient is extensively applied in the standards of ASCE 7 (2010). The Equivalent Lateral Force (ELF) procedure, the response spectrum analysis (RSA), and the linear response history analysis procedure each make use of the factor to estimate inelastic demands on the structure. Forces are reduced by the factor $1/R$, and displacements are reduced by C_d/R, where C_d is the deflection amplification factor. A third seismic response factor is the overstrength factor Ω_0, which is used to amplify forces for components that cannot be assumed to possess reliable inelastic performance. In general, the R values are based on engineering judgment and past experience and lack any firm technical basis for determination (FEMA 2009a, Uang 1991, Whittaker et al. 1999). Table 12.2-1 of ASCE 7 (2010) contains the code values of

R, C_d, and Ω_0 for various structural systems. The values of R vary between 1 and 8; C_d varies between 1 and 6.5; and Ω_0 varies between 1.25 and 3. The FEMA P-695 project *Quantification of Building Seismic Performance Factors* (FEMA 2009b) is an attempt to make the calculation of R, C_d, and Ω_0 a more rational procedure.

In is standard practice in current design procedures to apply R to all vibrational modes during the analysis. This inherently assumes that the inelastic behavior is spread equally throughout the modes. However, there has been some disagreement on this, with some researchers suggesting that R may apply only to the first mode, or to the modes contributing the most to the response of the structure. Pugh (2013) discusses this concept as it relates to shear demands in concrete walls. If the first mode only is reduced and the higher modes are elastic, this has the effect of making the second mode the dominant mode in many cases. Eibl and Keintzel (1988) propose that only the first mode response be reduced by the response modification factor. This concept is gaining recognition for potential inclusion in building codes. Additional research should be performed to assess its accuracy in terms of predicting inelastic behavior.

4.5 Modeling Concerns

4.5.1 Damping

Damping is the mechanism by which energy is dissipated in a vibrating structure. Sources of damping in real structures include the thermal effects of elastic straining, internal friction of deforming materials, friction at connections, opening and closing of concrete cracks, and friction between structural and nonstructural components (Chopra 2012). It is exceedingly difficult to model each independent source of damping, and so the concept of equivalent viscous damping is

used, in which the damping force is proportional to the velocity (related by the viscous damping coefficient c). Typically the damping in a system is expressed as a percentage of critical damping (ζ), calculated with the following equation:

$$\zeta = \frac{c}{2m\omega_n} \qquad (4.11)$$

where:

c = viscous damping coefficient
m = system mass
ω_n = circular natural frequency of the system

The most commonly assumed damping ratio for a structure is 5% of critical, although the range can vary from 2% for low levels of deformation in steel or lightly cracked concrete to 20% for high levels of deformation in wood structures with nailed joints (Chopra 2012). ASCE 7 (2010) implicitly assumes that linear response history analysis will be performed with damping ratio of 5% (0.05), because the mapped spectral coordinates (and therefore the design response spectrum) are calculated for a 5% critically damped system. For nonlinear analysis the viscous damping ratio is often lower than for linear systems, due to the damping associated with the hysteretic behavior of the structural elements.

When performing modal LRHA the system is decomposed into its mode shapes and each mode is analyzed separately and then recombined to form the final solution. In this case, the damping matrix does not need to be constructed and instead a damping ratio is specified for each individual mode. However, for direct integration LRHA the full damping matrix must be constructed. One of the most common methods of constructing the damping matrix is through the use of Rayleigh damping, in which the damping is proportional to both stiffness and mass. It should be noted that with Rayleigh damping the damping ratio of two modes is specified (usually

5%) and the other modes are calculated from these two anchor points. An issue with Rayleigh damping is its resulting overdamping of higher modes, which can lead to unconservative results if higher mode effects are significant.

4.5.2 Direction of Loading

ASCE 7 (2010) Section 12.5 contains provisions relating to the direction of loading. The requirements become more stringent for higher seismic hazard. For Seismic Design Category (SDC) B, each orthogonal direction of the structure may be analyzed separately and the orthogonal interaction can be ignored. For SDC C, the requirements of SDC B apply, unless the structure contains a Type 5 horizontal structural irregularity (nonparallel system). If the irregularity is present, then the designer has two options: (1) analyze each direction independently and then design the members for 100% of the loading in one direction and 30% of the orthogonal loading, or (2) use linear response history analysis and apply the ground motions simultaneously in both directions. Additional requirements exist for columns or walls forming part of an intersecting lateral system in SDC D, E, or F. Wilson et al. (1995) discuss the potential inaccuracy and unconservatism of the "30% rule" (or in some codes the "40 % rule"), and propose a method in which an SRSS combination of 100% of the loads in each direction is used. The SRSS rule, however, assumes that the orthogonal ground motions are statistically independent. Menun and Der Kiureghian (1998) propose an alternate formula, called CQC3, which accounts for the correlation and relative intensities between the components of ground motion.

More recently, Kostinakis et al. (2013) examine the effectiveness of the 30% (or 40%) rule for linear response history analysis. In general, they found that the 30% and 40% rules are dependent on the chosen reference system and the correlation between the ground motions. The percentage rules can be unconservative by as much as 70% compared to the maximum value over all incidence angles. Additional discussion of combination rules for multidirectional response can be found in Khaled et al. (2011) and Nie et al. (2010).

4.5.3 Vertical Acceleration

Although still somewhat unusual, consideration of the vertical component of ground motion is becoming more common in design practices. Vertical ground motions tend to be rich in high frequency content (as compared to horizontal ground motions), leading to higher spectral accelerations at short periods. This is significant because typical structures are much stiffer vertically than horizontally, meaning they are affected by the high frequency content of the vertical ground motions (Bozorgnia and Bertero 2004).

The vertical-to-horizontal (V/H) spectral ratio depends on several factors, including oscillator period, source distance, and local site conditions. V/H depends less on fault type and magnitude. In general, at short periods the V/H ratio is high (up to 1.8), but it drops sharply and is significantly less than unity at longer periods (meaning the horizontal spectral acceleration is larger than the vertical spectral acceleration). This dependence of the V/H ratio on oscillator period signifies that it is inappropriate to generate a vertical response spectrum based a constant scale factor applied to a horizontal response spectrum (Bozorgnia et al. 1999).

ASCE 7 (2010) does not require explicit consideration of vertical ground motions. Instead, the vertical effects of the seismic loading is included through the use of an approximation (see equation below) which relates the vertical load to the short period spectral acceleration (S_{DS}) and the dead load (D).

$$E_v = 0.2 S_{DS} D \qquad (4.12)$$

where:

E_v = effect of vertical seismic forces

The vertical effects (E_v) are added to the horizontal seismic effects (E_h) to produce E (the total seismic effect) for use in the ASCE 7 load combinations. The commentary of FEMA P-750 (FEMA 2009a) contains a proposed new Chapter 23 for ASCE 7. In this chapter a vertical design response spectrum is defined for vertical periods of vibration ranging from 0 to 2.0 seconds. The spectrum is a function of C_V (the vertical coefficient), T_V (the vertical period of vibration), and S_{DS} (the horizontal short period spectral acceleration). This chapter was developed in response to research which suggested that the previous method of applying a 2/3 factor to the horizontal spectrum to generate a vertical spectrum is inadequate.

4.5.4 Dependent Actions

Dependent actions, such as axial-moment interaction, are better handled using response history analysis than the equivalent lateral force (ELF) procedure or the response spectrum analysis (RSA) procedure. This is because the ELF and RSA procedure produce values of peak response, but give no guidance relating to *when* these peaks occur. For this reason, the engineer must use some method to estimate design values when designing for concurrent forces (Menun and

Kiureghian 2000). It would be overly conservative to simply assume that the maxima occur at the same time.

For response history analysis, the most rigorous approach to designing for concurrent forces is to plot the loading history (called the response trajectory) of the concurrent forces on top of the interaction curve for the member in question. If the entire response trajectory is bound by the interaction curve, the design is acceptable. If the response trajectory exceeds the interaction curve at any time, this indicates an unacceptable load combination. Note that the response trajectory should include all appropriate loads (with their associated load factors), including earthquake, live, and dead load. Figure 4-5 shows an example of a response trajectory (axial load vs. moment) and the corresponding interaction curve. Note that the response trajectory values have been normalized by the nominal axial and nominal moment capacities. In this particular case, the design of the member would be considered acceptable because the response trajectory is bound by the interaction curve.

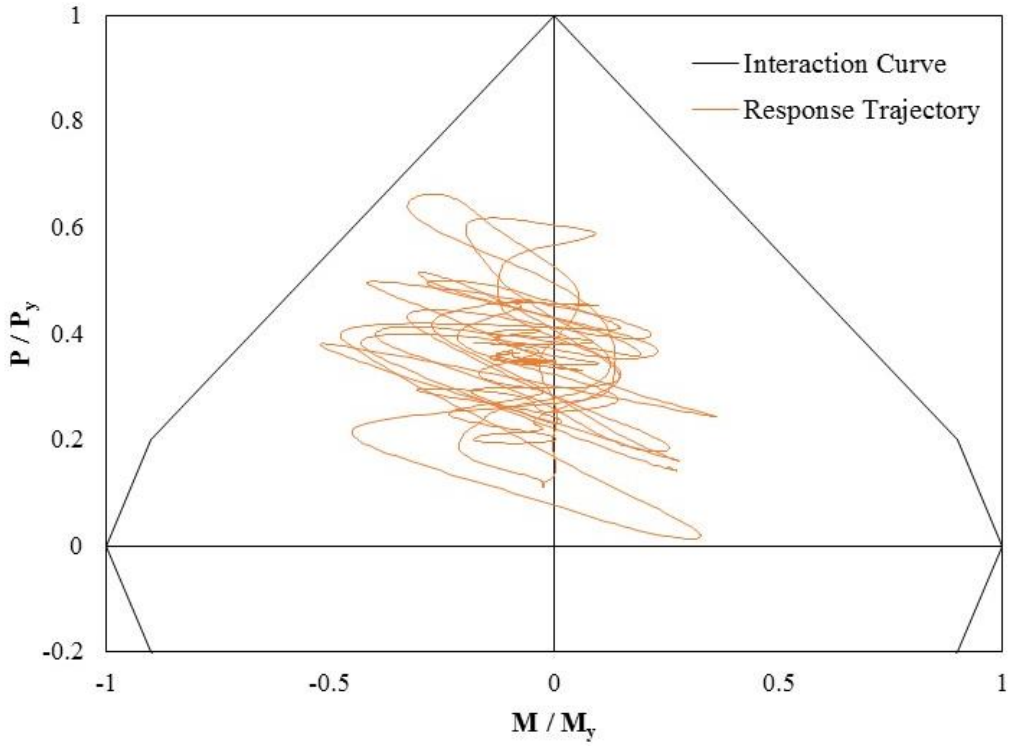

Figure 4-5. Response Trajectory and Interaction Curve

4.5.5 Accidental Torsion

Accidental torsion in a building arises due to a combination of inherent unaccounted for asymmetry in the structure and the spatial variation of the ground motion. Accidental torsion must be accounted for in some approximate way, such as offsetting the center of mass or applying a rotational component of ground motion (which is not typically recorded at seismic recording stations). Chopra (2012) provides an example of the calculated torsional response of a two story structure in Pomona, California and compares the results to the actual recorded torsional response. The response is calculated by applying a rotational ground motion $a_{g\theta}(t)$ and solving by decoupling the modes and using modal LRHA with only the purely torsional vibrational modes. The rotational ground motion is estimated by examining two recordings of the base acceleration at opposite ends of the structure. If no rotational ground motion component existed, the two components would be identical (in this case, they were not identical). The

rotational acceleration is the difference between the two recordings (at the same level) divided by the distance between the accelerographs.

De la Llera and Chopra (1994) propose two simplified analysis methods which are intended to produce similar results to response history analysis. The first of these methods is a computed design accidental eccentricity, in which the center of mass is offset by some amount. The offset varies with respect to the lateral translational period and the rotational period. In most cases, with the exception being for systems with short (< 0.5 sec) lateral periods, the eccentricities calculated are less than the typical code recommended value of 0.05*b*, where *b* is the plan dimension perpendicular to the applied force. The second method is the response spectrum method in which the results from the lateral case and the torsional case are combined using the SRSS combination rule. Additional static methods of accounting for accidental torsion can be found in Tola (2010).

A common approach for dynamic analyses is to remove a portion of the total mass of the floor and shift it laterally such that the center of mass is moved a specified distance (e.g. 5% of the overall building width). This procedure is generally acceptable, although its effect on the rotational moment of inertia should be considered. Other possible, although not often used, procedures include applying a rotational component of ground motion or applying two slightly different ground motions at opposite ends of the structure, representing the spatial variation of the ground motion across the building site. For a thorough review of accidental torsion and how various building codes handle it, refer to Tola (2010). Tola recommends that static procedures be allowed only when Ω is greater than 1, where Ω is the ratio of the uncoupled fundamental translational period to the fundamental rotational period. When Ω is less than 1 a dynamic

analysis is recommended, where the center of mass is shifted by moving a percentage of the mass laterally.

4.6 Overview of Current Procedures

4.6.1 ASCE 7

4.6.1.1 Design Acceleration Response Spectrum

ASCE 7 (2010) defines a "Design Response Spectrum" in Section 11.4.5. This response spectrum is a smoothed estimate of the actual seismic demand at the site of interest. It is defined by two design spectral acceleration response parameters, S_{DS} and S_{D1}. A summary of the equations used to generate the design response spectrum is shown in Figure 4-6, where S_{DS} and S_{D1} are the design spectral acceleration responses at 0.2 sec and 1 sec, respectively, T is the fundamental period of the structure, T_S is the ratio S_{D1}/S_{DS}, T_0 is $0.2T_S$, and T_L is the long-period transition period.

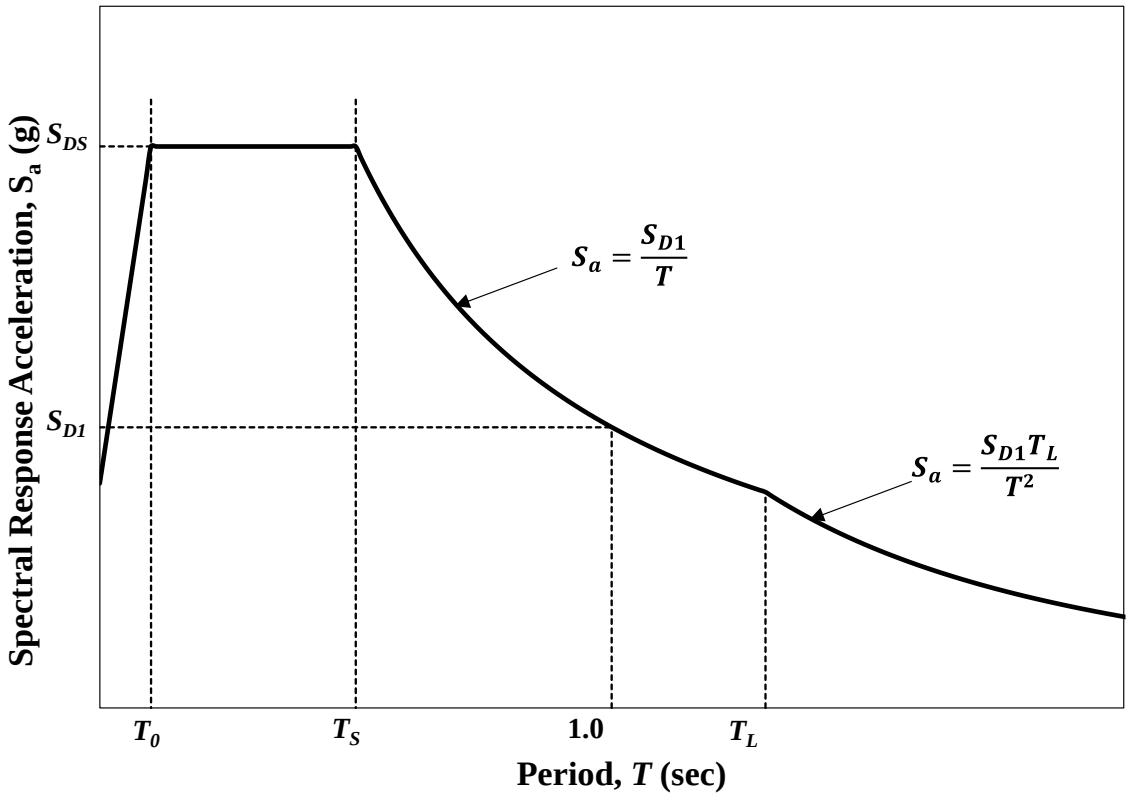

Figure 4-6. ASCE 7 (2010) Design Response Spectrum

4.6.1.2 Equivalent Lateral Force Procedure

The most commonly used seismic analytical procedure is the Equivalent Lateral Force procedure (ELF), detailed in Section 12.8 of ASCE 7 (2010). The procedure is relatively simple and easy to implement. The applied forces are static and the mathematical model is linear. The procedure involves first calculating the seismic base shear, *V*, and then vertically distributing the base shear as applied lateral loads to the upper stories of the structure. The base shear is defined by the following equation:

$$V = C_S W \qquad (4.13)$$

where:

C_S = seismic response coefficient = $\frac{S_a}{\left(\frac{R}{I_e}\right)}$

S_a = design spectral acceleration at the approximate fundamental period, T_a
R = seismic response modification coefficient (see Table 12.2-1 of ASCE 7-10)
I_e = importance factor (see Section 11.5.1 of ASCE 7-10).

In addition, there are minimum values for C_s defined by equations 12.8-5 and 12.8-6 of ASCE 7-10. Because the fundamental period of the structure cannot be calculated before the design is completed, the code specifies the approximate fundamental period T_a for use in the ELF procedure. The equation for T_a depends only on the height of the structure and the lateral system type. It should be noted that the equations given for T_a by the code are conservative and will typically provide period estimates shorter than the period determined using an eigenvalue analysis. Assuming a shorter fundamental period is conservative because it leads to a higher design spectral acceleration parameter.

The vertical distribution of forces is determined equations 12.8-11 and 12.8-12. The distribution of the base shear to a particular story is based on the height of the story and the effective seismic weight assigned to the story.

4.6.1.3 Response Spectrum Analysis

The modal response spectrum analysis procedure (RSA) is often the method used by designers when the ELF procedure is not permitted by the code. The RSA procedure uses the same design response spectrum at the ELF procedure (except that for the ELF procedure, the response spectrum does not descend to $0.4S_{DS}$ at T = 0 sec), but includes higher modes in the analysis. ASCE 7 (2010) describes the procedure in Section 12.9. The analysis must include the minimum

number of modes to reach a cumulative modal mass participation equal to 90% or more of the actual mass in each direction of interest.

A key aspect of the ASCE 7-10 RSA procedure is the requirement that when the base shear determined with the RSA procedure is less than the base shear determined with the ELF procedure, the forces from the RSA procedure must be scaled up such that the base shear is not less than 85% of the ELF base shear. This means that no greater than a 15% reduction in base shear can be obtained using the RSA procedure, as compared to the ELF procedure.

4.6.1.4 Linear Response History Analysis

Chapter 16 of ASCE 7 (2010) contains the linear and nonlinear response history analysis procedures. For linear response history analysis (LRHA), a suite of at least three ground motions must be used (for 3D analysis orthogonal pairs of ground motions are used). The ground motions must be recorded from an actual seismic event, and the earthquakes' magnitudes, fault distances, and source mechanisms must be "consistent with those that control the maximum considered earthquake." Simulated ground motions are permitted where recorded ground motions are not available. When at least seven ground motions are used, the design member forces and drifts are permitted to be taken as the average of the forces and drifts determined for each ground motion. When at least three but less than seven ground motions are used the design member forces and drifts are to be taken as the maximum of the forces and drifts determined for each ground motion.

When scaling for 2D analysis, the code permits any combination of scale factors such that the average of the 5 percent damped response spectra for the suite of ground motions does not fall below the design response spectrum, over the period range 0.2T to 1.5T. For 3D analysis, a square root sum of the squares (SRSS) spectrum is constructed for each pair of ground motions, where the same scale factor is applied to each pair. The average of the SRSS 5 percent damped response spectra for the suite of ground motions does not fall below the design spectrum, over the period range 0.2T to 1.5T.

The forces determined by the LRHA are multiplied by the factor I_e/R and the drifts are multiplied by the factor C_d/R, where I_e is the importance factor, R is the response modification coefficient, and C_d is the deflection amplification factor. Additionally, the member forces and drifts are subject to scaling requirements if the value of the base shear calculated with the LRHA procedure is less than that predicted by the minimum C_s value of equations 12.8-5 and 12.8-6.

4.6.1.5 Nonlinear Response History Analysis

The nonlinear response history analysis (NRHA) procedure is generally the most accurate yet most difficult and time consuming of the permitted procedures. It is described in Section 16.2 of ASCE 7 (2010). In general, the ground motion selection and scaling requirements are the same for the NRHA procedure as for the LRHA procedure. However, the procedure does not make use of the R-factor. Instead, the mathematical model explicitly includes inelastic behavior. The model must account for yielding, hysteretic behavior, strength degradation, and stiffness degradation.

4.6.2 Other Codes

4.6.2.1 National Building Code of Canada (NBCC)

The National Building Code of Canada (NRCC 2010a) utilizes a design response spectrum similar to ASCE 7. However, where ASCE 7 uses two spectral acceleration parameters, the NBCC response spectrum is defined using four spectral acceleration parameters for periods 0.2, 0.5, 1.0, and 2.0 seconds. At a period of 4.0 seconds the spectral acceleration is defined to be 50% of the value at 2.0 seconds. Linear interpolation is used to define the spectrum at periods between the five defined points. Figure 4-7 shows the construction of the NBCC design response spectrum.

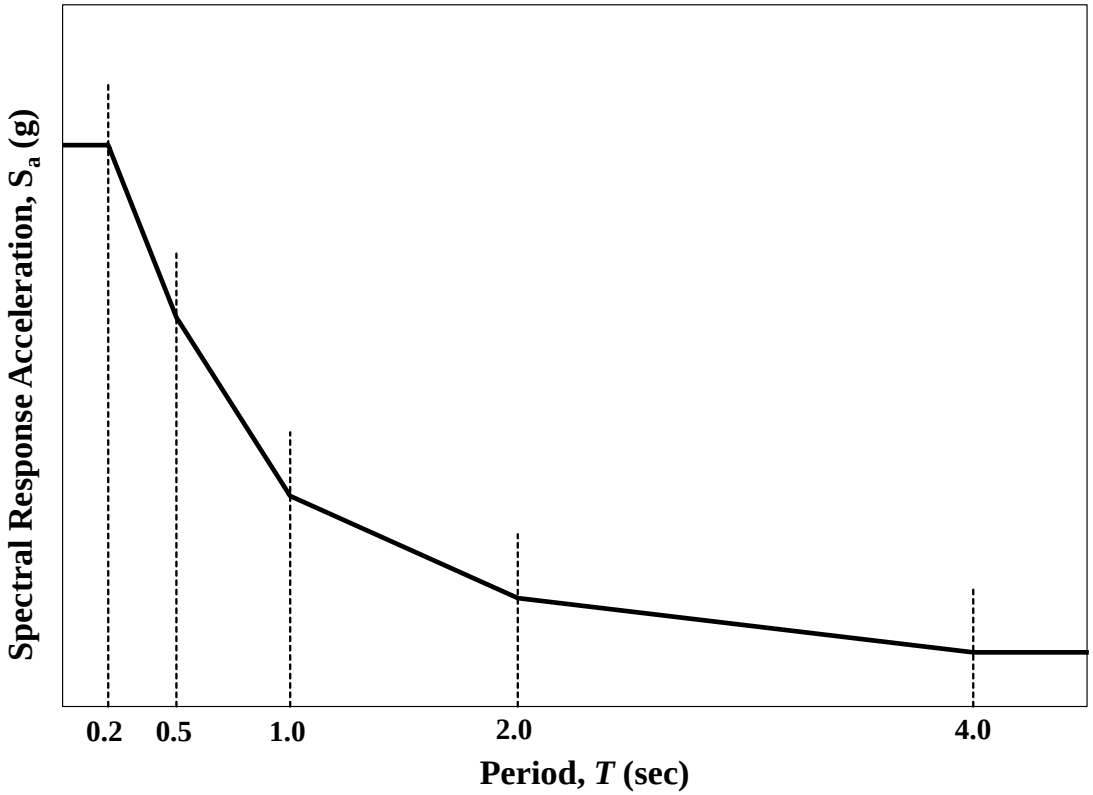

Figure 4-7. NBCC (NRCC 2010) Design Response Spectrum

The NBCC requires a dynamic analysis to be performed unless a structure meets certain requirements which qualify it for the Equivalent Static Force (ESF) Procedure. When a dynamic

analysis is performed, the NBCC allows three options: modal response spectrum method, numerical integration linear time history method (LRHA), or a non-linear dynamic procedure (NRHA).

The Commentary of the NBCC (NRCC 2010b) provides some guidance on the selection and scaling of ground motions for LRHA. A suite of at least three ground motions should be used, but at least seven is recommended. The code recommends actual recorded acceleration histories, but allows artificial or synthetic ground motions where no recorded histories are available. Any acceleration history used for LRHA must be "spectrum-compatible," which is defined as having a response spectrum greater than or equal to the design response spectrum over the period range of interest. The Commentary indicates that the upper limit for scaling should be the fundamental period of the structure, but it provides no requirements on the lower limit, except to say that the period range of interest should include "the periods of the modes contributing to the response of the particular structure." Similar to ASCE 7 (2010), the NBCC limits the reduction in base shear that can be achieved when using a linear dynamic analysis procedure. The base shear cannot fall below 80% of the base shear calculated with the equivalent static procedure.

4.6.2.2 Eurocode 8

Eurocode 8 (EC8) is the seismic design standard for the countries of the European Union (CEN 2004). EC8 contains an elastic response spectrum and design response spectrum similar to ASCE 7 (2010), although they are defined in a different manner. Section 3.2.3 of EC8 discusses the use of acceleration time histories for response history analysis. Unlike ASCE 7 and the NBCC, there

are instances when EC8 requires the vertical component of the ground motion to be used (whenever a spatial model of the structure is required).

In terms of ground motion selection, EC8 specifically allows artificial and simulated ground motions in addition to actual recorded accelerograms. In all cases at least three ground motions must be used. The ground motions must be scaled such that the "mean of the zero period spectral response acceleration values (calculated from the individual time histories) should not be smaller than the value of $a_g S$ for the site in question." The value $a_g S$ is the design peak ground acceleration modified by the soil factor *S*. Furthermore, the mean 5% damped spectrum cannot fall below 90% of the design spectrum over the period range $0.2T_1$ to 2.0 T_1. This period range is larger than that required by ASCE 7 and the scaling procedure is made unique by the requirement that the mean response spectrum exceed the design peak ground acceleration at the site.

EC8 does not contain provisions for a LRHA procedure. The allowed procedures in the standard are the lateral force method of analysis (similar to ELF), the modal response spectrum analysis, the nonlinear static (pushover) analysis, and the nonlinear response history analysis. The ground motion selection and scaling requirements discussed previously are specifically intended for use with NRHA.

4.6.2.2 New Zealand Standard

The New Zealand Building Code NZS 1170.5:2004 (NZS) dealing with seismic loading, design, and analysis contains specific provisions for linear response history analysis. NZS (2004)

Section 5.5 discusses the selection and scaling of ground motions. The standard requires at least three ground motions to be used. The ground motions must be representative of the hazard at the site (consistent magnitude, source characteristics, and distance) and have been recorded with an instrument located on similar soil conditions as the site of interest. Simulated ground motions are permitted when recorded ground motions are unavailable. The standard contains a requirement that when a site is close to a fault at least one third of the selected ground motions must "have a forward directivity component" to account for near-source effects.

The NZS contains a detailed two-factor scaling procedure. The first factor (the record scale factor) k_1 is determined by scaling the ground motion component so that the function $\log(k_1 SA_{\text{component}}/SA_{\text{target}})$ is minimized (using the least mean square approach), where $SA_{\text{component}}$ is the ground motion's 5% damped response spectra and SA_{target} is the target response spectra, over the period range $0.4T_1$ to $1.3T_1$. For pairs of ground motions the principal component is defined as the component in the pair with the smallest k_1 factor. A component with a k_1 factor below 0.33 or above 3.0 is disallowed by the code. Furthermore, the standard provides a check of the fit of the component's response spectra to the target spectra, as well as guidance on how closely the periods must be spaced when calculated the response spectra. The formula for checking the adequacy of the fit of the component's response spectra to the target is provided below (NZS 2004):

$$D_1 = \sqrt{\frac{1}{(1.5-0.4)T_1}\int_{.4T_1}^{1.5T_1}\left[\log\left(\frac{k_1 SA_{component}}{SA_{target}}\right)\right]^2 dT} \qquad (4.14)$$

where:

D_1 = fitness criterion
T_1 = fundamental period of the structure in the direction of interest

ΔT = Period increment between adjacent periods in the response spectrum

The standard requires that $D_1 \leq \log(1.5)$. This requirement generally means that the calculated response spectrum is within approximately 50% of the design spectrum within the period range of interest. In most cases this requirement is not restrictive.

The second scale factor in the NZS is the family scale factor k_2. This factor is determine such that for "every period in the period range of interest, the principal component of at least one record spectrum scaled by its record scale factor k_1, exceeds the target spectrum." The general procedure to determine k_2 would be to determine a value of k_2 for each individual component (i.e. determine the scale factor required to insure that the calculated response spectra is above the target over the entire period range of interest), and then to select the smallest value of k_2 as the overall family scale factor. The factor k_2 must be at least 1.0, but if it is above 1.3 then the standard presents options to the engineer, including proceeding with the large scale factor, or substituting one of the ground motions in the set for another so that the family scale record is smaller.

In general, the selection and scaling procedure required by the NZS is the most complex of any of the procedures surveyed. It contains explicit scaling steps, rather than simply stating that the mean spectrum must be above a certain threshold relative to the target spectrum (as in ASCE 7-10). It also contains provisions which disallow ground motions based on excessively large or small scale factors or a poor fit to the target spectrum.

Per section 6.1.3.3 of the NZS, the LRHA procedure is allowed to be used for the design of any structure, provided that a 3D analysis be performed for torsionally sensitive structures. The analysis procedure itself is described in Section 6.4. The standard specifies the maximum size of the analysis time step as the following, but also small enough to guarantee convergence:

(i) $T_1/100$

(ii) T_n

(iii) 0.01 sec

where:

$T1$ = the fundamental period of the structure

Tn = period required to reach 90% mass participation

4.6.2.4 ASCE 4-98

ASCE 4-98 Seismic Analysis of Safety-Related Nuclear Structures and Commentary (ASCE 2000) contains provisions for four analysis methods: the response history method (linear or nonlinear), the response spectrum method, the complex frequency response method, and the equivalent-static method.

The LRHA method of ASCE 4-98 can be either modal superposition or direct integration. The code provides a check of the suitability of modal superposition (as an alternative to direct integration) related to decoupling the equation of motion. The standard recommends that the number of modes included in the LRHA be enough such that the inclusion "all of the remaining modes does not result in more than 10% increase in total responses of interest."

The standard states that the average responses may be used when at least two sets of acceleration histories are used as input, although strictly speaking only one input ground motion is required. The ground motions may be actual recorded, modified, or synthetic. The standard requires that the selected (or developed) time histories contain amplitude and duration which is proper for the earthquake's duration and distance. Additional ASCE 4-98 time history requirements are listed below.

- The mean of the peak ground accelerations for the time histories must be greater than or equal to the design ground acceleration.
- Within the frequency range of interest the average ratio of the mean spectrum to the target spectrum must equal or exceed 1.

- At no point can the mean spectrum fall below the target spectrum by more than 10%.
- The average of the power spectral densities of the individual components must have adequate power within the frequency range of interest.

4.6.2.5 ASCE 43-05

ASCE 43-05 Seismic Design Criteria for Structures, Systems, and Components in Nuclear Facilities (ASCE 2005) contains provisions for a linear equivalent static analysis, a response spectrum analysis, a linear response history analysis, a nonlinear static (pushover) analysis, and a nonlinear response history analysis. ASCE 43-05 is intended to be used in conjunction with ASCE 4-98.

ASCE 43-05 contains the following requirements for synthetic or modified recorded ground motions for use in LRHA. It is stated that actual recorded ground motions are preferred for nonlinear analysis, but that modified recorded ground motions are acceptable if they also meet the following requirements.

- Records must have a Nyquist frequency of 50 Hz and a duration of at least 20 seconds. The Nyquist N_y frequency is defined as:

$$N_y = \frac{1}{2\Delta t} \qquad (4.15)$$

where:

Dt = time increment of the ground motion

- The 5% damped acceleration spectra must be computed with a minimum of 100 points per frequency decade.

- The mean of the spectra cannot fall more than 10% below the target spectrum. Where the mean spectrum falls below the target spectrum, the window of frequencies possessing spectral accelerations less than the target must be no larger than ±10% of the frequency around which the window is centered.
- The power spectral density (PSD) check of ASCE 4-98 may be neglected if the 5% damped mean response spectra does not exceed the target spectra by more than 30% over the frequency range of 0.2 Hz to 25 Hz. If this requirement is not met, the PSD check of ASCE 4-98 must be performed to ensure that no significant energy gaps exist over the frequency range.
- Synthetic ground motions must have strong motion durations, V/A ratios, and AD/V^2 ratios (where A, V, and D are the peak acceleration, velocity, and displacement, respectively) similar to recorded earthquakes of the magnitude and distance which controls the hazard for the site.
- Ground motions be statistically independent when applied simultaneously to a structure. The pairs are considered statistically independent if the directional correlation coefficient between them is less than 0.30.

4.6.2.6 FEMA P-750

FEMA P-750 is the NEHRP Recommended Seismic Provisions for New Buildings and Other Structures (FEMA 2009a) and forms the basis for the seismic provisions of ASCE 7. The Commentary section of FEMA P-750 discusses the advantages and disadvantages of LRHA, with the most significant disadvantage being the requirement to select and scale ground motions. The Commentary of FEMA P-750 specifically allows the use of spectral matched ground

motions to contribute to the ground motion suite, pointing out that a suitable estimate of the mean response can be obtained through the use of a smaller number of spectral matched ground motions.

4.7 References

Abrahamson, NA. 1992. "Non-stationary spectral matching." *Seismological research letters* no. 63 (1):30.

Adekristi, Armen. 2013. *Algorithm for Spectral Matching of Earthquake Ground Motions using Wavelets and Broyden Updating*, Virginia Tech, Blacksburg, VA.

Al Atik, Linda, and Norman Abrahamson. 2010. "An improved method for nonstationary spectral matching." *Earthquake Spectra* no. 26 (3):601-617.

ASCE. 2000. Seismic Analysis of Safety-Related Nuclear Structures and Commentary. Reston, VA: American Society of Civil Engineers.

ASCE. 2005. Seismic Design Criteria for Structures, Systems, and Components in Nuclear Facilities. Reston, VA: American Society of Civil Engineers.

ASCE. 2010. Minimum design loads for buildings and other structures. Reston, VA: American Society of Civil Engineers.

Athanatopoulou, AM. 2004. "Critical orientation of three correlated seismic components." *Engineering structures* no. 27 (2):301-312.

Bozorgnia, Y, KW Campbell, and M Niazi. 1999. Vertical ground motion: Characteristics, relationship with horizontal component, and building-code implications. Paper read at SMIP99 Seminar on Utilization of Strong-Motion Data, at San Francisco, CA.

Bozorgnia, Yousef, and Vitelmo V Bertero. 2004. *Earthquake engineering: from engineering seismology to performance-based engineering*: Crc Press.

CEN. 2004. BS EN 1998-1:2004. In *Eurocode 8: Design of Structures for Earthquake Resistance–Part 1: General Rules*.

Charney, F.A. 2013. Class Notes for CEE 6984. Virginia Tech, Blacksburg, VA.

Charney, Finley Allan. 2010. *Seismic loads : guide to the seismic load provisions of ASCE 7-05*. Reston, Va.: ASCE Press.

Chopra, A.K. 2012. *Dynamics of structures: Theory and applications to earthquake engineering*. Vol. 2. Upper Saddle River, NJ: Prentice Hall.

De la Llera, Juan C, and Anil K Chopra. 1994. "Accidental torsion in buildings due to base rotational excitation." *Earthquake engineering & structural dynamics* no. 23 (9):1003-1021.

Eibl, Josef, and Einar Keintzel. 1988. Seismic shear forces in RC cantilever shear walls. Paper read at Proceedings of the 9th Conference on Earthquake Engineering.

Fahjan, Y, and Z Ozdemir. 2008. Scaling of earthquake accelerograms for non-linear dynamic analyses to match the earthquake design spectra. Paper read at The 14th World Conference on Earthquake Engineering, Beijing, China.

FEMA. 2009a. 2009 NEHRP Recommended Seismic Provisions. In *FEMA P-750*. Washington, D.C.: Building Seismic Safety Council.

FEMA. 2009b. Quantification of Building Seismic Performance Factors. In *FEMA P695*. Washington, D.C.: Federal Emergeny Management Agency.

Grant, D.N. 2010. "Response spectral matching of two horizontal ground-motion components." *Journal of Structural Engineering* no. 137 (3):289-297.

Grant, Damian N, Paul D Greening, Merrick L Taylor, and Barnali Ghosh. 2008. "Seed record selection for spectral matching with RSPMatch2005." *Engineer* no. 3:1.

Hancock, Jonathan, and Julian J Bommer. 2007. "Using spectral matched records to explore the influence of strong-motion duration on inelastic structural response." *Soil Dynamics and Earthquake Engineering* no. 27 (4):291-299.

Hancock, Jonathan, Jennie Watson-Lamprey, Norman A Abrahamson, Julian J Bommer, Alexandros Markatis, EMMA McCOY, and Rishmila Mendis. 2006. "An improved method of matching response spectra of recorded earthquake ground motion using wavelets." *Journal of Earthquake Engineering* no. 10 (spec01):67-89.

Heo, YeongAe, Sashi K Kunnath, and Norman Abrahamson. 2011. "Amplitude-Scaled versus Spectrum-Matched Ground Motions for Seismic Performance Assessment." *Journal of Structural Engineering* no. 137 (3):278-288.

Hines, EM, LG Baise, and SS Swift. 2011. "Ground-Motion Suite Selection for Eastern North America." *Journal of Structural Engineering* no. 137 (3):358-366.

Huang, Yin-Nan, Andrew S Whittaker, Nicolas Luco, and Ronald O Hamburger. 2011. "Scaling Earthquake Ground Motions for Performance-Based Assessment of Buildings." *Journal of Structural Engineering* no. 137:311.

Kadas, Koray, Ahmet Yakut, and Ilker Kazaz. 2011. "Spectral Ground Motion Intensity Based on Capacity and Period Elongation." *Journal of Structural Engineering* no. 137 (3):401-409.

Kaul, Maharaj K. 1978. "Spectrum-consistent time-history generation." *Journal of the Engineering Mechanics Division* no. 104 (4):781-788.

Khaled, A., R. Tremblay, and B. Massicotte. 2011. "Effectiveness of the 30%-rule at predicting the elastic seismic demand on bridge columns subjected to bi-directional earthquake motions." *Engineering Structures* no. 33 (8):2357-2370.

Kostinakis, KG, AM Athanatopoulou, and VS Tsiggelis. 2013. "Effectiveness of percentage combination rules for maximum response calculation within the context of linear time history analysis." *Engineering Structures* no. 56:36-45.

Lilhanand, Kiat, and Wen S Tseng. 1988. Development and application of realistic earthquake time histories compatible with multiple-damping design spectra. Paper read at Ninth World Conference on Earthquake Engineering.

Luco, Nicolas, and Paolo Bazzurro. 2007. "Does amplitude scaling of ground motion records result in biased nonlinear structural drift responses?" *Earthquake Engineering & Structural Dynamics* no. 36 (13):1813-1835.

Masi, Angelo, Marco Vona, and Marco Mucciarelli. 2010. "Selection of Natural and Synthetic Accelerograms for Seismic Vulnerability Studies on Reinforced Concrete Frames." *Journal of Structural Engineering* no. 137 (3):367-378.

Menun, Charles, and Armen Der Kiureghian. 1998. "A replacement for the 30%, 40%, and SRSS rules for multicomponent seismic analysis." *Earthquake Spectra* no. 14 (1):153-163.

Menun, Charles, and Armen Der Kiureghian. 2000. "Envelopes for seismic response vectors. I: Theory." *Journal of Structural Engineering* no. 126 (4):467-473.

Naeim, Farzad, and Marshall Lew. 1995. "On the use of design spectrum compatible time histories." *Earthquake Spectra* no. 11 (1):111-127.

NEHRP. 2011. NIST GCR 11-918-15: Selecting and Scaling Earthquake Ground Motions for Performing Response-History Analyses. National Institute of Standards and Technology.

Nie, Jinsuo, R Morante, Manuel Miranda, and Joseph Braverman. 2010. On the Correct Application of the 100-40-40 Rule for Combining Responses due to Three Directions of Earthquake Loading. Paper read at Proceedings of the ASME 2010 Pressure Vessels & Piping Division Conference (PVP2010).

NRCC. 2010a. National Building Code of Canada. Ottawa, Canada: National Research Council of Canada.

NRCC. 2010b. User's Guide - NBC 2010 Structural Commentaries (Part 4 of Division B). Ottawa, Canada: National Research Council of Canada.

NZS. 2004. NZS 1170.5 Structural Design Actions. In *Part 5: Earthquake actions*. Wellington, NZ: Standards New Zealand.

Preumont, André. 1984. "The generation of spectrum compatible accelerograms for the design of nuclear power plants." *Earthquake engineering & structural dynamics* no. 12 (4):481-497.

Pugh, Joshua Stephen. 2013. *Numerical Simulation of Walls and Seismic Design Recommendations for Walled Buildings*.

Rizzo, PC, DE Shaw, and SJ Jarecki. 1975. "Development of real/synthetic time histories to match smooth design spectra." *Nuclear Engineering and Design* no. 32 (1):148-155.

Stewart, Jonathan P, Norman A Abrahamson, Gail M Atkinson, Jack W Baker, David M Boore, Yousef Bozorgnia, Kenneth W Campbell, Craig D Comartin, IM Idriss, and Marshall Lew. 2011. "Representation of bidirectional ground motions for design spectra in building codes." *Earthquake Spectra* no. 27 (3):927-937.

Tola, Adrian. 2010. *Development of a Comprehensive Linear Response History Analysis Procedure for Seismic Load Analysis*, Civil and Environmental Engineering, Virginia Tech, Blacksburg, VA.

Uang, Chia-Ming. 1991. "Establishing R (or R w) and C d factors for building seismic provisions." *Journal of Structural Engineering* no. 117 (1):19-28.

Whittaker, Andrew, Gary Hart, and Christopher Rojahn. 1999. "Seismic response modification factors." *Journal of Structural Engineering* no. 125 (4):438-444.

Wilson, Edward L, Iqbal Suharwardy, and Ashraf Habibullah. 1995. "A clarification of the orthogonal effects in a three-dimensional seismic analysis." *Earthquake Spectra* no. 11 (4):659-666.

5 Conference Paper (10NCEE)

The preceding literature review is in support of the conference paper submitted to EERI's *Tenth U.S. National Conference on Earthquake Engineering* titled "A Simple Linear Response History Analysis Procedure for Building Codes." The article is presented in its entirety below.

A SIMPLE LINEAR RESPONSE HISTORY ANALYSIS PROCEDURE FOR BUILDING CODES

Kevin Aswegan[1] and Finley A. Charney[2]

ABSTRACT

This paper describes a Linear Response History (LRH) analysis procedure that is intended as an alternate to the Linear Modal Response Spectrum approach that is currently part of Chapter 12 of ASCE 7-10. The main motivation for providing the response history procedure is that it preserves the signs of computed quantities (which are lost in the SRSS or CQC computations of the response spectrum procedure). In addition, a simple linear response history procedure provides a means for analysts to become familiar with response history analysis before attempting the much more complex nonlinear approaches provided in Chapter 16.

Key to the proposed LRH method is the use of spectral matched ground motions that would be automatically calculated and provided to the analyst by a simple web-based application. The only parameters needed to create the motions are the design accelerations S_{DS} and S_{D1}, and the periods defining the scaling range. Spectral matching is the non-uniform scaling of a ground motion such that its pseudoacceleration response spectrum closely matches a target response spectrum. Other important aspects of the procedure include methods for enveloping dependent actions such as axial-force and bending moment, and the

[1] Graduate Research Assistant, Dept. of Civil Engineering, Virginia Tech, Blacksburg, VA 24060
[2] Professor, Dept. of Civil Engineering, Virginia Tech, Blacksburg, VA 24060

application of accidental torsion. Special consideration is provided to the scaling of individual modal responses by the design parameters R and C_d. The method, as written, is applicable to the analysis of three-dimensional systems only.

Examples are presented to show that the results of the LRH analysis are comparable to those obtained by the response spectrum analysis procedure. Code language for the new response history analysis procedure is proposed for inclusion in Part 1 of the 2014 NEHRP Recommended Seismic Provisions and, ultimately, Chapter 12 of the 2016 edition of ASCE 7.

Introduction

Linear Response History (LRH) analysis is the determination of the response of a structural model to actual recorded, simulated, or artificial earthquake records. ASCE 7 (2010) defines LRH as "an analysis of a linear mathematical model of the structure to determine its response, through methods of numerical integration, to suites of ground motion acceleration histories compatible with the design response spectrum for the site." The traditional steps in the procedure are 1) create a linear mathematical model of the structure, 2) select at least three ground motion records, 3) scale the records to the ASCE 7 design response spectrum, 4) calculate the response of the model to the scaled ground motions using a numerical time-stepping algorithm, and 5) scale the responses using the seismic response parameters (e.g. R and C_d) of ASCE 7.

Advantages of LRH are its ability to preserve the signs of component forces, reactions and displacements as well as its explicit handling of dynamic behavior, as opposed to response spectrum analysis (RSA) in which the signs are lost due to the modal combination rules. LRH

can also serve as a link between RSA and nonlinear response history analysis (NRH) by familiarizing analysts with the use of ground motions. Additionally, LRH can verify results from other design and analysis methods or serve as an analysis step ultimately culminating with NRH.

The purpose of this paper is to encourage and generate discussion on the topic of LRH, as well as serve as a position paper to promote the inclusion of a linear response history analysis procedure in the 2016 edition of ASCE 7. In most practical applications the proposed procedure will serve as an alternative to response spectrum analysis. Key characteristics are its use of spectral matched ground motions, its handling of dependent actions such as axial-force and bending moment interaction, its scaling of responses using the seismic response parameters, and its relocation from Chapter 16 (which will be dedicated to nonlinear analysis) to Chapter 12.

Response Spectrum Matching

Response spectrum matching (also called spectral matching) is the non-uniform scaling of actual or artificial ground motion such that its pseudoacceleration response spectrum matches a target spectrum. In most cases the target spectrum is the same spectrum used for scaling actual recorded ground motions (i.e. the ASCE 7 design spectrum). Spectral matching can be contrasted with amplitude scaling, in which a uniform scale factor is applied to the ground motion. The prime advantage of spectral matching is that fewer ground motions, compared to amplitude scaling, can be used to arrive at an acceptable estimate of the mean response (NIST 2011). Figure 1(a) shows the response spectra of ground motions that have been spectral matched and Figure 1(b) shows the response spectra of the original ground motions. In both cases the ground motions are normalized to match the target response spectrum at a period of 1.10 sec.

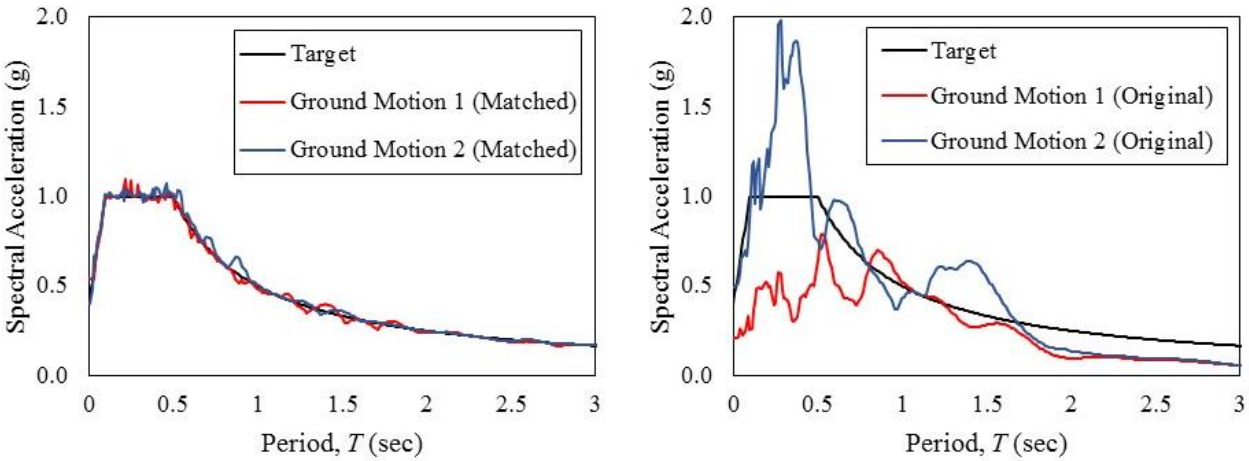

(a) Spectral Matched Ground Motions **(b) Amplitude Scaled Ground Motions**

Figure 1. Spectral Matching vs. Amplitude Scaled Response Spectra

Figure 2 contains the acceleration histories which were used to generate the response spectra of Figure 1. Figure 2(a) shows Ground Motion 1 and Figure 2(b) shows Ground Motion 2. Note that a qualitative inspection of Ground Motion 2 reveals better preservation of the characteristics of the original ground motion.

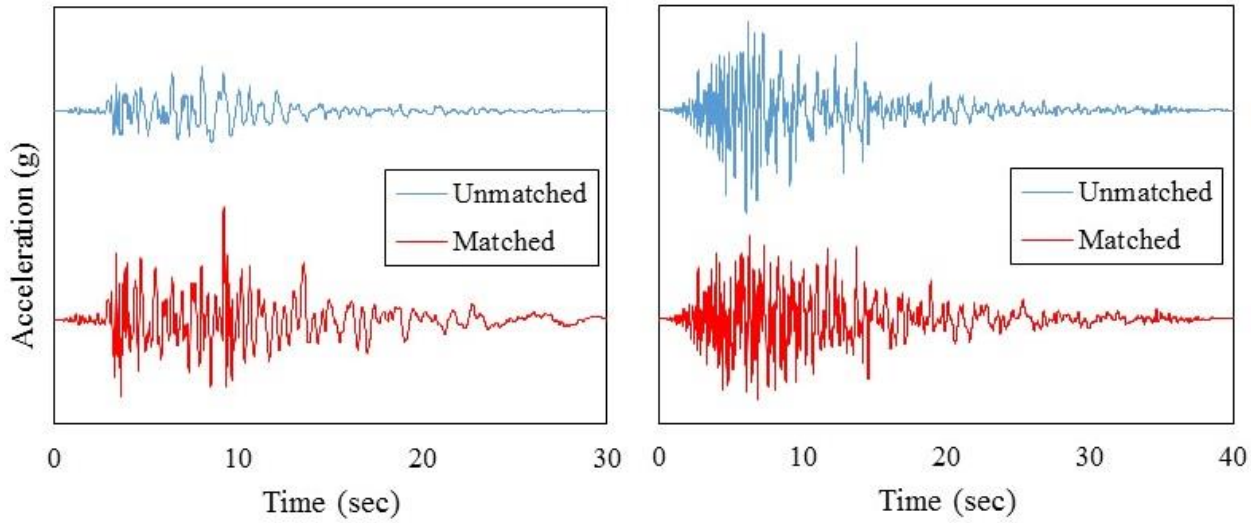

(a) Ground Motion 1 **(b) Ground Motion 2**

Figure 2. Spectral Matched vs. Amplitude Scaled Ground Motions

There are several spectral matching methods. The methods generally fall into one of two categories: matching in the frequency domain and matching in the time domain. Frequency

domain methods work by altering the Fourier amplitude spectrum of the ground motion and then reconstructing the matched ground motion using the inverse Fourier transform function. The resulting ground motions provide a close fit to the target spectrum, but often will possess distorted velocity and displacement records as well as exaggerated energy contents (Hancock et al. 2006). Spectral matching in the time domain consists of adding acceleration wavelets to the original ground motion. While more complex than frequency domain methods, spectral matching in the time domain possess superior convergence properties and typically better conserves the nonstationary characteristics of the ground motion (Al Atik and Abrahamson 2010). A time domain algorithm for spectral matching is implemented in the popular computer program RspMatch. The program uses a seed ground motion (preferably an actual recorded ground motion) and iteratively adjusts the ground motion history through the addition of wavelets. The most recent version of the program (2009) is described in Al Atik and Abrahamson (2010).

The spectral matching performed for this paper was completed using RspMatch. It is envisioned that for the proposed LRH building code procedure a simple web-based application will provide analysts with suites of spectral matched ground motions. The application will have access to a database of spectral matched ground motions corresponding to various design response spectra (defined by the value T_S which is S_{D1}/S_{DS}). The application would require only the design spectral response acceleration parameters S_{D1} and S_{DS} along with the period range for scaling. Alternatively, the analyst could perform the spectral matching using an off-line program or procedure.

Selection and Scaling of Ground Motions

The traditional approach to response history analysis is to select actual recorded ground motions and scale them to the target spectrum over a specified period range. ASCE 7 (2010) requires a minimum of three pairs of ground motions be used for 3D analysis when taking the design response quantity as the maximum response from all of the ground motions. When at least seven ground motions are used, the average response can be used for design. The code provides little guidance on the important characteristics of the selected ground motions, only stating that each ground motion "shall be obtained from records of events having magnitudes, fault distance, and source mechanisms that are consistent with those that control the maximum considered earthquake." No direction is given related to deaggregation of the seismic hazard or how to determine consistency with the maximum considered earthquake.

For 3D analysis ASCE 7 requires the construction of a square root sum of the squares (SRSS) spectrum for each ground motion pair. The average of the SRSS spectra for the ground motion suite is then scaled to equal or exceed the design spectrum over the period range $0.2T$ to $1.5T$, where T is the fundamental period of the structure. The code does not specify if T is the longer (or shorter) of the fundamental periods in the two orthogonal building orientations or some average of the two. In general it is conservative to use the longer T for the upper bound of the range and the shorter T for the lower bound of the range. Specifying a period range which extends beyond T is a requirement rooted in nonlinear analysis, because as the model yields and fractures the period will elongate. A linear model, however, will not experience any response in modes with periods longer than the first-mode period.

Accidental Torsion

Accidental torsion provisions in building codes account for multiple sources of torsion, including unconsidered mass distributions, uncertainties related to actual strength and stiffness, spatial variations in the ground excitation (i.e. base rotation), and other sources not explicitly considered in the design process (De la Llera and Chopra 1995). Accidental torsion is a separate concern from inherent torsion, which arises due to intrinsic and anticipated asymmetry in the floor plan, mass, stiffness, and strength.

There are several methods to account for accidental torsion in LRH. The most common are conducting a static analysis, in which the applied loads are offset from the center of mass (CM), or a dynamic analysis, in which the response history procedure is performed with the center of mass shifted some distance from its geometric center. The distance the center of mass must be shifted (the eccentricity) is defined by ASCE 7 (2010) to be 5% of the width of the building perpendicular to the applied loading. The mass should be shifted in the direction that produces the "worst case" response, which need not necessarily be the same for each response quantity of interest.

To shift the CM and maintain the same total mass, some amount of mass must be removed from the model and relocated some distance away from the CM, in the direction of the mass offset. The following equation can be used to determine the amount of mass to be uniformly subtracted from the level and added as a point mass (or in some other way, such as a line or area mass).

$$\alpha = \frac{0.05L}{x_p - \bar{x}} \tag{1}$$

where α is the factor defining the amount of mass to be offset, L is the total width of the structure parallel to the mass offset, $\bar{x}$ is the location of the center of mass, and x_p is the location (in the x-direction) of the point where the mass is shifted. For example, Figure 3 shows a floor with total mass M and geometric centroid located at 53.6' from the left side. Using Eq. (1), L = 120', $\bar{x}$ = 53.6', x_p = 120', and α is calculated to be 0.0903. This indicates that 0.0903M of the total mass must be relocated from the centroid to the point marked in the figure on the right edge of the floor, thus reducing the mass at the centroid to $(1-0.0903)M$.

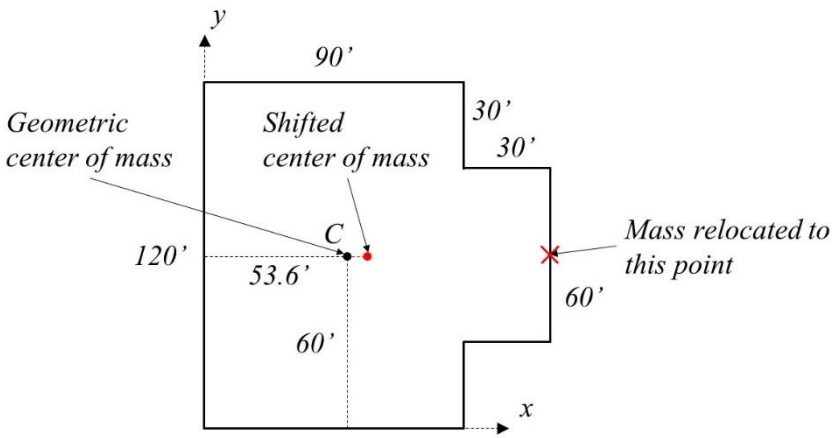

Figure 3. Example of Center of Mass Shift

Dependent Actions

Dependent actions, such as axial-moment interaction, can be more accurately handled using linear response history analysis than response spectrum analysis. This is because the precise point in time of the pair (or triplet) of responses can be known. This is contrasted with response spectrum analysis, which estimates the maximum values of each response, but requires some combination method to be used to design for concurrent forces (Menun and Der Kiureghian 2000). Using these maximum values the engineer must then determine how to design for interaction between the responses. It is overly conservative to assume that the two (or three) maxima occur at the same point in time. Using LRH the engineer can plot the loading history of

the responses (e.g. axial load vs. moment) over the interaction curve to determine acceptance (if the plot is bound by the interaction curve, the design is acceptable).

Figure 4 shows an example of an interaction curve used to verify the design of a steel column and the response trajectory for axial force vs. moment at the top of the column. The response trajectory represents loading from the appropriate controlling load combination (i.e. including dead and live load). In the case of Figure 4, the plot shows that the design is acceptable because the response trajectory is bound by the interaction curve.

To better quantify the performance of the member loaded under simultaneous actions, the usage ratio is employed. The usage ratio is defined as l_u/l_n, where l_u is the length of a line drawn from the origin to a point along the response trajectory, and l_n is the length of a line drawn from the origin to the interaction curve, at the same angle as the line drawn to the response trajectory (see Figure 4). If the usage ratio is at all times less than unity then the design is acceptable. If the usage ratio exceeds unity, the design is unacceptable. The maximum usage ratio of the response trajectory shown in Figure 4 is 0.92 (adequate design). The figure shown represents only axial load and bending about the strong axis of the column. To be complete, when simultaneous bending about both axes is significant, a three dimensional interaction surface should be created and compared to the three-dimensional response trajectory (P-M-M interaction).

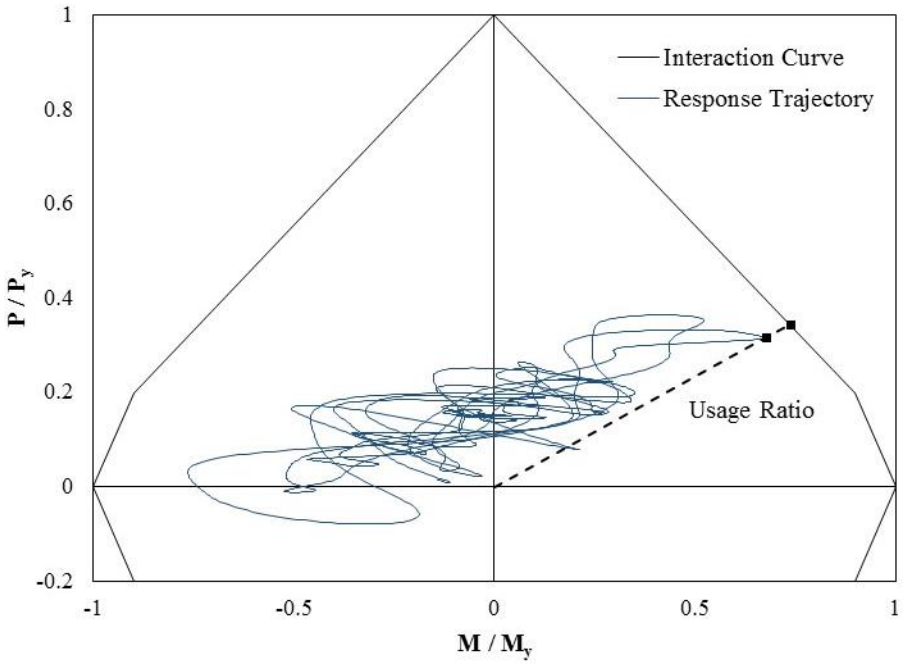

Figure 4. Axial Load vs. Moment Response Trajectories

Scaling of Responses

Results obtained from linear response history analysis are the elastic responses and must be scaled by some factor to account for inelasticity in the system. ASCE 7 (2010) uses the response modification coefficient R and the deflection amplification factor C_d. The response modification coefficient is the ratio of the forces developed in the system assuming it is perfectly linear-elastic to the design forces in the system (FEMA 2009). It primarily accounts for system ductility and overstrength, although other factors play a smaller role, including damping, engineering judgment, and past experience. Deflections are multiplied by the deflection amplification factor C_d in order to obtain inelastic drifts and deformations. The seismic response parameters of ASCE 7 are central to the linear seismic analysis procedures and will remain in any proposed building code procedure.

When the calculated base shear is less than 85% of the static base shear determined using the equivalent lateral force (ELF) procedure, all force values must be multiplied by $0.85V/V_d$,

where V is the static base shear and V_d is the dynamic base shear. This requirement is consistent with the base shear scaling requirement of the modal response spectrum analysis procedure.

Recommended Procedure

The following is a brief description of the recommended LRH procedure. The proposed procedure will be located in Chapter 12 of ASCE 7, immediately following the response spectrum analysis procedure. Spectral matched ground motions are required (in order to produce a better mean estimate of response with fewer ground motions). To simplify the procedure and to make the effort similar to that required for response spectrum analysis, only one spectral matched ground motion pair is required. While reduced variability in the mean response could be obtained through requiring additional ground motion pairs, the ultimate goal is a simple procedure with validity equal to or exceeding that of the ELF or RSA methods. If particular ground motion qualities are desired (e.g. velocity pulses), the seed ground motions should contain these qualities and a spectral matching technique should be employed which preserves as best as possible the characteristics of the input records (NIST 2011).

The ground motions are scaled to the target spectrum over the period range defined by the period range T_1 to T_2. The upper bound period, T_2 is the greatest horizontal first-mode period of the two orthogonal directions of response. The lower bound, T_1, of the period range is defined by the period of the mode required for the structural model to reach 90% modal mass participation in each orthogonal horizontal direction. The ground motion components should be spectral matched such that over the period range the response spectrum of the matched motions does not deviate from the target spectrum by more than 10%.

The mathematical model of the structure must be linear elastic and contain at least enough elastic vibration modes to achieve 90% modal mass participation in each direction. The modal should be as accurate as possible, accounting for P-Delta effects, any expected diaphragm flexibility, soil-structure interaction, and accidental torsion. Accidental torsion is modeled by offsetting the center of mass of the structure 5% in each orthogonal direction. In order to be consistent with the design response spectrum, inherent damping in the model should not exceed 5% equivalent viscous damping in any mode when performing a modal response history analysis.

The responses from the response history analysis are the elastic design values. Force responses are multiplied by I_e/R, where I_e is the importance factor and R is the response modification coefficient. Drift values are multiplied by C_d/R, where C_d is the deflection amplification factor. When the dynamic base shear (V_d) is less than 85% of the ELF static base shear (V), all forces response values must be scaled by $0.85V/V_d$.

Examples

Example 1 - Four Story Building

Figure 5 shows the structural model used in this example. The building is modeled after the four story steel special moment frame structure found in the report NIST GCR 10-917-8 (NIST 2010), identified as Archetype Design ID Number 3RSA in Performance Group PG-2RSA. The main lateral force resisting system is composed of two steel special moment frames in each direction, originally designed using the response spectrum analysis procedure. The building is regular in plan, measuring 140’ in the long direction and 100’ in the short direction. The columns forming the lateral system are fixed at the base while the gravity columns and all

gravity connections are assumed pinned. Panel zone deformations are included in the model. The fundamental period of vibration is 1.61 sec in the *X*-direction and 1.60 sec in the *Y*-direction, and the fundamental torsional period is 1.59 sec. The diaphragm is modeled as rigid.

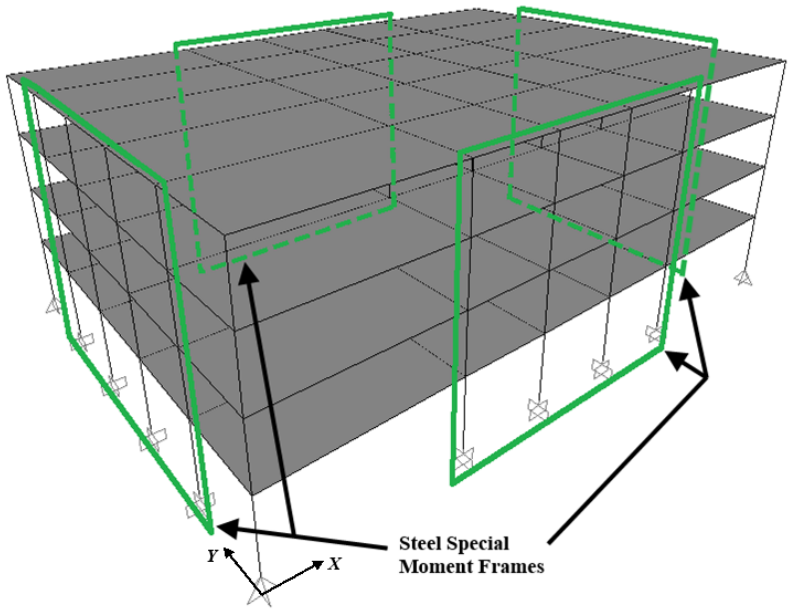

Figure 5. Four Story Building Model

Four different analysis cases are performed for the building and the results are compared (none of the analyses include accidental torsion). The analyses employ the ASCE 7-10 design response spectrum, three spectral matched ground motions, and three actual recorded ground motions (the original seed ground motions used for the spectral matching). The analysis cases are: 1) response spectrum analysis with the ASCE 7-10 design spectrum, 2) response spectrum analysis with the response spectra from three spectral matched ground motions, 3) linear response history analysis with the three spectral matched ground motions, and 4) linear response history analysis with the three actual recorded seed ground motions scaled using the ASCE 7-10 Chapter 16 SRSS scaling procedure. Figure 6 shows the ASCE 7 elastic design spectrum, the average of the spectral matched response spectra in the *X*- and *Y*-directions, and the SRSS response spectra for the original amplitude scaled records. For the site in question S_{DS} = 1.00g

and S_{D1} = 0.50g. In Figure 6(a) the ground motions are scaled such that the average of the response spectra in each direction does not fall below the target spectrum by more than 10%.

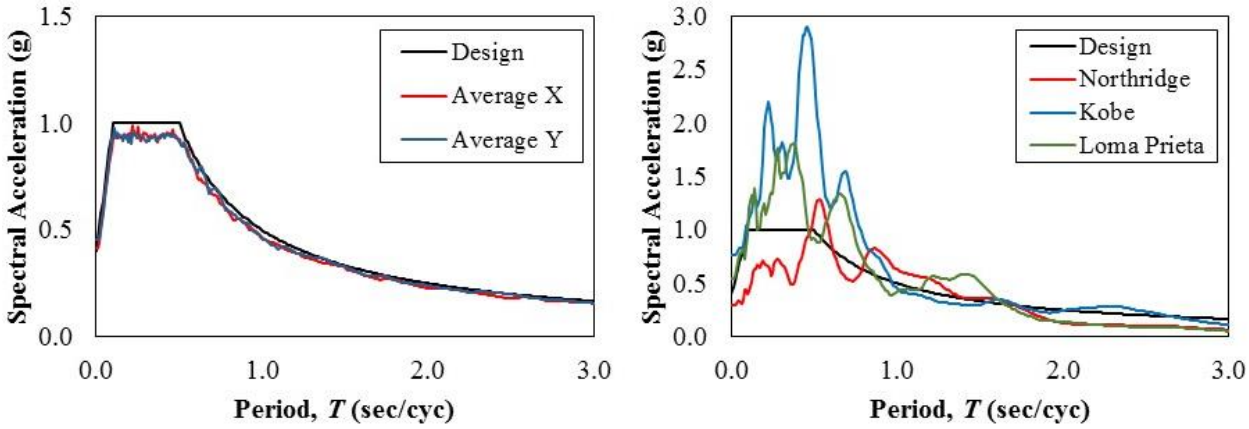

(a) Spectral Matched Ground Motions **(b) Amplitude Scaled Ground Motions**

Figure 6. Elastic Response Spectra for Four Story Building

Table 1 contains the results of the four analysis cases, comparing the base shears (divided by R) and interstory drift ratios (multiplied by C_d/R) in the two horizontal directions. The interstory drift ratios are measured at the corners of the building. This provides a consistent measure for comparison when the center of mass is shifted for the accidental torsion cases. The results from the response spectrum analysis using the ASCE 7 spectrum are used as the baseline for comparisons. As expected, the RSA responses based on the response spectra from the spectral matched ground motions are the closest to the responses from the RSA with the ASCE 7-10 response spectrum. On average, the responses are 94% of the ASCE 7-10 RSA. The difference is explained by the inexact match provided by the spectral matching algorithm as well as the fact that the ground motions are permitted to fall below the target spectrum by up to 10%. The three spectral matched LRH cases produce results which are, on average, equal to 93% of the responses generated by RSA with the ASCE 7-10 response spectrum. The three original ground motions produce results with a wide variation. The base shears are, on average, 15%

higher than the response spectrum analysis base shears. The interstory drift ratios are, on average, 19% higher than the response spectrum analysis results.

Table 1. Base Shear and Interstory Drift Ratios for Example 1

Analysis Type	Loading	Base Shear (kips)		Interstory Drift Ratio (%), X-direction				Interstory Drift Ratio (%), Y-direction			
		x	y	1st St.	2nd St.	3rd St.	4th St.	1st St.	2nd St.	3rd St.	4th St.
RSA	ASCE 7-10 Spectrum	213	214	1.07	1.28	1.35	1.04	1.07	1.28	1.35	1.04
RSA	Northridge (Matched) Response Spectrum	199	200	0.99	1.20	1.26	0.97	1.00	1.20	1.26	0.96
RSA	Kobe (Matched) Response Spectrum	197	202	0.99	1.20	1.26	0.96	1.01	1.21	1.27	0.97
RSA	Loma Prieta (Matched) Response Spectrum	202	203	1.01	1.20	1.28	0.99	1.02	1.22	1.28	0.98
LRH	Northridge (Matched)[1]	177	174	0.87	1.21	1.34	1.11	0.89	1.16	1.38	1.08
LRH	Kobe (Matched)[1]	189	193	0.94	1.18	1.18	1.03	0.97	1.19	1.21	0.95
LRH	Loma Prieta (Matched)[1]	211	195	1.02	1.23	1.38	1.23	0.98	1.20	1.18	0.91
LRH	Northridge (Original)[2]	208	240	1.10	1.50	1.62	1.15	1.18	1.46	1.62	1.26
LRH	Kobe (Original)[2]	275	301	1.21	1.28	1.98	1.85	1.42	1.74	1.69	1.43
LRH	Loma Prieta (Original)[2]	321	125	1.63	2.02	1.98	1.49	0.60	0.75	1.08	0.86

1. Scaled using the proposed scaling procedure (average of spectra in each direction does not fall the target by more than 10%.
2. Scaled using the current ASCE 7-10 SRSS 3D scaling procedure, with the period range $0.2T$ to $1.5T$.

For this example accidental eccentricity is accounted for by offsetting the center of mass of each floor 5% of the width of the building (7’ in the long direction, 5’ in the short direction). Table 2 presents the effects of shifting the mass of the structure on the calculated periods and modal mass participation ratios. The “No Shift” case represents the model in which the center of mass has not been altered in any way. The other two cases represent a mass offset equal to 5% of the width. In general, shifting the center of mass does not significantly change the periods of vibration. In fact, in the lateral direction parallel to the mass offset the periods and modal mass participation ratios are unchanged. Shifting the center of mass does, however, have a significant effect on the calculated modal mass participation ratios of the torsional modes and the lateral modes perpendicular to the mass offset. A second important effect is that the mass offset tends to couple the torsional and lateral modes (once again, those perpendicular to the mass offset). Because this particular structure is symmetric and regular, the effect on the periods and mass

participation ratios of shifting the mass in the positive *X*- (or *Y*-) direction is the same as shifting it in the associated negative direction.

Table 2. Comparison of Periods and Modal Mass Participation Ratios for Example 1

Mode	No Shift				Shifted 5% in *x* -direction				Shifted 5% in *y* -direction			
	Period	x (%)	y (%)	Rot. (%)	Period	x (%)	y (%)	Rot. (%)	Period	x (%)	y (%)	Rot. (%)
1	1.609	83.9	-	-	1.653	-	50.3	39.9	1.642	53.8	-	34.6
2	1.603	-	84.0	-	1.609	83.9	-	-	1.603	-	84.0	-
3	1.586	-	-	84.2	1.529	-	33.6	44.3	1.550	30.0	-	49.5
4	0.519	11.9	-	-	0.532	-	7.0	5.8	0.530	7.7	-	4.8
5	0.516	-	11.9	-	0.519	11.9	-	-	0.516	-	11.9	-
6	0.512	-	-	11.8	0.493	-	4.9	6.0	0.500	4.3	-	7.0
7	0.266	3.1	-	-	0.274	-	1.8	1.5	0.272	2.0	-	1.2
8	0.264	-	3.1	-	0.266	3.1	-	-	0.264	-	3.1	-
9	0.263	-	-	3.0	0.253	-	1.3	1.5	0.257	1.1	-	1.8
10	0.170	1.1	-	-	0.173	-	0.6	0.5	0.173	0.7	-	0.4
11	0.168	-	1.0	-	0.170	1.1	-	-	0.168	-	1.0	-
12	0.168	-	-	1.0	0.161	-	0.5	0.5	0.164	0.4	-	0.6

LRH is performed using the same spectral matched ground motions applied to the models with center of mass offsets. Note that in this case results are only shown for the center of mass offset in the *+X* and *+Y* directions. Table 3 shows the results of the two accidental eccentricity cases. The values reported are the averages of the responses from the three ground motion pairs. In general, the base shears are unchanged in the direction parallel to the mass offset, but decrease in the direction perpendicular to the mass offset. The trend for interstory drift ratios, however, shows that the interstory drift ratios generally increase when the mass is offset.

Table 3. Comparison of Responses from Accidental Eccentricity Cases

Eccentricity	Base Shear (kips)		Interstory Drift Ratio (%), *X* -direction				Interstory Drift Ratio (%), *Y* -direction			
	x	y	1st St.	2nd St.	3rd St.	4th St.	1st St.	2nd St.	3rd St.	4th St.
No Eccentricity	192	187	1.37	1.76	1.89	1.63	1.38	1.72	1.83	1.43
+5% in *X* -direction	192	173	1.46	1.87	2.05	1.76	1.40	1.76	1.86	1.40
+5% in *Y* -direction	185	187	1.57	1.94	2.01	1.55	1.40	1.79	1.90	1.63

Example 2 - Twelve Story Building

While the first example studied a low-rise symmetric building, this example will examine the response of a taller irregular structure. Figure 7 shows a twelve story steel perimeter steel moment frame. A slightly different version of this structure is used in the Analysis chapter of FEMA P-751 (2012), which contains more detailed information related to the original design of the structure. The first story of the structure is 18' and the remaining stories are 12.5'. The base of the structure is composed of seven bays at 30' in the long direction, and 7 bays at 25' in the short direction.

This example uses the same seed ground motions as the previous example. However, the ground motions are spectral matched to a target spectrum defined by S_{DS} = 1.10g and S_{D1} = 0.66g. Figure 8 shows the average response spectra for the two orthogonal building directions. The average spectra are less than the design spectrum by a small amount due to the fact that the proposed procedure allows the response spectra to fall below the target spectrum by as much as 10%.

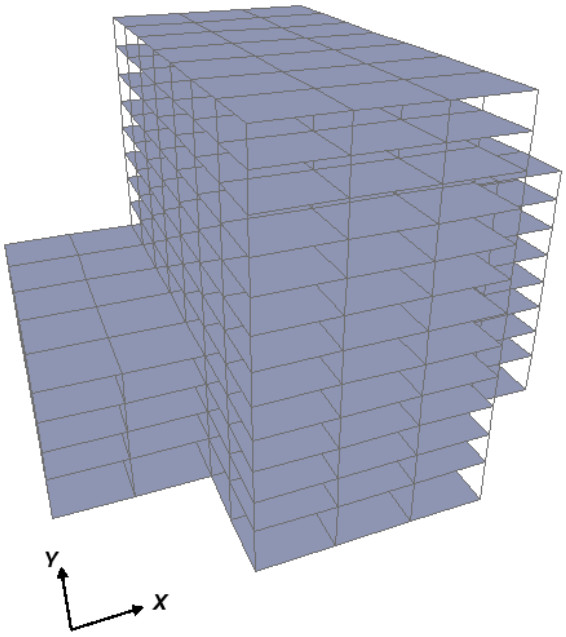

Figure 7. Twelve Story Building Model

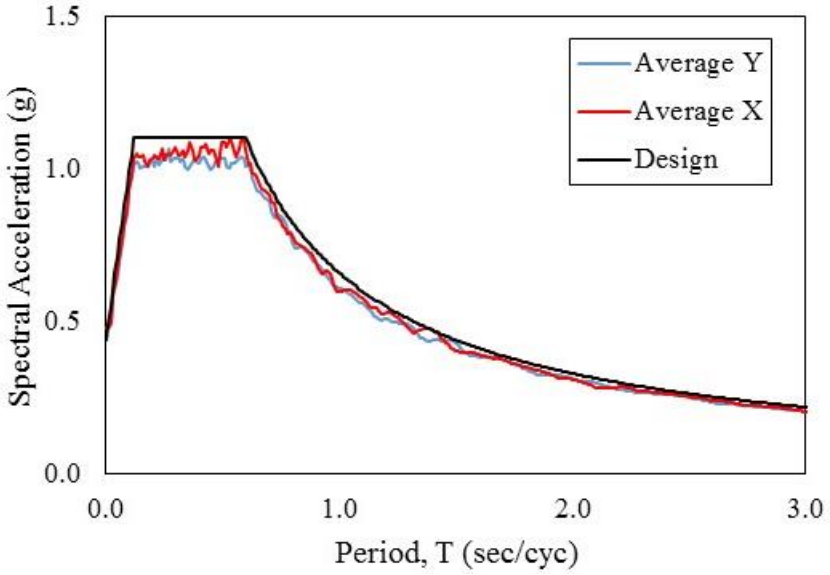

Figure 8. Elastic Response Spectra for Twelve Story Building

This example compares only the results from the response spectrum analysis case using the ASCE 7 response spectrum to the results from the linear response history case using the spectral matched ground motions. Table 4 shows the base shears calculated for both cases. Also shown is the ratio of the average base shear from the LRH cases to the base shear from the RSA case. Note that in the *x*-direction, the LRH analysis produces results greater than the RSA response, and the in *y*-direction the LRH procedure produces results less than the RSA response. Also calculated in this example are the interstory drift ratios at each level of the building. Figure 9 compares these values over the height of the structure, showing lines representing the interstory drift ratios in the *x*- and *y*-directions for both the RSA and the average values from the LRH cases.

Table 4. Base Shears for Example 2

Analysis Type	Loading	Base Shear (kips)	
		x	y
RSA	ASCE 7-10 Spectrum	897	988
LRH	Northridge (Matched)	990	980
LRH	Kobe (Matched)	970	1028
LRH	Loma Prieta (Matched)	816	796
(Average LRH) / RSA		1.031	0.946

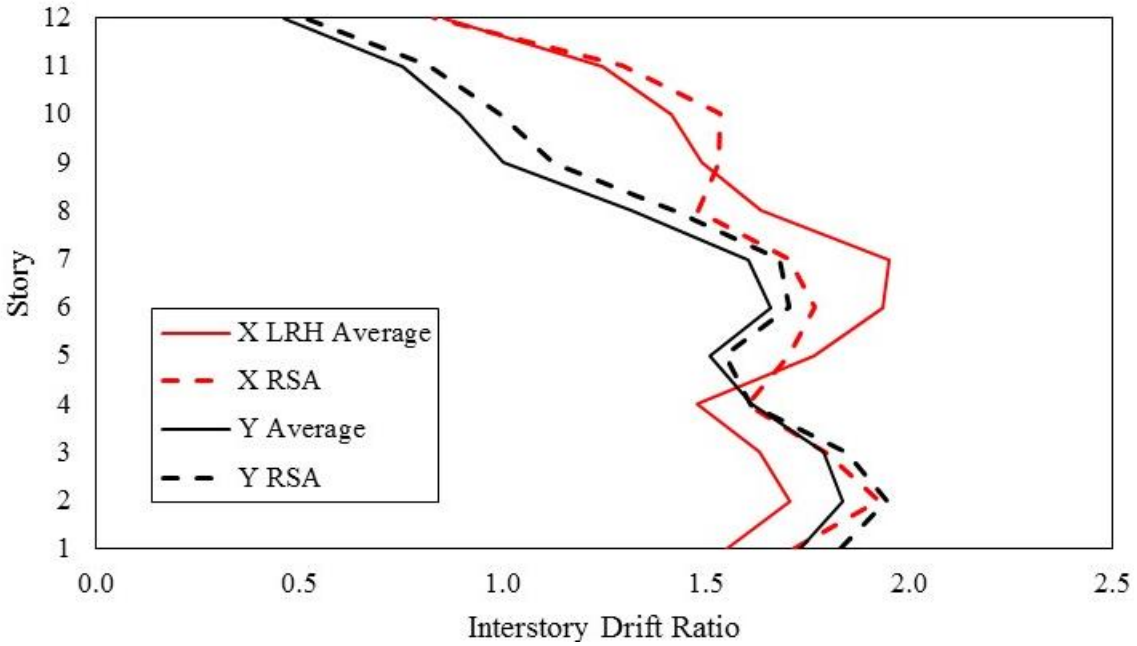

Figure 9. Comparison of Interstory Drift Ratios for Example 2

For this particular structure accidental eccentricity is not a significant design consideration, although it should still be considered. This is due to the fact that shifting the center of mass 5% in each orthogonal direction has little effect on the computed lateral periods and modal participation ratios, and only a moderate effect on the torsional periods and modal participation ratios. Table 5 shows the results of the center of mass shifts.

This and the previous example demonstrate the compatibility between the proposed linear response history procedure and the current modal response spectrum procedure of ASCE 7 (2010). Although not shown, the next steps for the examples include establishing the

acceptability of the design, through the verification of section capacities against calculated loads (including consideration of concurrent forces) and the comparison of the calculated drifts to the acceptable drift limits.

Table 5. Comparison of Periods and Modal Mass Participation Ratios for Example 2

Mode	No Shift				Shifted 5% in +*x* -direction				Shifted 5% in +*y* -direction			
	Period	*X* (%)	*Y* (%)	Rot. (%)	Period	*X* (%)	*Y* (%)	Rot. (%)	Period	*X* (%)	*Y* (%)	Rot. (%)
1	2.789	79.9	-	26.2	2.789	79.9	-	23.4	2.791	80.0	-	32.4
2	2.565	-	82.5	40.1	2.577	-	82.7	46.4	2.565	-	82.5	37.3
3	1.588	-	-	18.1	1.590	-	-	14.8	1.619	-	-	14.3
4	1.106	12.5	-	3.6	1.106	12.5	-	3.3	1.115	12.5	-	4.4
5	0.971	-	11.6	2.3	0.960	-	11.4	3.0	0.971	-	11.5	2.5
6	0.695	-	-	3.0	0.701	-	-	2.4	0.699	-	-	2.1
7	0.673	2.8	-	-	0.673	2.9	-	-	0.683	3.3	-	1.0
8	0.573	-	2.2	2.0	0.582	-	2.1	2.2	0.572	-	2.1	1.8
9	0.433	-	-	-	0.433	-	-	-	0.433	-	-	-
10	0.419	2.2	-	-	0.420	2.2	-	-	0.423	2.2	-	-
11	0.385	-	2.2	-	0.387	-	2.2	1.1	0.385	-	2.2	-
12	0.328	-	-	-	0.328	-	-	-	0.332	-	-	-

Conclusions

The linear response history analysis procedure in ASCE 7 (2010) is underused and contains several obstacles to its utilization by the design community. These drawbacks include the ground motion selection and scaling requirements and its location in Chapter 16 of the code. The procedure proposed in this paper remedies these drawbacks by employing spectral matched ground motions (to reduce the required number of analyses) and relocating the procedure to Chapter 12, alongside the alternate linear analysis procedures. It is expected that the spectral matched ground motions will be available to designers through the use of a web-based application.

The intention of this paper is to advance discussion on the topic of linear response history analysis in building codes and to propose a procedure for future editions of ASCE 7. It is

recommended that additional work be completed to further explore the topics of accidental torsion, scaling of responses, and other topics as they relate to linear response history analysis.

Acknowledgments

Funding for author K. Aswegan was partially provided by the Charles E. Via Endowment of the Virginia Tech Department of Civil and Environmental Engineering and by a grant from the National Institute of Standards and Technology (NIST).

References

Al Atik, L., and N. Abrahamson, 2010. "An improved method for nonstationary spectral matching," *Earthquake Spectra*, 26(3), 601-617.

ASCE, 2010. Minimum design loads for buildings and other structures, American Society of Civil Engineers, Reston, VA.

De la Llera, J. C., and A. K. Chopra, 1995. "Estimation of Accidental Torsion Effects for Seismic Design of Buildings," *Journal of Structural Engineering*, 121(1), 102-114.

FEMA, 2009. NEHRP Recommended Seismic Provisions for New Buildings and Other Structures, *FEMA P-750*. Prepared by the Building Seismic Safety Council for the Federal Emergency Management Agency, Washington, D.C.

FEMA, 2012. NEHRP Recommended Seismic Provisions: Design Examples, *FEMA P-751*. Prepared by the Building Seismic Safety Council for the Federal Emergency Management Agency, Washington, D.C.

Hancock, J., J. Watson-Lamprey, N. A. Abrahamson, J. J. Bommer, A. Markatis, E. McCoy, and R. Mendis, 2006. "An improved method of matching response spectra of recorded

earthquake ground motion using wavelets," *Journal of Earthquake Engineering*, 10(1), 67-89.

Menun, C., and A. Der Kiureghian, 2000. "Envelopes for Seismic Response Vectors. I: Theory," *Journal of Structural Engineering*, 126(4), 467-473.

NIST, 2011. Selecting and Scaling Earthquake Ground Motions for Performing Response-History Analyses, *NIST GCR 11-918-15*. Prepared by the NEHRP Consultants Joint Venture for the National Institute of Standards and Technology Gaithersburg, MD.

NIST, 2010. Evaluation of the FEMA P-695 Methodology for Quantification of Building Seismic Performance Factors, *NIST GCR 10-917-8*. Prepared by the NEHRP Consultants Joint Venture for the National Institute of Standards and Technology, Gaithersburg, MD.

Appendix. Proposed Linear Response History Analysis Code Language

12.10 MODAL RESPONSE HISTORY ANALYSIS

12.10.1 General Requirements

Modal response history analysis shall consist of the superposition of the numerical response of individual elastic modes of a mathematical model of the structure subjected to spectrally matched ground motions. The analysis shall be performed in accordance with the requirements of this section.

12.10.2 General Modeling Requirements

A three-dimensional model of the structure is required. All other modeling considerations shall be in conformance with Section 12.7.3.

12.10.3 Period Range

An analysis shall be conducted to determine the natural modes of vibration of the structure. The response of all modes with periods greater than or equal to T_1 and less than or equal to T_2 shall be included in the analysis. T_1 is the period of vibration at which 90% of the actual mass has been recovered in each of the two orthogonal directions of response. T_2 is the larger of the two orthogonal fundamental periods of vibration.

12.10.4 Damping

Damping in each mode of vibration shall be equal to 5% critical.

12.10.5 Ground Motion Selection and Scaling

Ground acceleration histories used for analysis shall consist of two orthogonal components of a single artificial or recorded ground motion event, spectrally matched to the target response spectrum. The target response spectrum shall be developed in accordance with in Sections 11.4.5 or 21.3, as applicable.

12.10.5.1 Period Range for Spectral Matching

Each component of the ground motion shall be spectrally matched over the period range T_1 to T_2. Over the same period range the ordinates of the response spectrum computed from each component of the spectrally matched motions shall not fall below the target spectrum by more than ten percent.

12.10.5.2 Quality of Spectral Matching

Histories of ground velocity that are computed from time integrals of the spectrally matched ground acceleration histories shall have terminal velocities not greater than 1.0 percent of the peak ground velocity from the unmatched record.

12.10.5.3 Orientation of Ground Motions

Where one component of ground motion is rotated at a given angle about a vertical axis, the second orthogonal component shall be rotated about the same angle.

12.10.6 Application of Ground Acceleration Histories

Ground motion shall be applied to the base of the structure. Orientation of loading shall be in accordance with the requirements of Section 12.5.

12.10.7 Accidental Torsion

The analysis shall consider the effect of both inherent and accidental torsion. Accidental torsion shall be included by offsetting the center of mass each way (i.e. plus or minus) from its expected location by a distance equal to 5 percent of the horizontal dimension of the structure at the given floor measured parallel to the direction of mass offset. The required 5 percent offset of the center of mass need not be applied in both orthogonal directions at the same time.

12.10.8 Design Response Values

For each direction of ground motion analyzed, the individual response parameters shall be multiplied by the following scalar quantities:

a. Force quantities shall be multiplied by I_e/R. Where force interaction effects must be considered in design, concurrent quantities shall be used.

b. Drift quantities shall be multiplied by C_d/R.

12.10.9 Scaling Design Response Values

A static base shear, V, shall be calculated in each of two orthogonal directions in accordance with Section 12.8.1.

12.10.9.1 Scaling of Forces

A dynamic base shear, V_d, shall be computed for each application of ground motion using design force results determined in accordance with Section 12.10.8a. Where the dynamic base shear is less than $0.85V$ in any direction of response, all force results obtained for that direction of response shall be multiplied by $0.85V/V_d$.

12.10.9.2 Scaling of Drifts

Scaling of design drift quantities is not required.

12.10.10 P-Delta Effects

P-Delta effects shall be satisfied in conformance with Section 12.8.7. The story deflection Δ and the story shear V_x used in Eqn. 12.8-16 shall be concurrent values computed in the direction of interest.

12.10.11 Soil Structure Interaction

Soil structure interaction effects may be included in the analysis using generally accepted procedures approved by the authority having jurisdiction.

6 Conclusions

6.1 Summary

The two procedures proposed in this thesis aim to improve the design process related to wind drift in steel structures and linear response history analysis. The wind drift design procedure is a rational method which utilizes concepts taken from performance based earthquake engineering. Multiple mean recurrence intervals are considered, shear strain is taken as the damage measure of interest, and fragility curves are recommended for setting shear strain limits. Chapter 2 contains the literature review related to wind drift serviceability and Chapter 3 contains the *Engineering Journal* paper which describes the proposed procedure.

The steps of the recommended wind drift design procedure are: 1) select an appropriate mean recurrence interval, 2) determine wind speeds and loading for the selected MRIs, 3) accurately model the structure, 4) calculate the deformation damage indices (DDIs), 5) select rational drift limits using fragility curves, 6) compare the DDIs to the damage limits, 7) repeat steps 1-6 until and economical design is achieved or other loading cases control.

The linear response history analysis procedure proposes code language for the next edition of ASCE 7. The proposed procedure utilizes spectral matched ground motions to reduce the required number of analyses, as well as a ground motion scaling procedure which is believed to be consistent with future nonlinear response history analysis code language. Chapter 4 contains

the literature review related to linear response history analysis and Chapter 5 contains the conference paper which describes the proposed procedure.

6.2 Conclusions

The wind drift design procedure addresses the lack of a standardized wind serviceability design procedure for steel buildings. The proposed design method introduces fragility curves as a means to quantify performance at various hazard levels, while advocating for the use of shear strains as the damage measure and the most accurate possible mathematical building model. The most significant future work recommended for the procedure is its extension to include consequences of damage, most importantly cost. This could be accomplished using the cost relationships developed for performance based earthquake engineering. The procedure's extension to include cost would provide the decision makers valuable information related to the performance and acceptability of the design.

The proposed linear response history analysis procedure addresses shortcomings of the current LRH procedure. It simplifies the procedure by requiring only one ground motion to be used. The accuracy of the produce is maintained through the use of spectral matched ground motions, which allow fewer analyses to be performed in order to arrive at an acceptable estimate of the mean response. It is intended that the procedure be used as an alternative to the other linear procedures of ASCE 7 (the equivalent lateral force procedure and the modal response spectrum analysis procedure). The proposed code language includes a redefined period range for scaling and spectral matching as well as a new scaling procedure. The new scaling procedure applies separate and independent scale factors to the individual ground motion components. This is

acceptable due to the fact that the ground motions are spectral matched, and the inherent intensity differences between the orthogonal seed components has been removed. Ultimately, the goal of the proposed procedure is inclusion in the 2014 NEHRP Recommended Seismic Provisions and the 2016 ASCE 7 seismic provisions.